

UNIVERSITÀ DEGLI STUDI DI NAPOLI “FEDERICO II”

FACOLTÀ DI INGEGNERIA



Dipartimento di Ingegneria dei Materiali e della Produzione

DOTTORATO DI RICERCA IN

INGEGNERIA DEI MATERIALI E DELLE STRUTTURE

XXIV CICLO

**NANOSTRUCTURED PLATFORMS WITH CONTROLLED DRUG DELIVERY
FOR PERIODONTAL TISSUE REGENERATION**

Relatori:

Ch.mo Prof. Luigi Ambrosio

Dr. Ing. Vincenzo Guarino

Coordinatore

Prof. Giuseppe Mensitieri

Candidato:

Wan Khartini Wan Abdul Khodir

Triennio 2008 – 2011

To my beloved parents, Wan Abdul Khodir and Rohani Awang,
for their continuous guidance
and patience, and to my brothers and sisters, for their support

ABSTRACT

Electrospinning/electrospraying technique is currently represent a challenging route to produce polymer micro and nanoscaffolds with fibers and/or particles aspect. The design of integrated platforms based on the synergistic use of electrospinning and electrospraying technique offer the chance to design powerful scaffolds for tissue engineering and drug delivery applications. PCL and Chitosan are biocompatible materials to consider as 'ideal' candidates for cell material interation. In particular, PCL fibers may be electrospun to form submicrometric fibrous networks able to mimic the structural organization of the collagen fibres in the native ECM. Process parameters, i.e, voltage, flow rate, may be finely controlled optimize fiber size, distribution and beads occurrence. Meanwhile, chitosan particles processed by electrospraying can be successfully used as carrier of antibiotics, i.e, tetracycline for the use in periodontal surgery as confirmed by the fast release completed after 24 hours. Finally, the biological response of integrated systems was ultimately explored to validate the use of PCL/CHI scaffolds as periodontal patches.

Table of contents

Abstract

Table of contents

Chapter 1	Micro to Nanostructured Scaffolds for Tissue Engineering	1
1.1	Scaffold Design: Basic Knowledge	1
1.2	Nanotechnology in Scaffold Design: State of Art	4
1.3	Electrospun Nanofibrous Scaffold to Mimic Natural ECM.	6
1.4	The Challenges of Electrical Forces: Electrospinning and Electrospaying Techniques	8
1.5	Aim of this study	10
1.6	Summary of Covered Subjects	10
	References	11
Chapter 2	Electrospinning: Alternatives Routes towards Nanotechnology	13
2.1	History at a glance	13
2.2	Basic Requirement: Tailoring Polymer Solution Properties	14
2.2.1	Polymer Molecular Weight	14
2.2.2	Intermolecular and Solvent Interaction in Polymers	15
2.2.3	Surface Tension	16
2.2.4	Conductivity	17
2.3	Electric Field Driven Process Technologies	18
2.3.1	Basic Principles	18
2.3.2	Electrospaying	20
2.3.3	Electrospinning	22
2.4	Basic Parameters to Control Morphologies	24
2.4.1	Polymer/Solvent System	24
2.4.2	Molecular Weight and Viscosity	27
2.4.3	Processing Parameters	28
2.5	Electrospun/Electrosprayed Devices in Drug Delivery Applications	30
2.5.1	Oral Drug Delivery	33
2.5.2	Other Examples of Drug Delivery System	35
	References	36
Chapter 3	Investigation of PCL Electrospun Membranes: Effect of Co- Solvent and Process Parameters	
3.1	Introduction	40
3.2	Materials	43
3.3	Methods	45
3.4	Results and Discussion	46
3.5	Conclusion	58
	References	58
Chapter 4	Chitosan Nanoparticles for Drug Delivery System	

4.1	Introduction	60
4.2	Materials and Methods	66
4.3	Results and Discussion	71
4.4	Conclusion	81
	References	82
Chapter 5	Integrated System of PCL Nanofibers/Chitosan Particles for Periodontal Tissue Engineering	
5.1	Introduction	84
5.2	Materials and Methods	87
5.3	Results and Discussion	92
5.4	Conclusion	105
	References	106
	Summary	107
	Acknowledgements	110

CHAPTER 1

Micro to Nanostructured Scaffolds for Tissue Engineering

1.1 Scaffold Design: Basic Knowledge

Tissue engineering is an interdisciplinary field that applies the principles of chemistry, physics, materials science, engineering, cell biology and medicine to the development of biological substitutes that restore, maintain or improve tissue/organ functions [1].

Since its inception, there has been a considerable effort to develop an "ideal" tissue-engineering scaffold. The field has been governed by the generic concept of combining cell, scaffold (artificial extracellular matrix), and bioreactor technologies in the design and fabrication of neo-tissues/organs. This is logical since every tissue or organ in our body is composed of parenchymal cells (functional cells) and mesenchymal cells (support cells) contained within an extracellular matrix (ECM) to form a microenvironment. These microenvironments collectively form our tissues and organs. In terms of development and maintenance of the tissues and organs, our body is the "bioreactor", exposing the cell and ECM microenvironments to biomechanical forces and biochemical signals. Composition (i.e., biomaterials of synthetic or natural origin) and architecture of a tissue engineered scaffold result in cell–environment interactions that determine the structure's fate. The ultimate goal is to enable the body (cellular components) to heal itself by introducing a tissue engineered scaffold that the body recognizes as "self", and in turn, uses to regenerate "neo-native" functional tissues. In order to duplicate all of the essential intercellular reactions and promote native intracellular responses, the ECM must be mimicked. These synthetic ECMs or scaffolds must be designed to conform to a specific set of requirements [2].

The design requirements of a tissue engineering scaffold specific to the structure and function of the tissue to be regenerated have been identified as crucial for the production of tissue engineering scaffolds [2,3], which is;

1. The material must be biocompatible and bioresorbability to function without interrupting other physiological processes. This functionality includes an ability to promote normal cell growth and differentiation while maintaining a three-

dimensional orientation/space for the cells. The most widely utilized scaffold materials are poly(α -hydroxy esters) such as PGA, PLA, and PLGA. They have been fabricated into thin films, fibers, porous foams, and conduits and investigated as scaffolds for regeneration of several tissues [4],

2. Should not induce or initiate any adverse response and, be easily fabricated into a variety of shapes and sizes,
3. The scaffold should possess interconnecting pores of appropriate scale to favor tissue integration and vascularisation with respect to nutrient supply to transplanted and regenerated cells,
4. For clinical and commercial success, scaffold must have appropriate surface chemistry to regenerate tissue, thus engineered scaffolds act as hosts to cells harvested from natural tissue and begun to mimic the extracellular matrix (ECM) and facilitate the development of a 3-D structure [5,6]. With the ability and advantages of scaffolds (have a high surface to- volume ratio) is able to enhance cell adhesion [5], migration, proliferation and differentiated function [7].
5. Possess adequate mechanical properties to match the intended site of implantation and handling. For load-bearing tissues such as bone, the scaffold should be strong enough to withstand physiological stresses to avoid collapse of the developing tissue. Also, transfer of load to the scaffold (stress shielding) after implantation may result in lack of sufficient mechanical stimulation to the in growing tissue. For the regeneration of soft tissues such as skin, the scaffolds are required to be pliable or elastic. The stiffness of the scaffold may affect the mechanical tension generated within the cell cytoskeleton, which is critical for the control of cell shape and function [8].
6. Once implemented in vitro or in vivo, the material must either be removed via degradation and absorption or incorporated via innate remodeling mechanisms, leaving only native tissue. For example the degradation products are released gradually by surface erosion, whereas during bulk degradation, the release of degradation products occurs only when the molecular weight of the polymer reaches a critical value. This late-stage burst effect may cause greater local pH drop. The rate of scaffold degradation is tailored to allow cells to proliferate and secrete their own ECM while the polymer scaffold vanishes over a desired time

period (from days to months) to leave enough space for new tissue growth. Since the mechanical strength of a scaffold usually decreases with degradation time, the degradation rate may be required to match the rate of tissue regeneration in order to maintain the structural integrity of the implant. Therefore, understanding and controlling the degradation process of a scaffold and the effects of its degradation products on the body is crucial for long-term success of a tissue-engineered cell–polymer construct [5].

Beyond these generalized requirements, one of the principle methods behind tissue engineering involves growing the relevant cell in vitro into the required three-dimensional (3D) organ or tissue. Rather, a dynamic three-dimensional inter-relation is constantly kept in balance and influenced by both internal and external stimuli.

Thus, any scaffold material must in nanostructure and able to interact with cells in three dimensions and facilitate this communication. It is because, in the native tissues, the structural ECM proteins (50–500 nm diameter fibers) are 1 to 2 orders of magnitude smaller than the cell itself to allow the cell to be in direct contact with many ECM fibers, thereby defining its three dimensional orientation. This biomimetic features and excellent physiochemical properties of nanoscaffold played a key role in stimulating cell growth and chemical signals can be exchanged between cells and the environment as well as guide tissue regeneration. It is may be a crucial factor in determining the success or failure of a tissue engineering scaffold. [1, 2].

Generally, three-dimensional scaffolds can be fabricated from natural and synthetic polymers, ceramics, metals, composite biomaterials, and cytokine release materials. There are some common methods for fabrication an emulated scaffold to imitate the structure and functional biology of native ECM. Self assembly, phase separation, and electrospinning have been utilized to produce nanofibrous scaffold [9].

Therefore, nanofibrous scaffolds will be preferred due to their similarity to ECM fibrils in both dimension and morphology. Indeed, the advantages of nanofibrous scaffold in promoting cell growth and maintaining the proper cell phenotype have been demonstrated in a numerous studies [2,10], which is considered as the synergistic result of both nanotopography and chemical signaling of the scaffold [11,12,13,14].

1.2 Nanotechnology in Scaffolds Design: State Of Art

With increasing interest in cutting-edge nanotechnology, development of biomimetic design of nanoscaffolds mimics natural extracellular matrix (ECM) at a multiscale level, from the composition morphology, topography, to spatial organization is having a new momentum. Since conventional polymer processing techniques have difficulty in producing fibers smaller than 10 μm in diameter, which are several orders of magnitude larger than the native ECM fibrils diameter which is in the range of 50–500 nm, there has been a concerted effort to develop methods of producing nanofibers to more adequately simulate the ECM geometry. Three distinct techniques have proven successful in routinely creating nanofibrous tissue engineering structures: self assembly [15], phase separation [2], and electrospinning [11, 16].

The drawing is a process similar to dry spinning in fiber industry, which can make one-by-one very long single nanofibers. However, only a viscoelastic material that can undergo strong deformations while being cohesive enough to support the stresses developed during pulling can be made into nanofibers through drawing. The template synthesis, as the name suggests, uses a nanoporous membrane as a template to make nanofibers of solid (a fibril) or hollow (a tubule) shape. The most important feature of this method may lie in that nanometer tubules and fibrils of various raw materials such as electronically conducting polymers, metals, semiconductors, and carbons can be fabricated. On the other hand, the method cannot make one-by-one continuous nanofibers. The phase separation consists of dissolution, gelation, and extraction using a different solvent, freezing, and drying resulting in nanoscale porous foam. The process takes relatively long period of time to transfer the solid polymer into the nano-porous foam. The self-assembly is a process in which individual, pre-existing components organize themselves into desired patterns and functions. However, similarly to the phase separation the self-assembly is time-consuming in processing continuous polymer nanofibers. Thus, the electrospinning process seems to be the only method which can be further developed for mass production of one-by-one continuous nanofibers from various polymers [12] and the formation of a thin fiber via electrospinning is based on the uniaxial stretching (or elongation) of a viscoelastic jet derived from a polymer solution or melt [14].

In a new innovation in the electrospinning for biomedical application, researchers generate new hybrid materials in the platform of nanofibrous scaffolds with specific and desired properties (used the schemes of copolymerization and polymer mixtures). The performance of the

electrospun scaffold can be further controlled by adjusting the diameter and morphology of the nanofibers with desirable 3D patterns (eg., layered structures). For certain applications in tissue engineering, scaffolds with aligned fibers are often more desirable to guide the cell growth with desired anisotropy. It has been reported by Xu et al. [17] that poly(l-lactid-co-ε-caprolactone) [P(LLA-CL)] nanofibrous scaffold with aligned fibrous structure showed human coronary artery smooth muscle cells (SMCs) attached and migrated along the axis of the aligned nanofibers and expressed a spindle-like contractile phenotype. Furthermore, they found the adhesion and proliferation rate of SMCs on the aligned nanofibrous scaffold was significantly improved when compared with those on solid polymer films.

A multilayered electrospinning and/ or mixing electrospinning is a new way to design a 3-D multilayered non-woven nanofibrous mesh, in which a hierarchically ordered structure composed of different polymer meshes could be obtained. In mixing electrospinning, two different polymer solutions were simultaneously electrospun from different syringes under different processing conditions. The spun polymer fibers were mixed on the same target collector, resulting in the formation of mixed fibers mesh. Recently, Kidoaki et al. [18] fabricated composite scaffolds containing different polymer by using multilayer electrospinning and also mixing electrospinning techniques. In their study, three layered scaffolds, containing segmented polyurethane, styrenated gelatin and type I collagen, fabricated by using the multilayered electrospinning technique, and co-mingled nanofibrous scaffold, containing segmented Polyurethane and poly(ethylene oxide), fabricated by using the mixing electrospinning technique had been demonstrated. The multilayered electrospun scaffolds have been further used for controlled drug release system [19] and guided bone regeneration [20].

The two-phase electrospinning process, using a single spinneret, provides a viable means to incorporate small molecules and/or macromolecules, including drugs and proteins in the nanofibrous scaffolds, provided that the molecules could withstand the electrospinning process. The encapsulated bioactive molecules could be immobilized for a long time and then released in a controlled manner. In Sanders and co-workers [21], study, they developed an electrospun fibrous mat, containing distinct two-phase structures by using immiscible polymer solutions such as poly (ethylene-co-vinyl-acetate) in dichloromethane and bovine serum albumin (BSA) in phosphate-buffered saline (PBS). Therefore, the techniques may offer potentially useful advantages over other electrospinning techniques in the applications of drug delivery and tissue engineering.

Scaffolds of either natural or synthetic polymers display certain limitations. Natural polymers, such as gelatin and collagen, have very good biocompatibility for cell adhesion and proliferation, but their mechanical strength is not sufficient to support the scaffold during healing process. On the other hand, synthetic polymers, such as PCL, have very good mechanical properties but the therapeutic effectiveness is not as good as that of natural polymers. Therefore, there is a need to develop a novel structure to overcome these limits for tissue engineered scaffolds. The core-sheath structure is an excellent candidate to solve this problem. By using co-axial electrospinning technology, core-shelled nanofibers can be fabricated. Basically, two polymer solutions were co-electrospun without direct mixing. Recently, Zhang et al. [22] and Han et al [23], developed a biodegradable core-shelled structure with PCL being the shell and gelatin being the core. It showed that, the electrospun core shelled scaffold exhibits better mechanical properties compared to gelatin scaffold [23].

This technique can be particularly useful in producing surface-modified nanofibers, functional nanocomposites and even continuous hollow fibers. Another advantage of the core-shelled fiber is that the shell protects the material in the core during the electrospinning process. This feature is even more attractive when bio-related materials are employed to form nanofibrous scaffolds.

For instance, Jiang et al. [24], electrospun a fiber with poly (ϵ -caprolactone) as the shell and BSA together with dextran and the protection of the shell, BSA was nearly intact during the electrospinning process. A release of BSA in a controlled manner was achieved by the formation of the core-shelled fibers.

1.3 Electrospun Nanofibrous Scaffold to Mimic Natural ECM

Electrospun fibrous scaffold produced from electrospinning techniques are widely used for tissue engineering applications. Native ECMs in different tissues or organs have specifically defined architectures which play important role in determine tissue functions. Previous studies have shown that specific topological architectures of the materials mimicking ECMs could promote favorable biological responses, such as enhanced protein adsorption, as well as enhanced cell adhesion, proliferation and migration [25]. Therefore, efforts have been made to develop electrospun materials with ordered microstructures and patterns [26] by controlling the spatial arrangement of collected nanofibers.

Depending on the materials used and electrospinning conditions, nonwoven fibrous meshes with microscale variation, have been successfully produced. Thus, when deposited as a nonwoven mat, the resulting fabrics are highly porous, i.e., they have a large interconnected void volume in the range of 50% to even greater than 90% and possess one of the highest surface-to-volume ratios among all cohesive porous materials. The entangled fibrous geometry has a pseudo-bicontinuous structure; the pore volume is essentially continuous and interconnected (Figure 1b), whereas woven fabrics compartmentalize the pore volume more regularly (Figure 1a). The mechanical stability of nonwoven structures, which depends on the chemical composition and processing procedure, can be improved further. For example, the crossing points of those fibers can be annealed and attached together (Figure 1c) [27].

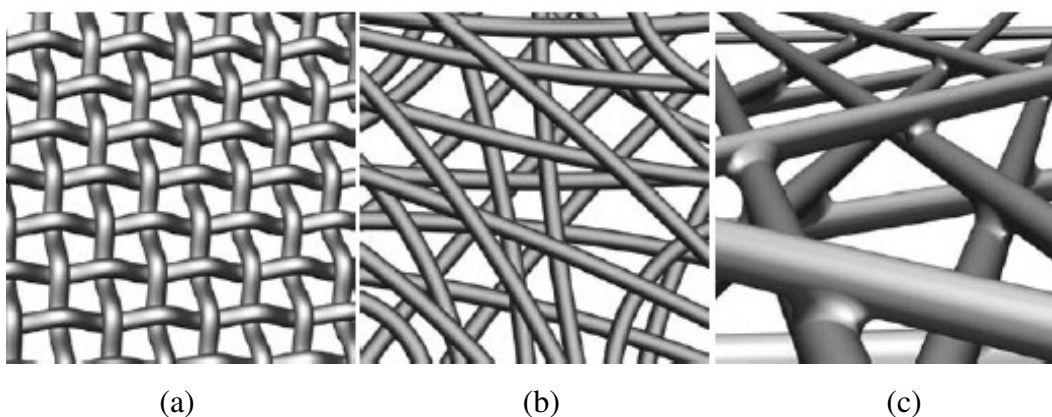


Figure 1 Artistic representations of woven and non woven fabrics. (a) Woven fabrics. (b) Nonwoven fabrics. (c) Non woven electrospun mat with soldered junction.

According to Agarwal et al. 2008 [18], the scaffold architecture is very important and affects cell binding. The cells binding to scaffolds with microscale architecture flatten and spread as if cultured on flat surfaces. The scaffolds with nanoscale architecture have bigger surface area for absorbing proteins and present more binding sites to cell membrane receptors. The adsorbed proteins further can change the conformations, exposing additional binding sites, expected to provide an edge over microscale architectures for tissue generation applications.

Functionalization of nanofiber scaffolds can be achieved through one of three main methods [28]: (1) mixing bioactive agents with the biodegradable polymer solutions to prepare bioactive composite nanofibers, (2) surface modification of the whole nanofibrous scaffolds; or (3) employing a coaxial electrospinning, to produce fibers with core-shell structure. Therefore, it is

essential to develop a system that can deliver drugs/morphogens of interest at the appropriate time, for appropriate duration, and at precise target location.

In particular, many *in vivo* tissues and organs exhibit hierarchical layered structures with distinct ECM composition and arrangement in each layer. These anisotropic properties not only offer the cells with distinct signalling information, but also provide the tissues with a unique mechanical performance to accommodate the physiological requirement. Therefore, it is highly desirable to incorporate these hierarchical features into multiscale design of nanoscaffolds using the electrospun nanofibers. Additionally, the spatial organization of various types of cells in the hierarchically layered tissues is often recognized, which offers the tissue with specialized function for each layer. For instance, two distinct cell layers are identified in the skin, where the epidermal layer (mainly keratinocytes) stays at the outmost region of the skin and is connected to the underneath dermal layer (mainly fibroblasts) via basement membrane. In this regard, it is also preferred for the scaffolds to help the organization of cells with a distinct and controllable spatial distribution. Electrospinning holds a great promise in allowing the bottom-up assembly of various types of cells into layered nanofiber/cells constructs [29].

1.4 The Challenge of Electrical Forces: Electrospinning and Electrospaying Techniques

Electrospinning and electrospaying is a subject of intensive research due to their unique properties and intriguing applications especially in tissue engineering area. Modern electrospinning technology, developed by a number of researchers, is able to make continuous fibers with diameters in the range of nanometers to a few micrometers. However, in electrospaying technology, researchers are competent to produce small droplets or particle which is formed as a result of the varicose break-up of the electrified jet that is often present with a solution of low viscosity. Both of these techniques involve the use of a high voltage to induce the formation of a liquid jet.

Electrospinning has the unique ability to produce nanofibers of different materials and also allow some degree of control over fiber orientation within the scaffold. The motion of the mandrel and focusing of the electrical field during the process provide this control. In this way, electrospinning can be used to fabricate practically any composite structure desired in order to replicate and mimic the ECM of the tissue of interest. The thickness of the scaffolds or

individual layers can also be controlled by simply adjusting the electrospinning time; scaffold thickness can range from a single fiber to several millimeters [11, 12]. The relatively high production rate and simplicity of the setup make electrospinning highly attractive in tissue engineering and drug delivery application.

Electrospraying was used for fine particle production. When a charged droplet evaporates, the fine powder suspended in it forms a tight cluster. For a droplet produced from a solution, the remaining substance crystallises forming a solid particle. The size of such particles can be controlled by changing the concentration of dissolved or suspended substance [30]. This technique had an added advantage of not making use of an external dispersion/emulsion phase which often involves ingredients that are undesirable for biomedical applications [31]. Apart from this, Kumbar et al. employed precision electrospraying and demonstrated its potential in uniform coating of various medical implants to enhance their biocompatibility and efficacy, thus avoiding various nonspecific reactions with the natural body [32].

Nevertheless, challenges using electrospun fibers are generally associated with defining the appropriate cell populations and controlling the effects of matrix composition and signaling on the cells of interest. One of the key factors is to accurately control the fiber deposition, probably in nanometer scale, in order to achieve a more precise mimicking of ECM. Therefore, a further understanding is critical of the mechanisms and key parameters that determine the nanofiber formation and deposition. It will accelerate the development of electrospinning techniques and setups, and electrospun materials will then find more potential applications in the field of tissue engineering and drug delivery. In addition, it is also critical to further understand the cellular reaction to electrospun materials with different composition, fiber orientation and microstructures. Currently, although numerous studies have demonstrated the great potential of electrospun fibrous materials, fewer *in vivo* studies have been carried out.

For drug delivery applications, more sophisticated electrospinning techniques need to be further developed according to the requirements of biomedical applications. The joint efforts from both material scientists and biologists are needed for more interdisciplinary research on the development of electrospun techniques [33]. As the next frontier in nanotechnology research, toxicity concerns of nanomaterials and nanoparticles during manufacturing and/or implantation will be covered as well [34].

1.5 Aim of This Study:

1. To develop and characterize electrospun membranes scaffold from a morphological point of view.
2. To prepare micro/nanospheres using electro spraying techniques for controlled drug delivery
3. To design and develop integrated system of multicomponent PCL fibers/ chitosan particles for periodontal application.

1.6 Summary of Covered Subjects:

This thesis concerns nano- and micro-structures generated by electrostatic processes like electrospinning and electro spraying as powerful tools in medical and pharmaceutical applications, for specific interaction with living cells in a tissue engineering approach and oral drug delivery combined with controlled and retarded drug release.

Chapter 2 gives a brief overview on the history, and theory of electrostatic processes and the state of art in several biomedical applications.

Chapter 3 describes the preparation and characterization of electrospun polycaprolactone fibers and discusses possibilities to control morphology and fibre assembly (i.e, fiber size scale and size distribution, fiber defects, etc.).

Chapter 4 presents the generated monodisperse particles with drug encapsulation by using electro spraying for oral drug delivery and adjusting their release behavior.

Chapter 5 describes a simple and versatile integrated method of electro spraying and electrospinning consisting of PCL nanofiber and chitosan nanoparticles for tissue engineering. Therefore, explanation includes in vitro and cells attachment study.

References

- [1] Langer & Vacanti. **1993**. *Science*. 920-926.
- [2] Barnes, C. P., Sell, S. A., Boland, ED., Simpson, DG., Bowlin, G. L. **2007**. *Adv Drug Deliv Rev*, 59(14),1413-33.
- [3] Hutmacher DW. **2001**. *J Biomat Science Poly Edit 2001*, 2:107-
- [4] Liao, S., Li, B., Ma, Z., Wei, He., Chan, C. & Ramakrishna, S. **2006**. *Biomed. Mater. R45–R53*.
- [5] Mikos, A., Lu, L., Temenoff, JS. & Tessmar, JK. **2004**. *Bioresorbable Polymer Scaffolds Biomaterials science: an introduction to materials in medicine* / edited by Buddy D. Ratner et al 2nd ed. 735-749.
- [6] Flemming, R., Murphy, C., Abrams, G., Goodman, S., and Nealey, P. **1999**. *Biomaterials*. 20, 573.
- [7] Kim, TG. & Park, TG. **2006**. *Tissue Engineering*. 12(2): 221-233.
- [8] Chicurel, M. E., Chen, CS., & Ingber, DE. **1998**. *Curr. Opin. Cell Biol*. 10: 232–239.
- [9] Kanani, A.G. & Bahrami, SH. **2010**. *Trends Biomater. Artif. Organs*, Vol 24(2) 93-25.
- [10] Ashammakhi & Ndreu, A & Yang, Y & Ylikauppila, H & Nikkola, L. **2008**. *Eur J Plast Surg*. (Published Online).
- [11] Pham, Q. P., Sharma, U., Mikos, A. G., **2006**. *Tissue Eng* 12, (5), 297-122.
- [12] Huang, ZM., Zhang, YZ., Kotakic, M., & Ramakrishna, S. **2003**. *Composites Science and Technology* (63) 2223–2253.
- [13] Agarwal, S., Wendorff, J.H. & Greiner, A. **2008**. *Polymer* (49): 5603-5621.
- [14] Li, D. & Xia, Y. **2004**. *Adv. Mater.* 16 (14):251-270.
- [15] Paramonov S E, Jun H W and Hartgerink J D. **2006**. *J. Am. Chem. Soc.* 128 7291–7298.
- [16] Matthews, JA., Wnek, G E., Simpson, DG., Bowlin, G. L., **2002**. *Biomacromolecules*, 232-238.
- [17] Xu, CY., Inai, R, Kotaki, M. & Ramakrishna, S. **2004**. *Biomaterials*. 25: 877–886.
- [18] Kidoaki, S., Kwon IK & Matsuda, T. **2005**. *Biomaterials*. 26: 37-46.
- [19] Okuda, T., Tominaga, K. & Kidoaki, S. **2010**. *Journal Controlled Released*. 258-264.
- [20] Gupta, D., Venugopal. J. Mitra, S., Dev, G. & Ramakrishna, S. **2009**. *Biomaterials*. 30: 2085–2094.
- [21] Sanders, EH., Kloefkorn, R., Bowlin, GL., Simpson, DG. & Wnek, GE. **2003**. *Macromolecules*. 36: 3803-3805.

- [22] Zhang, YZ., Huang, ZM., Xu, XJ., Lim, CT. & Ramakrishna, S. **2004**. *Chemistry of Materials*. 3406-3409.
- [23] Han, D., Boyce, ST. & Steckl, AJ. **2008**. *Mater. Res. Soc. Symp. Proc.* Vol. 1094.
- [24] Jiang, H., Hu, Y. Zhao, P. Li, Y. & Zhu, K. **2006**. *Journal of Biomedical Material Research Part B, Appl. Biomater* 79B: 50-57.
- [25] Li W, Tuli R, Okafor C, Derfoul A, Danielson K, Hall D & Tuan R. **2005**. *Biomaterials* 26: 599.
- [26] Teo W and Ramakrishna S **2006** *Nanotechnology* 17 R89.
- [27] Burger, C., Hsiao, BS. & Chu, B. **2006**. *Annu Rev Mater Res*.36: 333-368.
- [28] Zhang YZ, Venugopal J, Huang ZM, Lim CT, Ramakrishna S. **2005**. *Biomacromolecules*. 6:2583.
- [29] Yang, X., Shah, JD. & Wang, H. **2009**. *Tissue Engineering Part A*.15 (4): 945-956.
- [30] Jaworek. **2007**. *Powder Technology* 176: 18–35.
- [31] Arya, N., Chakraborty, S., Dube, N., Katti, DS. **2008**. *J Biomed Mater Res Part B: Appl Biomater* 88B: 17–31.
- [32] Kumbar SG, Bhattacharyya S, Sethuraman S, Laurencin CTA. **2007**. *J Biomed Mater Res Part B: Appl Biomater*; 81B:91–103.
- [33] Cui, W., Zhou, Y. & Chang, J. **2010**. *J. Sci. Technol. Adv. Mater.* (2) 014108.
- [34] Zhang, L. & Webster, TJ. **2009**. *Nano Today*. 4: 66-80.

CHAPTER 2

Electrospinning: Alternatives Routes towards Nanotechnology

2.1 History at a Glance

The origin of electrospinning as a viable fiber spinning technique is established since early 1930s. Anton Formhals, a quarter century later in 1934, patented an improved version of the electrospinning process and apparatus. His first patents on electrospinning of cellulose acetate from acetone used a fiber collection system that could be moved, allowing some degree of fiber orientation during spinning. He recognized the importance of adequate drying of the fibers prior to the nanofibers being collected on a grounded surface. Since 1944, several patents on improved processes and claimed methods to electrospun even multi-component webs that contain more than one type of nanofiber.

Sir Geoffrey Taylor's contribution in the 1960s towards the fundamental understanding of the behavior of droplets placed in an electric field helped further develop the technique [1]. He studied the shape of the polymer droplet produced at the tip of needle when an electric field is applied and showed that it is a cone and the jets are ejected from the vertices of the cone. This conical shape of the jet was later referred to by other researchers as the 'Taylor Cone' in subsequent literature. By a detailed examination of different viscous fluids, Taylor determined that an angle of 49.3 degrees is required to balance the surface tension of the polymer with the electrostatic forces. The conical shape of the jet is important because it defines the onset of the extensional velocity gradients in the fiber forming process. Peter Baumgarten designed an apparatus with an infusion pump to electrospun acrylic fibers, and discovered that the diameter of fibers could be controlled by the polymer feed rate from the infusion pump.

Although this early work laid down the basic technique of electrostatic spinning, the present understanding of the process is mainly due to more recent work especially that carried out within the last 10–15 years. The recent, surging interest in nanotechnology has engendered renewed

attention to this convenient, economical technology that enables researchers to produce nanofibers for various applications.

2.2 Basic Requirement: Tailoring Polymer Solution Properties.

2.2.1 Polymer Molecular Weight

As polymer chains are made of repeating units, the molecular weight of the polymer is the sum of the molecular weight of the individual monomers. Generally, a higher molecular weight increases the polymer's resistance to solvent dissolution. The molecular weight of the polymer also has a direct influence on its viscosity. There are numerous ways to obtain the molecular weight, M_n (Number average), M_v (Viscosity average), M_w (Weight average) and M_z (z average). M_n is the total weight of the individual molecular weight by the number of molecules. M_n is independent on molecular size but is highly sensitive to small molecules present in the mixture. A typical molecular weight distribution along with these molecular weight averages is shown in Figure 2.1. For a heterogeneous molecular weight system [2], $M_z > M_w > M_n$.

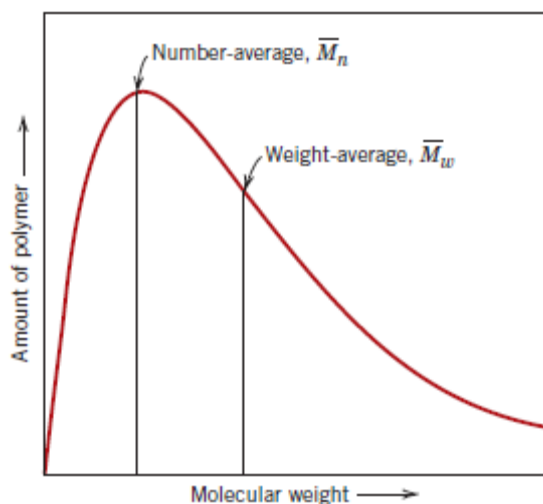


Figure 2.1 Distribution of molecular weights for a typical polymer [3]

2.2.2. Intermolecular and Solvent Interaction in Polymers.

There are two stages when a polymer dissolves in the solvent. Firstly, solvent molecules diffuse slowly into the polymer bulk to produce a swollen gel. If the polymer-polymer intermolecular forces are high as a result of cross-linking, crystallinity or strong hydrogen bonding, the polymer-solvent interactions may not be strong enough to break the polymer-polymer bond. The second stage of solution will only take place when the polymer-polymer bond is broken to give ideal solution [2].

The structure of the polymer has an impact on its solubility in the solvent. Generally, a polymer with higher molecular weight is less soluble and takes a much longer time to dissolve than one with a lower molecular weight using the same solvent. The intermolecular forces between longer chain molecules are stronger and the solvent molecules take a longer time to diffuse into the polymer bulk. Cross linked polymers do not dissolve, as covalent bonding between the molecules is much stronger than the secondary forces exerted from polymer-solvent interactions. [2].

Moreover, the quality of solvent is also need to be considered. With a very good solvent, the solvent-repeat unit interactions are maximized, resulting in a relatively expanded free-draining polymer chain. Typically, a highly polar solvents and higher permittivity values ensured stronger polar interactions among the polymer chains mediated by solvent molecules, producing enhanced stretching of fibers and therefore the formation of thinner fibers [4]. In the other hand, in a very poor solvent, the polymer chains are close to their most compact average conformation, behaving similarly to rigid spheres suspended in solution. Both the expanded and contracted chains, however, behave very differently from ideal chains and the excluded volume effects change with the solvent [5]. In this case, whereas lower concentration of solutions indicates a higher level of solvent molecules and thus reduces the incidence of chain entanglements and also leads to bead formations [4].

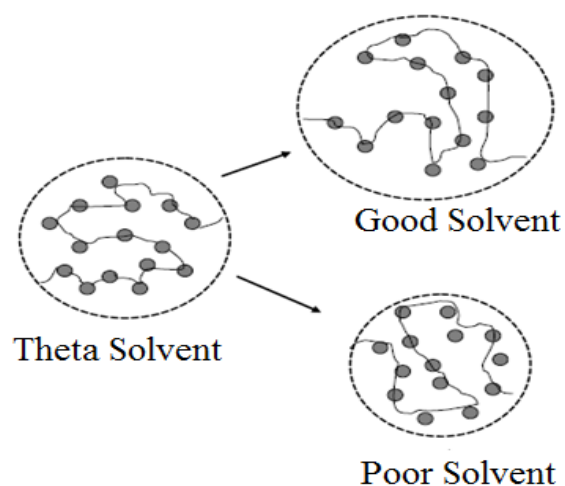


Figure 2.2 Illustration of the effect of solvent quality parameter on chain geometry [5]

2.2.3. Surface Tension

The inhomogeneous organization of the atoms at the surface of a condensed phase causes the phenomenon known as surface tension, γ . The surface tension is the reversible work needed to create a unit surface area in a substance. For a liquid molecule submerged within the solution, there is uniform attractive forces exerted on it by other liquid molecules surrounding it. However, for a liquid molecule at the surface of the solution, there is a net downward force as the liquid molecules below exert a greater attractive force than the gas molecules above as shown in Fig. 2.4. Thus the surface is in tension and this causes a contraction at the surface of the solution, which is balanced by repulsive forces that arise from the collisions of molecules from the interior of the solution. The net effect of the pulling of all the surface liquid molecules causes the liquid surface to contract thereby reducing the surface area. The surface tension is sometimes called the specific surface energy, the intrinsic surface energy, or the true surface energy. Surface tension has the cgs units of ergs/cm², or SI units of J/m². However, since work can be expressed as force times distance, the units are sometimes expressed as dyn/cm or N/m [2, 6]

The initiation of electrospinning requires the charged solution to overcome its surface tension. However, as the jet travels towards the collection plate, the surface tension may cause the formation of beads along the jet. Surface tension has the effect of decreasing the surface area per unit mass of a fluid. In this case, when there is a high concentration of free solvent molecules, there is a greater tendency for the solvent molecules to congregate and adopt a spherical shape

due to surface tension. A higher viscosity will mean that there is greater interaction between the solvent and polymer molecules thus when the solution is stretched under the influence of the charges, the solvent molecules will tend to spread over the entangled polymer molecules thus reducing the tendency for the solvent molecules to come together under the influence of surface tension [2]. The influence of surface tension of solvents in electrospinning is well discussed in the sub chapter 2.5.1.

2.2.4 Conductivity

Conductivity is a measure of electrical conduction and thus a measure of the ability of a material to pass a current. Generally, materials with conductivities less than 10^{-8} S/cm are considered insulators, materials with conductivities between 10^{-8} and 10^3 S/cm are considered semiconductors, and materials with conductivities greater than 10^3 S/cm are considered conductors [7]. For electrospinning process to be initiated, the solution must gain sufficient charges such that the repulsive forces within the solution are able to overcome the surface tension of the solution. Subsequent stretching or drawing of the electrospinning jet is also dependent on the ability of the solution to carry charges [2]. A minimal electrical conductivity in the solution is therefore essential for electrospinning; solutions of zero conductivity cannot be electrospun [3]. Generally, the electric conductivity of solvents is very low (typically between 10^{-3} to 10^{-9} ohm⁻¹m⁻¹) as they contain very few free ions, if any, which are responsible for the electric conductivity of solution. The presence of acids, bases, salts and dissolved carbon dioxide may increase the conductivity of the solvent. The electrical conductivity of the solvent can be increased significantly through mixing chemically non-interacting components. Substances that can be added to the solvent to increase its conductivity includes mineral salts, mineral acids, carboxylic acids, some complexes of acids with amines, stannous chloride and some tetraalkylammonium salts. For organic acid solvents, the addition of a small amount of water will also greatly increase its conductivity due to ionization of the solvent molecules [2]. Recently, composite substrates made of synthesized polyaniline (sPANi) and polycaprolactone (PCL) were investigated as platforms for cardiac tissue regeneration. sPANi composites scaffold are currently utilized as a temporary substrate to stimulate tissue formation by controlled electrochemical signals as well as continuous mechanical stimulation until the regeneration processes are completed. Among them, composites from the blending of conductive (CPs) and biocompatible polymers are powerfully emerging as a successful strategy for the regeneration of

myocardium due to their unique conductive and biological recognition properties able to assure a more efficient electroactive stimulation of cells [7]

2.3 Electric Field Driven Process Technologies

Electrospraying and electrospinning are unique approaches using electrostatic forces to produce fine particles and fibers. Electrospraying and electrospinning are processes by which a polymer solution or melt can be processed into smaller diameter particles and fibers using a high potential electric field. This generic description is appropriate as it covers a wide range of structures with submicron diameters that are normally produced by both processes. If a liquid or melt is subjected to an electrical field of sufficient strength, the shape of a droplet of this material will change into a cone and above a certain critical voltage either electrospraying or electrospinning will occur.

2.3.1 Basic Principles.

Electrostatic atomization occurs when the surface tension of a liquid is overcome by an applied electric field, thereby ejecting tiny droplets from the surface. Polymeric solutions behave differently compared to monomeric liquids during electrostatic atomization in that they persist as elongated jets over a much greater distance [8]. Electrospinning is possible only if there is a potential difference between the solution and the collector. Very often, an external electric field is used to control the charged electrospinning jet. Factors that affect the ability of the solution to carry charges, the electric field that surrounds the electrospinning jet and the dissipation of charges on the polymer fibers that are deposited on the collector will have an impact on the electrospinning process [2].

The region where there is an electric force caused by the presence of electric charges is known as an electric field. The force can either be attraction between opposite charges or repulsion between charges of the same polarity and is given by the Coulomb's Law:

$$F = \frac{q_1 q_2}{4\pi\epsilon_0 d^2} \quad (3)$$

Where;

q is the charge

ϵ_v is the absolute permittivity of the space between the charges

d is the distance between the charges

However, this law is only valid if the charges involved are point charges. In most practical cases, the electric field is more widely used and it is defined as a region where a charge feels a force created by other charges. The magnitude of the field is given by its field strength (4):

$$F=qE \quad (4)$$

Where

F is the force

q is the charge

E is the electric field strength

For a positive charge, the force has the same direction as the field strength while a negative charge will have the force at the opposite direction.

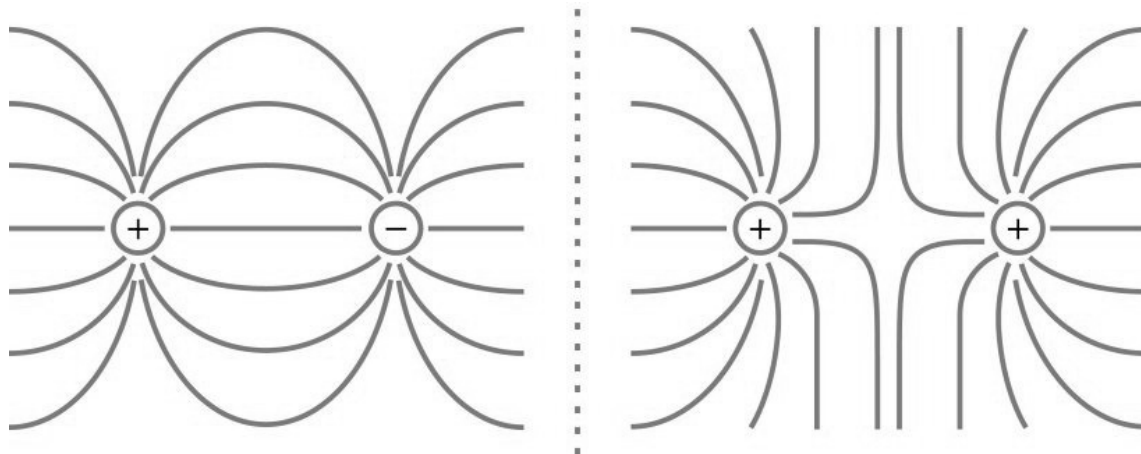


Figure 2.4 Electric flux lines from a source and a sink

In electrospinning, the liquid jet travels across the gap distance from the highly charged tip to the grounded collector plate. It is the presence of a surface charge that is responsible for the

acceleration of the initial jet towards the grounded collector, extending it as by as much as a million times during the short span of travel. In the process, along with mass transfer there is a corresponding charge transfer across the gap. The current flow due to this transfer can be measured and is generally found to increase smoothly with the applied voltage [5].

Theron and colleagues [9] expressed the volume and surface charge densities in terms of I, Q, and d as follows:

Volume charge density

$$q_v = I/Q \quad (5)$$

Surface charge density

$$q_s = q_v (0.25d) \times 10^{-7} \quad (6)$$

where

d (mm) is the diameter of the jet measured just below the Taylor's cone

2.3.2 Electro spraying.

Electrospraying (electrohydrodynamic spraying) is a process of simultaneous droplet generation and charging by means of electric field. Droplets produced by electrospraying are highly charged, that prevents their coagulation, and promotes self dispersion. When a droplet of liquid is subjected to strong electric field, due to mutual repulsion of electrical charges inside the droplet, it changes its shape to conical (cone-jet mode). If the electric field is strong enough, from the cone apex a thin liquid jet emerges, which quickly breaks up into the mist of fine droplets [10, 11]. To achieve a stable cone-jet, a minimum flow rate is required [12]. A diagram of the steps involved in micro- and nano-particle production is shown in Fig. 2.4. Electro spraying allows generation of fine droplets of charge magnitude close to one-half of the Rayleigh limit. The Rayleigh limit is the magnitude of charge on a drop that overcomes the surface tension force that leads to fission of the droplet. The solvent from the electrosprayed droplets evaporates, and the remaining solid material forms a fine powder. The particles are

produced from a solution or suspension of a solid material. For the solution based droplets, the remaining substance crystallizes forming solid particles. When a suspension is used for powder production, the nanosized particles suspended in the solvent form a tight cluster after the droplets dry. The size of such particles can be controlled by changing the concentration of the dissolved or suspended substance. The charge and size of the droplet can be easily controlled to some extent by adjusting the flow rate and voltage applied to the nozzle. Nevertheless, electrospaying allows the generation of particles of small size, down to 10 nm, and of high monodispersity [10,11].

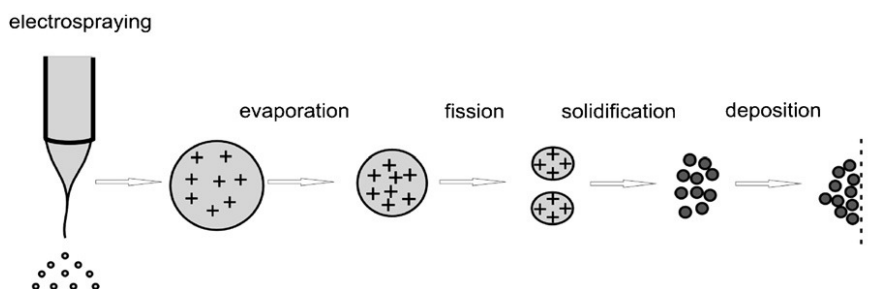


Fig. 2.4. Steps of micro- and nanoparticle production via electrospaying.

The electrospaying has some advantages over conventional mechanical spraying systems with droplets charged by induction [10]:

1. Droplets have size smaller than those available from conventional mechanical atomisers, and can be smaller than 1 μm .
2. The size distribution of the droplets is usually narrow, with low standard deviation; droplets can be of equal size only for dripping and microdripping modes, or for Rayleigh jet breakup due to varicose wave instability.
3. Charged droplets are self-dispersing in the space those results in absence of droplet agglomeration and coagulation.
4. The motion of charged droplets can be easily controlled (including deflection or focusing) by electric fields.
5. The deposition efficiency of charged spray on an object is much higher than for uncharged droplets.

Electrospaying process enables the production of microparticles or nanoparticles in the presence of biomacromolecules and even cells, without denaturing their bioactivity or destroying cell

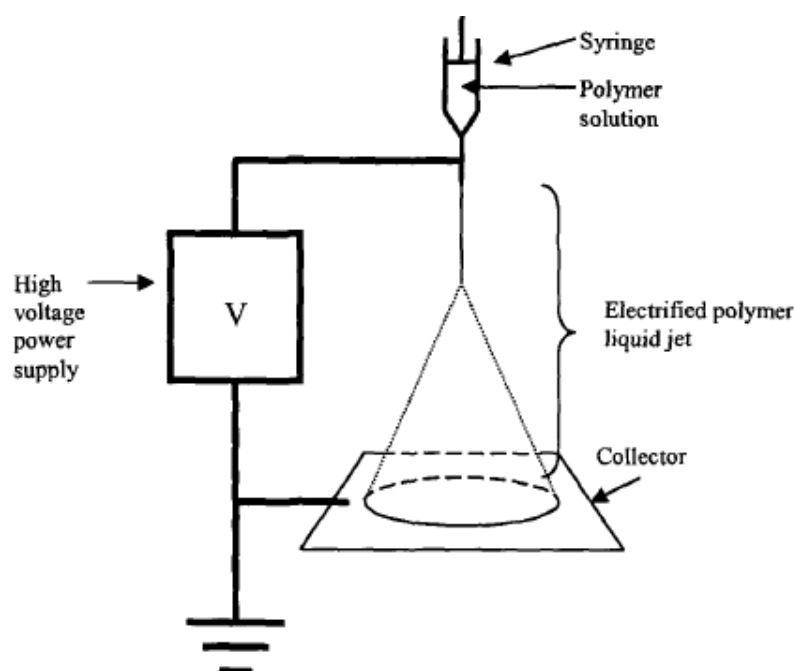
viability. The versatile microfabrication or nanofabrication schemes allow the production of drug delivery systems for a variety of biomedical applications. Arya and co-workers [13] fabricated biodegradable, polymeric chitosan microparticles by electro spraying process. In their works, Ampicilin (drug) was encapsulated with chitosan to produce microspheres and study the potential as delivery vehicles for bioactive agents. The drug loaded particles showed a sustained release over a period of 5 days. The micro/nanoparticles formed by electro spraying contained active drug as demonstrated by the zone of inhibition on *E. coli* lawn. The particles appear to be promising agents for sustained nasal and gastrointestinal tract delivery with the potential for better patient compliance and enhanced control of bacterial pathogenesis. Fantini et. al. [14], synthesized PS microspheres using electro spraying techniques and observed by using low molecular weight PS, microspheres with uniform dimensions and smooth surfaces had been obtained.

2.3.3 Electrospinning

Electrospinning is the process to form nanofibers using electrostatic force, which uniaxially stretches a viscoelastic solution as it solidifies. The electrospinning process that applies a high voltage on a highly viscous polymer solution to form a liquid jet for the initial stage of fiber formation is in the cone-jet mode, followed by the fiber formation in the whipping mode [14]. A long nanofiber thread is formed, and a nanofiber assembly is collected in a grounded collector. Nonwoven, aligned, patterned, or ordered nanofiber assemblies can be obtained in the grounded collector by manipulating the electric field or changing the configuration of the collectors. The diameter of nanofibers is related to the solution properties, including the concentration, viscosity, electrical conductivity of polymer, surface tension of the solvent, and process parameters, including the applied electric field, spinneret tip-to-collector distance, and flow rate.

Basically, a typical set up for electrospinning comprised a polymer solution supply, a high voltage power supply with positive or negative polarity, a capillary tube connected with spinneret (needle) and a conducting collector (a grounded collector). One electrode is attached into the spinneret and the other attached to the collector. The collector can be made of any shape according to the requirements, like a flat plate, rotating drum and etc. A schematic of the electrospinning process is shown in Figure 2.5. Initially, the polymer solution is supplied to the capillary tip in order to form a hemispherical droplet and the feed rate is controlled by a syringe

pump. The surface of a hemispherical liquid drop suspended in equilibrium at the end of a capillary will be distorted into a conical shape in the presence of an electric field. As the electric voltage is increased, the fluid jet ejected from the tip of needle to form a conical shape known as Taylor cone [1]. After the initiation from the cone, the jet undergoes a chaotic motion or bending instability and elongation process, with which allows the jet to become very long and thin. The jet is initially a straight line, then becomes unstable, and undergoes a bending or whipping stage, which is caused by the repulsive interactions between like charges in the electrified polymer jet [15]. Various instability modes that occur during the fiber forming process are expected to occur by the combined effect of both the electrostatic field and the material properties of the polymer. The bending instability of the electrified jet causes a reduction of the diameter of the fiber as the solvent evaporates. A long nanofiber thread is formed, and a nanofiber assembly is collected in a grounded collector. Nonwoven, aligned, patterned, or ordered nanofiber assemblies can be obtained in the grounded collector by manipulating the electric field or changing the configuration of the collectors. The diameter of nanofibers is related to the fluid properties, including the concentration, viscosity, electrical conductivity of polymer, and surface tension of the solvent, and the process parameters, including the strength of the applied electric field, spinneret tip-to-collector distance, and flow rate [16, 17, 18].



Figures 2.5. Illustration of Electrospinning

Important features of electrospinning are [2]:

- i. Suitable solvent should be available for dissolving the polymer.
- ii. The vapor pressure of the solvent should be suitable so that it evaporates quickly enough for the fiber to maintain its integrity when it reaches the target but not too quickly to allow the fiber to harden before it reaches the nanometer range.
- iii. The viscosity and surface tension of the solvent must neither be too large to prevent the jet from forming nor be too small to allow the polymer solution to drain freely from the pipette.
- iv. The power supply should be adequate to overcome the viscosity and surface tension of the polymer solution to form and sustain the jet from the pipette.
- v. The gap between the pipette and grounded surface should not be too small to create sparks between the electrodes but should be large enough for the solvent to evaporate in time for the fibers to form.

2.4 Basic Parameters to Control Fiber Morphologies.

Numerous parameters have been identified in affect on the final properties of the electrospun fibre. These parameters include (a) polymer/solvent system (c) governing variables for process parameters such as voltage, flow rate and working distance, (d) environmental conditions such as solution temperature, humidity and air velocity in the electrospinning chamber [18,19,20].

2.4.1 Polymer/Solvent System

In electrospinning process, foremost thing to go through is the selection of a desirable solvent system as the carrier of a particular polymer for the optimization of nanofibers. Solvent selection is pivotal in determining the critical minimum solution concentration to allow the transition from electro spraying to electrospinning, thereby significantly affecting solution spinnability and the morphology of the electrospun fibres [21]. Selection of solvent primarily determines (a) conformation of the dissolved polymer chains, (b) ease of charging the spinning jet, (c) cohesion of the solution due to surface tension forces and (d) rate of solidification of the jet on evaporation of the solvent. Unlike with droplets of low-molecular-weight liquids or monomers that subdivide into smaller droplets under a strong electric field, polymer solutions undergo a degree of

elongational flow and orientation in an electric field. It is the entanglement of the partially oriented, expanded conformations of polymer chains that makes their electrospinning possible in the first place. Solvents that yield open conformations of polymer chains and those solutions with high solids contents are therefore better suited for electrospinning [5]. For instance, water is suitable solvent for PEO system [22] and tetrahydrofuran (THF) is an excellent solvent for PVC system [23]. However, many researchers preferred to use binary solvent systems which lead to obtain smooth fibers. It had been confirmed by Fong et al. [22] study by added ethanol into the PEO/water system, attributed from the phenomenon of the higher viscosity, lower surface tension, and faster evaporation rate, thus, exhibit smooth fibers with larger diameters. Furthermore, Shenoy et al. [24] also mentioned in their study that by mixing solvents of lower solubility with higher solubility can produce electrospinnable solutions at lower critical concentrations. In the latest study by Luo et al. [21], is proposed to use solubility and spinnability maps drawn on the Teas graph which provide a reasonable guidance for the solubility of binary solvent system for a particular polymer, especially for the prediction of non-solvent and good solvent mixtures.

The effect of the solvent system on the solvent properties such as net charged density, boiling point, solubility parameter, dipole moment, dielectric constant and conductivity of a various solvents had a significance influence on productivity and morphological appearance of electrospun fibers [25, 26]. In addition to the work done by Mit Uppatham et al. [19] that reported by using m-cresol (co-solvent) together with formic acid (solvent) enhanced the viscosity of the mixed solvents while the conductivity values were decreased. Instead of that, a solvent must have high enough values of both the dipole moment and the conductivity and the resulting polymer solutions are high enough boiling point of the solvent (in order to prevent dryness on the tip of needle during the electrospinning [27]).

The formation of beads along the as-spun fibers could be a result of viscoelastic force and also the surface tension upon the reduction of the Coulombic force once the fibers are in contact with the grounded target that drives the formation of the beads [22]. A surface tension has the effect of decreasing the surface area per unit mass of a fluid [2]. Hence, decreased in surface tension of the solvent solution will favored the formation of smooth fibers. As in the study of Fong et al. [22], the addition of Ethanol (co-solvent) makes the solution viscosity higher, and the surface tension lower.

As the ejected charged jet is affected by electrical forces, a polymer solution needs to have high electrical properties such as good dielectric constant to enhance the density of charges at the surface of jet for better stretching and uniform formation of fibers with proper morphology [26]. Higher dielectric constant is related to the dipole moment of solvents and tend to give higher electrical susceptibility of the solutions when they are subjected to an electrostatic field, in turn, help increase the mass throughput of the solutions from a spinneret, therefore reflects the polarity of the molecules [25]. In the Lee et al. [23] works, demonstrated binary solvent system consisted THF (dielectric constant; 7.6 at 25 °C and dipole moment; 1.7 D) and DMF solvent (dielectric constant; 36.7 at 25 °C and dipole moment; 3.8 D) obtained diameters of fibers less than 1 μ m. However, a large difference between the values of the dielectric constant of Polystyrene (PS) and a solvent enhances the difference in the distribution of charges in the solvent-rich and polymer-rich regions [25].

Electrospinning involves stretching of the solution caused by repulsion of the charges at its surface. Thus if the conductivity of the solution is increased, more charges can be carried by the electrospinning jet. The conductivity of the solution can be increased by the addition of ions [2]. In Mit Uppatham et al. [20] work, the addition of inorganic salts (eg, NaCl, LiCl and MgCl₂) resulted in a marked reduction in the viscosity values and a marked increase in the conductivity values. The increase in the fibers diameters with increasing amounts of salt could be a result of the increase in the viscoelastic force (i.e. for fibers obtained from solutions containing NaCl and LiCl) and the increase in the mass flow (due to the increase in the electrostatic force acting on the jet segments) [20]. Demir and co workers [28] also reported an increase in the mass flow with the addition of triethylbenzylammonium chloride to a solution of Polyurethane (PU) in dimethylformamide (DMF).

In fact, the addition of the salt should not change the entanglement number; as it has a positive effect on the electrospinning number. Thus, the electrical energy is increased [24]. Beads formation will occur if the solution is not fully stretched. Therefore, when a small amount of salt or polyelectrolyte is added to the solution, the increased charges carried by the solution will increase the stretching of the solution. As a result, smooth fibers are formed which may otherwise yield beaded fibers [2].

The amount of evaporating solvent is determined by a number of factors: the boiling point of the solvent, the initial concentration of the solution, the solution and the ambient temperatures, the diameter of the charged jet which continuously decreases during its flight to the target and the total path length the charged jet travels from the nozzle to the target which significantly depends on the extent of the bending instability that occurs [29,30]. In Lee et al. [23] study, THF with low boiling point (65°C) was rapidly evaporated after the splaying and splitting of an unstable jet, but for the solutions prepared from a mixed solvent of THF and DMF, the jet become stable due to the DMF higher boiling point (153°C). Moreover, in Wannatong et al. [25] study, they found that ‘dryness’ of the charged jet developed and mainly controlled by the amount of solvent that can evaporate during the flight of the charged jet to the target. The ‘dryness’ was found to increase as the density and the boiling point of the solvents decrease. Consequently, the ‘dryness’ halted the production of fibers. However, if the boiling point is such a high, the charged jet from the solution did not have enough time to ‘dry’ prior to depositing on the target. The ‘rather wet’ depositing jet then fused with adjacent depositing jets to form the blobs of solution observed in Mit Uppatham et al. [19] experiments.

2.4.2 Molecular Weight and Viscosity

As mentioned in Chapter 2.2.1, one of the factors that affect the viscosity of the solution is the molecular weight of the polymer. Generally, when a polymer of higher molecular weight is dissolved in a solvent, its viscosity will be higher than solution of the same polymer but of a lower molecular weight. One of the conditions necessary for electrospinning to occur where fibers are formed is that the solution must consists of polymer of sufficient molecular weight and the solution must be of sufficient viscosity [2]. In fact, the molecular weight of the polymer represents the length of the polymer chain, which in turn has an effect on the viscosity of the solution since the polymer length will determine the amount of entanglement of the polymer chains in the solvent [2]. Therefore, at low viscosity values (low degree chain entanglements), the viscoelastic force was comparatively smaller than the Coulombic force. This resulted in the over-stretching of a charged jet, hence the break-up of the charged jet into many small spherical droplets as a result of the surface tension [19]. When the concentration is too low, electrospaying can be occurred [31]. Therefore, it is really important to require a sufficient level of intermolecular interaction that will help to damp the fluid instabilities and prevent jet break-up. Fong et al. [22] observed a bead-on-a-string morphology. The reason for this is that the

coiled macromolecules of the dissolved polymer are transformed by the elongation flow of the jet into oriented, entangled networks that persist as the fiber solidifies. The contraction of the radius of the jet, which is driven by surface tension, causes the remaining solution to form beads.

Though, it is slowly becoming more spindle-like and merging into the fiber as the concentration increases. An increase in the solution concentration resulted in an increase in the solution viscosity, hence an increase in the viscoelastic force (from the Coulombic repulsion) [20,27]. Indeed, the charged jet did not break up into small droplet, a direct result of the increased chain molecular entanglements (and hence an increase in the viscoelastic force) which were sufficient to prevent the break-up of the charged jet and allow the Coulombic stress to further elongate the charged jet during its flight to the grounded target [8]. It is well known that the fiber diameter increase with polymer concentration [19,28].

2.4.3 Processing Parameters

- Applied Voltage

The applied voltage is one of the important parameters in electrospinning and had been confirmed by many authors [2,16,24,31,32]. In fact, the spinning current is founded to increase with increasing voltage [30]. In the study of Jaruwannasapoom et al. [27] showed that when the number of charge carriers in a jet segment increased, the electrostatic and the Coulombic forces (voltage) also increased. The voltage will induce the charges on the solution and charge transport across the gap between the charged needle and the electrically grounded target. The only mechanism of charge transport is the flow of polymer from the tip to the target. Thus, an increase in the electrospinning current generally reflects an increase in the mass flow rate from the capillary tip to the grounded target [2,31]. Taking into the account, the applied voltage was proportionally decreased with deposition distance [8]. At lower applied voltages the Taylor cone formed at the tip of the pendant drop; however, as the applied voltage was increased the volume of the drop decreased until the Taylor cone was formed at the tip of the capillary, which was associated with an increase in bead defects. Indeed, an increase in applied voltage (above critical voltage) is depended on the number of charge carriers in a jet and caused a change in the shape of the jet initiating point (instability mode), increased the deposition rate and hence the structure and morphology of fibers (bead defects) [16,27,31]. In more detailed, Buchko et al. [8] had observed a decreased in the fiber diameter with an increase in the applied voltage. Though, based

on the work by Deitzel et al. [31], and others it is evident that there is an optimal range of electric field strengths for a certain polymer/solvent system, as either too weak or too strong a field will lead to the formation of beaded fibers.

- Flow Rate

The flow rate of the polymer influences the jet velocity and the material transfer rate. Taylor 1969 recognized that the cone shape at the tip of the capillary cannot be maintained if the flow of solution through the capillary is insufficient to replace the solution ejected as the fiber jet. Therefore, flow rate had been used as a control parameter for stabilization of the Taylor cone as in the Shin et al. [33] experiments. In the work of Yuan et al. [34], observed a low flow rate was shown to form very thin and dry fibers because the solvent have more time to evaporate promptly avoid a bead formation. However, Shin et al. [33], demonstrated with increased flow rates the fibers became much thicker and beads-on-a-string fibers were formed. It also been confirmed by Megelski et al. [35], both fiber diameter and pore size increase with increasing flow rate. Theron et al. [32] confirmed that the volume charge density decreased with increasing flow rate for all the solution tested in their experiments. Additionally, at high flow rates significant amounts of bead defects were noticeable, due to the inability of fibers to dry completely before reaching the collector. In complete fiber drying also leads to the formation of ribbon shaped fibers [35].

- Deposition Distance

The structure and morphology of electrospun fibers is easily affected by the nozzle to collector distance because of their dependence on the deposition time (total flight time), evaporation rate and bending instability. Buchko et al. [8] examined the morphological change occurred upon decreasing the distance collector. In their study showed that reduced collector distance produces wet fibers and beaded structures, from round to flat shape. The same phenomenon also observed by Megelski et al. [35], a bead formation in electrospun PS fibers, which attributed to inadequate drying of the polymer fiber prior to reaching the collector. As such in some cases increasing the working distance results in thinner fibers [30] due to more time for the bending instability to develop and hence more time for the solvent to evaporate [34] so the jet have enough time to be stretched. Even, use a volatile solvent (eg, formic acid; b.p 100 °C) required less deposition distance to form a solid product under ambient conditions [8].

On the other hand, the working distance together with the electrostatic potential can effect on the strength of the electric field. It had been studied by Buchko et al. [8] that lower deposition distances required lower applied voltages to create sufficient field strength. Otherwise, too long or too short of a distance collector can cause electric field being too weak or strong thus affect the morphology of fibers.

- Environmental Conditions.

Few studies focused on the effects of ambient parameters like humidity, temperature, atmosphere composition and pressure on electrostatic processes. The morphology of the electrospun fibers is also affected by the percentage of humidity. The surface of the electrospun fibers tends to form pores if the humidity is above a certain percentage. This could be attributed to the water on top of the fiber surface. As the humidity increases, the pores on the surface of the fibers also increase due to the evaporation of water [35,36]. Increasing the humidity resulted in the appearance of small circular pores on the surface of the fibers; increasing the humidity further leads to the pores coalescing.

Mit-Uppatham et al. [20] spun polyamide-6 fibers at temperatures ranging from 25 to 60°C. They found that increasing the temperature yielded fibers with a decreased fiber diameter, and they attributed this decline in diameter to the decrease in the viscosity of the polymer solutions at increased temperatures. The study by Kim et al. [37] found that increasing the local temperature resulted in the solvent evaporating faster and provided a simple solution to solvents with a low rate of evaporation. For excessively volatile solvents the Taylor cone will dry out. It is possible to introduce a local flow of gas saturated with the solvent around the cone to prevent evaporation at the cone [38]. Spinning has also been performed under vacuum in order to obtain higher electric fields; doing so produced fibers and yarns with larger diameters [29].

2.5 Electrospun/Electrosprayed Devices in Drug Delivery Applications.

There has been extensive research on drug delivery by biodegradable polymeric devices since bioresorbable surgical sutures entered the market two decades ago. Among the different classes of biodegradable polymers, the thermoplastic aliphatic poly(esters) such as poly (lactide) (PLA), poly (glycolide) (PGA), and especially the copolymer of lactide and glycolide referred to as poly

(lactide-co-glycolide) (PLGA) have generated tremendous interest because of their excellent biocompatibility, biodegradability and mechanical strength. They are easy to formulate into various devices for carrying a variety of drug classes such as vaccines, peptides, proteins and macromolecules. Most importantly, they have been approved by the United States Food and Drug Administration (FDA) for drug delivery.

In a drug delivery system, size of therapeutic agents is one of the important key factors for a need of an appropriate dosage of therapeutic agents to be function at the right time and a right location. In general, the smaller the dimensions of the drug and the coating material required to encapsulate the drug, the better the drug to be absorbed by human being [18]. Hence, polymeric microstructured or nanostructured (nanofibers and nanoparticles) systems show a great potential to stabilize therapeutic agents and had overcome transport barriers by controlled the size and surface properties. In many therapeutic programs, it is desirable to provide for slow release of a drug to the body at a constant rate over a prolonged period of time. Ideally, such a rate release has zero order time dependence, that is, the rate of release is independent of time. The simplest configuration of a controlled release device is where a drug is either dissolved in high concentration or suspended as particles in a monolithic polymer such as a cylindrical polymer. The release of the drug from it may occur via: (1) Diffusive transfer through the polymer matrix to the surrounding tissue. (2) Release of the dissolved or suspended drug due to slow biodegradation or erosion of the surface layers of the polymer (3) Slow release of covalently bonded drug via hydrolytic cleavage of the linkages and (4) Rapid delivery of the drug due to dissolution of the polymer [5]

The design and fabrication of specific drug delivery system using an electrostatic generator to produce therapeutic agent is a new approached. A high-voltage electric field can be imposed on a polymer liquid to produce nanoparticles through electrospraying or nanofibers through electrospinning process. The addition of an electric field results in charging the components of the system and the resulting electrostatic interactions. Because electrostatic forces become meaningful at the nanoscale, electrostatic technologies attract much attention in microfabrication or nanofabrication [5,12].

Nanoparticles had become an important area of research in the field of drug delivery because they have the ability to deliver a wide range of drugs to varying areas of the body for sustained

periods of time. Nanoparticles had a further advantage over larger microparticles, because they are better suited for intravenous delivery. The smallest capillaries in the body are 5-6 μm in diameter. The size of particles being distributed into the bloodstream must be significantly smaller than 5 μm , without forming aggregates, to ensure that the particles do not form an embolism. Clearly, a wide variety of drugs can be delivered using nanoparticulate carriers via a number of routes. Nanoparticles can be used to deliver hydrophilic drugs, hydrophobic drugs, proteins, vaccines, biological macromolecules, etc. they can be formulated for targeted delivery to the lymphatic system, brain, arterial walls, lungs, liver, spleen or made for a long-term systemic circulation. Therefore, numerous protocols exist for synthesizing nanoparticles based on the type of drug used and the desired delivery route. Once a protocol is chosen, the parameters must be tailored to create the best possible characteristic for the nanoparticles. Four of the most important characteristics of nanoparticles are their size, encapsulation efficiency, zeta potential (surface charge) and release characteristics [39].

Meanwhile, electrospun nanofibers can be designated as a carrier with therapeutic drugs as well. Thus, the electrospun polymer nanofibers with pharmaceutical compositions (drugs) are expected to enhance the dissolution rate of drugs with poor water solubility. Electrospinning of solutions of drugs in polymers is expected to generate nanofibers having very large surface area. This extremely high surface area has profound influence on the bioavailability of a poorly soluble drug, since it is known that the increased surface area can lead to increased dissolution rate. A suitable dosage form, such as oral or parenteral, including aerosols, may be designed by judicious selection of polymeric carriers in terms of their physico-chemical properties as well as their regulatory status. Other pharmaceutically acceptable excipients may be included to ameliorate the stabilization and/or de-agglomeration of the drug nanoparticles. Electrospun pharmaceutical dosage forms may be designed to provide rapid, immediate, delayed, or modified dissolution, with sustained and /or pulsatile release characteristics since the principle of dissolution rate of a particulate drug increases with increasing surface area of both, the drug and the corresponding carrier if needed [18,40].

Using the electrospraying or electrospinning techniques a number of different drug loading methods had been utilized such as coatings, embedded drug and encapsulated drug (coaxial and emulsion electrospinning). These techniques can be used to give finer control over drug release kinetics [40]. Therefore, in a drug delivery system, nanoparticles and nanofibers are considered

as a potential drug carrier [2]. In this subchapter, will be reviewed recent work on the use of nanofibers and nanoparticles in a major noninvasive routes of administration specifically oral and the others drug delivery.

2.5.1 Oral Drug Delivery

Oral drug delivery is the most convenient route for drug administration. It is noninvasive and has good patient compliance. However, the bioavailability of macromolecules is limited because of gastrointestinal degradation and epithelial barriers. After oral administration, bioactive macromolecules need to survive the hostile gastrointestinal environment (pH acidic), adhere to intestinal cells and have efficient uptake by the epithelium followed by the systemic circulation and tissue distribution. Therefore, there is a great need in oral delivery of protein and peptide drugs, suitable devices for delivering the therapeutic agent incorporated microspheres selectively in the intestine [12]

Up to date, Zhang et.al [42] had used co-axial electrospray deposition as a promising formulation technology for oral delivery of poorly water-soluble drugs. In his experiments, a coreshell particles composed of griseofulvin and poly(methacrylic acid-co-methyl methacrylate) (Eudragit L-100), with a diameter of around 1 μm had been produced. The drug phase was in an amorphous state when the griseofulvin core was coated with the Eudragit L-100 shell. The in vitro dissolution and in vivo oral absorption studies revealed that the coreshell formulation significantly improved dissolution and absorption behaviors, presumably because of a reduction in particle size, improvement in dispersity, and amorphization. Results demonstrated that coaxial electrospray deposition possesses great potential as novel formulation technology for enhanced oral absorption of poorly water-soluble drugs.

Moreover, chitosan is a promising polymer for colon drug delivery since it can be biodegraded by the colonic bacterial flora and it has mucoadhesive character. Hence, there was a report of chitosan encapsulated with ampicillin by using electrospraying process. The average particle size of micro/nanospheres was 520 nm with zeta potential of 128.2 mV and encapsulation efficiency of 80.4%. The particles were characterized for drug release kinetics and results demonstrated an initial burst release followed by a sustained release over a period of 120 h. Further, antibacterial activity of drug loaded micro/nanospheres demonstrated that the encapsulated drug was in its active form post exposure to high voltage during electrospraying. The particles appear to be

promising agents for sustained nasal and gastrointestinal tract delivery with the potential for better patient compliance and enhanced control of bacterial pathogenesis [13].

Meanwhile, Bolgen et al. [43] examined PCL electrospun fiber loaded with a commercial antibiotic (Biteral[®]) for preventing abdominal adhesion. Adhesion was then examined in vivo using a rat model with defects in the abdominal wall in the peritoneum. Therefore, it's noted that the antibiotic containing electrospun PCL mat seemed to improve and accelerate the healing process as compared to the control and the unloaded PCL mat.

A work by Buschle Diller et al. [44], focuses on poly(L-lactic acid) (PLA) and poly(ϵ -caprolactone) (PCL) incorporating three different model antibiotics as well as bicomponent fibers made from PLA and PCL containing Tetracycline and chlorotetracycline hydrochloride, and amphotericin B as model drugs. Tetracycline was discharged from PCL at the highest rate while amphotericin B was slowest. PCL almost completely liberated any of the drugs over time while PLA only released about 10% total. By forming bicomponent PCL–PLA fibers surface and release characteristics could be modified to fit a sensible oral drug delivery specific in periodontal application.

Kenawy et al. [45] examined the release of tetracycline hydrochloride from electrospun mats composed of PLA, poly(ethylene-co-vinyl acetate) (PEVA), and a 50:50 blend of the two for periodontal disease application. In his study, both polymer composition and drug loading affected the rate of drug release with PEVA demonstrating quicker release than either the 50:50 PEVA/PLA blend or PLA. Additionally, the electrospun PEVA and 50:50 PEVA/PLA mats gave a relatively smooth release over a period of 5 days, while eliminating the initial burst seen with the films.

In Bottino et al. [46] study fabricated a novel, spatially designed and functionally graded periodontal membrane with osteoconductive/inductive behavior provided by nano-sized hydroxyapatite particles and metronidazole to combat periodontal pathogens. This electrospun FGM holds promise in terms of mechanical integrity, biodegradability and cell–membrane interactions. The advantages of the processing route employed in this study (multilayered electrospinning), such as mechanical and chemical tailoring, open an interesting route for the development of membranes with more predictable physico-chemical, mechanical and biological characteristics that could ultimately lead to enhanced periodontal regeneration.

2.5.2 Other Examples of Drug Delivery System

Recent work has examined the possibility of using nanoparticles and nanofibers as constructs for giving controlled release of a number of drugs including antibiotic and anticancer drugs; as well as protein carrier and DNA for applications in tissue engineering.

Taepaiboon et al. [47] had reported that mats of PVA nanofibers loaded with water insoluble drugs naproxen (NAP) and indometacin (IND), freely water soluble sodium salicylate were successfully prepared by the electrospinning process and were developed as carriers of drugs for a transdermal drug delivery system. Therefore, the drug loaded electrospun PVA mats exhibit better release characteristic of four model drugs than drug loaded as cast films.

Foremost, drug delivery field with the targeted and controlled delivery of anticancer drugs had been striving in a research world. The electrospun fibers had the ability to overcome drug loading limitations seen with other drug delivery devices, such as micelles and liposomes, and currently used for targeting tumors [41]. Therefore, Xu et al. [48] examined the incorporation of the anticancer drug BCNU into electrospun PEG-PLLA mats. The average fiber diameters depended on drug loading with values ranging from 690 to 1350 nm for drug loadings of 5 and 30 wt%, respectively. Both the release rate and the initial burst release increased with increasing BCNU loading. The effect of BCNU release from electrospun PEG-PLLA mats on the growth of rat Glioma C6 cells was also examined. While unloaded PEG-PLLA fibers did not have any effect on cell growth, BCNU loaded PEG-PLLA mats exhibited anticancer activity over a period of 72 h, while free BCNU began to lose its anticancer activity after 48 hours. Thus, by embedding the drug in the polymer fibers, protect it from degradation and preserve its anticancer activity.

While drug delivery is often associated with the delivery of therapeutic agents for the treatment of some disease state such as cancer, it can also apply to the delivery of bioactive agents such as proteins and DNA for tissue engineering applications. While the size scale and topography of electrospun nanofibers can help aid in cell attachment and proliferation due to their close approximation to the extracellular matrix, the ability to control the spatial and temporal delivery of bioactive agents can further augment the scaffolds ability to promote cell attachment, proliferation and differentiation [41].

Xie & Wang [49] had produced polymeric protein microparticles by using electrospinning in the cone-jet mode. In their study, Bovine serum albumin (BSA) was used as a model protein and dispersed in poly(lactide-co-glycolide) (PLGA) solution. Driven by a well-defined electrostatic potential difference between the nozzle and a ring electrode, BSA-PLGA emulsion was ejected from the nozzle and then broken up into monodispersed droplets. Microparticles were collected by evaporation of solvent during electrospinning process. These protein microparticles are about 20 μm in diameter, with an evenly distributed density of protein. These microparticles can realize the sustained release for more than a month while maintaining 80% of the bioactivity.

Liang et al. [50] examined the incorporation of DNA into electrospun PLGA scaffolds. Plasmid DNA was condensed in a poor solvent mixture, and then encapsulated in micelles composed of a triblock copolymer (PLA-PEG-PLA) giving encapsulated DNA nanoparticles. The micelles were then dissolved in a solution of DMF with PLGA and electrospun, resulting in the formation of PLGA fibers containing encapsulated DNA nanoparticles. The DNA was encapsulated in the PLA-PEG-PLA triblock copolymer in order to protect it from degradation during electrospinning with the PLGA copolymer. An in vitro release study demonstrated that approximately 20% of the encapsulated DNA was released after a period of 7 days.

References

- [1] Taylor, G. **1969**. *Proceedings of the Royal Society of London A: Mathematical, Physical & Engineering Sciences*, 313, 453-475
- [2] Ramakrishna, S., Fujihara, K., Teo, WE., Lim, TC & Ma, Z. **2005**. *An Introduction to Electrospinning and Nanofibers*. World Scientific Publishing Co.
- [3] Callister, WD. **2007**. *Materials Science and Engineering: An Introduction, 6th Edition*. John Wiley & Sons, Inc.
- [4] Guarino, V., Cirillo, V., Taddei, P., Alvarez, MA. & Ambrosio L. **2011**. *Macromolecular Science Journal* [DOI: 10.1002/mabi.201100204].
- [5] Andrad, A. L. **2008**. *Science and technology of polymer nanofibers*. John Wiley & Sons.
- [6] Sperling, L. H., **2006**. *Introduction to physical polymer science*. John Wiley & Sons, Inc.

- [7] Boriello, A., Guarino, V., Schiavo, L., Alvarez, MA & Ambrosio, L. **2011**. *J Mater Sci: Mater Med* 22:1053–1062.
- [8] Buchko C.J., Chen, LC., Shen, Y., Martin, DC. **1999**. *Polymer* (40) 7397–7407.
- [9] Theron, A., Zussman, E. & Yarin AL. **2001**. *Nanotechnology* (12) 384–390
- [10] Jaworek, A. & Sobczyk, AT. **2008**. *J. Electrostat.* 66 (3–4) (2008) 197–219.
- [11] Jaworek, A., Krupa, A., Lackowski, M., Sobczyk, AT., Czech, T., Ramakrishna, S., Sundarrajan, S., Pliszka, D. **2009**. *Journal of Electrostatics* (67) 435–438.
- [12] Xie, Y. & Castracane, J. **2009**. *IEEE Engineering in medicine and biology Magazine*. Jan/February. 23-30.
- [13] Arya, N., Chakraborty, S., Dube, N., Katti, DS. **2008**. *J Biomed Mater Res Part B: Appl Biomater* 88B: 17–31,
- [14] Fantini, D., Zanetti, M. & Costa, L. **2006**. *Macromolecular Rapid Communications* 27(23): 2038–2042.
- [15] Yarin, AL., Koombhongse, S & Reneker, DH. 2001. *J. Appl. Phys.*, 89 (5) 3018-3026
- [16] Subbiah, T., Bhat, GS., Tock, RW., Parameswaran, S. & Ramkumar, S. 2005. *Journal of Applied Polymer Science*, Vol. 96, 557–569.
- [17] Theron, A., Zussman, E. & Yarin, AL. **2004**. *Polymer*, 45 (6): 2017-2030.
- [18] Huang, ZM., Zhang, YZ., Kotakic, M., & Ramakrishna, S. **2003**. *Composites Science and Technology* (63) 2223–2253.
- [19] Mit-uppatham, C., Nithitanakul, M. & Supaphol, P. **2004**. *Macromol. Symp.* (216) 293-299.
- [20] Mit-uppatham, C., Nithitanakul, M. & Supaphol, P. **2004**. *Macromol. Chem. Phys.* (205) 2327.
- [21] Luo, C.J., Nangrejo, M. & Edirisinghe, M. **2010**. *Polymer* (51) 1654–1662.
- [22] Fong, H., Chun, I. & Reneker, DH. **1999**. *Polymer* (40) 4585–4592.

- [23] Lee, K.H., Kim, H.Y., La, Y.M., Lee, D.R & Sung, N.H. **2002**. *J.PolymSci Part B: Polym Phys* 40: 2259-2268.
- [24] Shenoy, S.L., Batesa, W.D., Frisch, H.L. & Wnek GE. **2005**. *Polymer* (46) 3372–3384.
- [25] Wannatong, L., Sirivat, A. & Supaphol, P. **2004**. *Polym Int* 53:1851–1859.
- [26] Kanani, A.G. & Bahrami, S.H. **2011**. *Journal of Nanomaterials*.1-10.
- [27] Jarusuwannapoom T., Hongrojjanawiwat, W., Jitjaicham, S., Wannatong, L., Nithitanakul, M., Pattamaprom, C., Koombhongse, P., Rangkupan, P., Supaphol, P. **2005**. *European Polymer Journal* (41) 409–421.
- [28] Demir, M.M., Yilgor, I., Yilgor, E. & Erman, B. **2002**. *Polymer*. 43(11) 3303-3309.
- [29] Reneker, D.H. & Chun, I. **1996**. *Nanotechnology*. (7) 216.
- [30] Reneker, D.H., Yarin, A.L. & Fong, H & Koombhongse, S. **2000**. *Journal of Applied Physics* 87 (9) 4531-4547.
- [31] Deitzel, J.M., Kleinmeyer, J., Harris, D. & Tan, N.C.B. **2001**. *Polymer* 42 26-272.
- [32] Theron, S.A., Zussman, E. & Yarin, A.L. **2004**. *Polymer* 45 2017-2030.
- [33] Shin, Y.M., Hohman, M.M., Brenner, M.P. Rutledge M.P. **2001**. *Polymer* (42) 9955-9967.
- [34] Yuan, X., Zhang, Y., Dong, C & Sheng, J. **2004**. *Polym Int* 53:1704–1710.
- [35] Megelski, S., Stephens, J.S., Chase, D.B & Rabolt, J.F. **2002**. *Macromolecules* 35: 8456-8466
- [36] Casper, C.L., Stephens, J.S., Tassi, N.G. Chase, D.B & Rabolt, J.F. **2004**. *Macromolecules*, 37:573-578.
- [37] Kim, S.J., Lee, C.K. & Kim, S.I. **2005**. *J Appl Polym Sci* 96: 1388–1393.
- [38] Larsen, G., Spretz, R. & Velarde-Ortiz, R. **2004**. *Advanced Materials* 16 (2):166–169.
- [39] Hans, M.L., Lowman, A.M. **2002**. *Current Opinion in Solid State and Materials Science* (6) 319–327.

- [40] Ignatious, F., Sun, L., Lee, CP. & Baldoni, J. **2010**. *Pharmaceutical Research*, 27 (4); 576-588.
- [41] Sill, TJ. & Recum, H.A. **2008**. *Biomaterials*. (29) 1989-2006.
- [42] Zhang, S., Kawakami, K., Yamamoto, M., Masaoka, Y., Kataoka, M., Yamashita, S. & Sakuma, S. **2011**. *Mol. Pharmaceutics* (8) 807–813.
- [43] Bolgen N, Vargel I, Korkusuz P, Menciloglu YZ, Piskin E. **2007**. *J Biomed Mater Res B Appl Biomater* 81(2):530-543.
- [44] Buschle-Diller, G., Cooper, J., Xie, Z., Wu, Y., Waldrup, J. & Ren X. **2007**. *Cellulose* 14:553–562.
- [45] Kenawy, ER, Bowlin GL, Mansfield K, Layman J, Simpson DG, Sanders EH. **2002**. *J Control Release* (81): 57-64.
- [46] Bottino, MC., Thomas, V. & Janowski, GM. **2011**. *Acta Biomaterialia* (7): 216–224.
- [47] Taepaiboon, P., Rungsardthong, U. & Supaphol, P. **2006**. *Nanotechnology* (17): 2317–2329.
- [48] Xu, X., Chen, X., Xu, X., Lu, T., Wang, X. & Yang, L. **2006**. *J Control Release*. 12; 114(3):307-316.
- [49] Xie, J. & Wang, CH. **2007**. *Biotechnol. Bioeng.* 97(5) 1278–1290.
- [50] Liang D, Luu YK, Kim K, Hsiao BS, Hadjiargyrou M, Chu B. **2005**. *Nucleic Acids Res* 33(19):170.

CHAPTER 3

Investigation of PCL Electrospun Membranes: Effect of Co-Solvent and Process Parameters

3.1 Introduction

Electrospinning or ‘electrostatic spinning’ is a unique technology and most convenient for nanofiber production. Well known as a simple process, elegant, reproducible, continuous and scalable technique. It is possible to fabricate fibers in the diameter range of ~ 3 nm– 6 μ m and several meters in length using the same experimental set-up. This process involves the subjecting of a polymer solution in a capillary to an electric field generated by high voltage differences. When the generated electric field exceeds the surface tension of the polymer solution, ejection of a polymer jet occurs. This polymer jet is targeted towards a grounded collector. Enroute to the collector plate, the polymer jet loses stability, leading to the stretching of the jet, with solid fibers deposited on the collector in the form of a nonwoven fabric. By the adjustment of solution and operating parameters, fiber diameter and porosity of fiber mats can be controlled during electrospinning [1-6], which makes this a promising technique for fabrication of tissue-engineered scaffolds. Further details of the physical phenomena governing the electrospinning process can be found in Chapter 2.

In an effort to minimize the instability due to the repulsive electrostatic forces, the jet elongates to undergo large amounts of plastic stretching that consequently leads to a significant reduction in its diameter and results in ultra-thin fibers. The resulting films from these nanoscaled fibers (nanofibers) have very large ratios of surface area to volume and very small pore sizes [7]. Due to special characterization of electrospun mat (high surface area to volume ratio, flexibility in surface functionalities, and mechanical properties superior to larger fibers), many research [1-8] have been performed to improve some potential applications of nanofibers included tissue engineering scaffolds, filtration devices, sensors, materials development, electronic applications and etc.. There is a strenuous interest in electrospun tissue engineered scaffold due to its great potential to pattern the native extracellular matrix (ECM). The basic requirements for a material

to be used for tissue engineering purposes is biocompatibility, although during the past two decades significant advances have been made in the development of biodegradable polymer so biodegradability is one of the most important properties, as the scaffold should degrade with time and be replaced with newly regenerated tissues. Nair and Laurencin [9] classified the most applicable ones: i.e. Poly(α -ester)s, especially lactic acids, glycolic acids and their copolymers with poly-caprolactone, which are the most commonly known and used among all biodegradable polymers for fabrication of novel materials for medical use and for tissue engineering applications [10].

Recently, there has been a gradual increase in the use of PCL for biomaterials and TE. PCL is an aliphatic linear polyester, with a glass transition temperature of 62 °C and a melting point of 55–60 °C, depending on the degree of crystallinity, which in turn is dictated by the molecular weight (normally 3000–100 000 g.mol⁻¹) and, to some extent, by the scaffold fabrication process [31–33]. It is biocompatible, bioresorbable and a low-cost synthetic polymer. Due to its semi-crystalline and hydrophobic nature, it exhibits a very slow degradation rate (2–4 years depending on the starting molecular weight) among the well-known biodegradable polyesters such as PGA, PLGA, and PLA. This fact is due to presence of five hydrophobic –CH₂ moieties in its repeating units [10]. Moreover, PCL shows mechanical properties suitable for a variety of applications and it is a Food and Drug Administration (FDA) approved material and has been clinically used as a slow release drug delivery device and suture material since the 1980s (i.e. Capronor ®, SynBiosys®, Monocryl® suture) [1]. However, its hydrophobic nature could often result in poor wettability, lack of cell attachment and uncontrolled biological interactions with the material [11]. Indeed, surfaces with moderate hydrophilicity are able to absorb adequate amount of proteins, while preserving their natural conformation, unlike hydrophobic or very hydrophilic surfaces, which have poor cell attachment. In order to rectify this issue, surface modification techniques can alter the chemical and/or physical properties of the surface, by modifying the existing surface or by coating it with differences materials [1].

In general, PCL and its copolymers have demonstrated this utility by being successfully used in electrospinning, gravity spinning, phase separation, solid freeform fabrication and microparticles. Hence, numerous reports on the production of PCL nanofibers are available in the literature. In electrospinning, a solvent system is important to be examined. This is due to the lack of invocal rules to establish when polymer/solvent solution may be efficaciously used for

the electrospinning. Therefore, a basic study of PCL nanofiber with various solvent systems is vital in the electrospinning research. PCL solutions just studied by Lee et al. [12], Jeun et al. [13] and also Qin et al. 2011 [14]. Effect of three different solvent (methylene chloride (MC), MC/DMF, and MC/toluene) on physical and mechanical properties of PCL nonwoven mats produced by electrospinning was reported by Lee et al. [12]. It is reported that for the MC as a single solvent, electrospun fibers had very regular diameter of about 5500 nm, but electrospinning was not facilitated, for the solvent system of MC/DMF, electrospinnability was enhanced and fiber diameter decreased with increasing DMF volume fraction. In MC/toluene system, with increasing toluene volume fraction, electrospinning is strictly restricted due to very high viscosity and low conductivity. In Jeun and co workers 2005 study the effect of various solvents such as methylene chloride, chloroform, dichloroethane, dimethylformamide (DMF), n-hexane and methanol with PCL. The fiber morphology was observed under a scanning electron microscope and the effects of the parameter including electric voltage, flow rate and solution parameters such as concentration and solvent had been examined. In their study, concluded that the use of non solvent allowed the solution viscosity and the thickness of the electrospun fibers to be controlled. Likewise, Qin et al. [14] examined PCL with N,N-dimethylformamide, 1-methyl-2-pyrrolidone, tetrahydrofuran, dichloromethane, acetone, chloroform and dimethyl sulfoxide as the solvent. When 1-methyl-2-pyrrolidone and acetone were used as the solvent for PCL electrospinning, all of them were composed of smooth and nanosized fibers with similar fiber surface morphologies. Meanwhile, when dichloromethane and chloroform were used as solvent, there were lots of holes in fibers due to high evaporation. The electrospinnability was good when acetone was chosen as solvent due to its lowest viscosity.

Beachley and Wen [15] reported the production of PCL electrospun nanofibers across two parallel plates for creating linearly oriented individual nanofiber arrays to investigate the nanofibers length. They explored the effect of electrospinning parameters such as solution concentration, plate size and applied voltage on the PCL nanofibers diameter and length [15]. They showed that relatively long continuous polycaprolactone (PCL) nanofibers with average diameters from approximately 350 nm to 1 nm could be collected across parallel plates at lengths up to 35-50cm. The effect of changing the applied voltage, flow rate, distance between needle, and collector on electrospun webs were investigated on the PCL microfiber and multilayer nanofiber/microfiber scaffolds [14]. Effect of nanofibers diameter on the mechanical properties

of web has been reported. Baji et al. [16] critically reviewed and evaluated the role of the microstructures on the fiber deformation behavior and presented possible explanations for the enhanced properties of the nanofibers. It was found that both modulus and strength of poly (ϵ -caprolactone) (PCL) fibers were increased significantly when the diameter of the fibers was reduced to below 500 nm [16]. In another work, electrospun nanofibers and films of PCL-grafted dextran (PGD) were prepared by electrospinning and solvent evaporation methods, respectively. The authors concluded that the selected polymer enabled the fabrication of nanofibers of an average diameter 412 nm and there was slight increase in the crystallization temperature along with linear increase in heat of fusion in both fibers and films during the progress of hydrolysis [16]. Accordingly, in this work we studied the effect of several parameters i.e. polymer concentration, solvent/ co solvent ratio, etc on the electrospinning processability of PCL solutions.

3.2 Materials

Poly(ϵ -caprolactone)

In this work, Poly(ϵ -caprolactone) (Figure 1) with a average of molecular weight; 42,500 kDa and 45,000 kDa was obtained from Aldrich Chemical and had been used without any purification. Recently, Sigma Aldrich had temporary stopped the production of PCL with average molecular weight, 42,500 kDa which is currently out of stock in worldwide. They replaced with another PCL, this time with a broad molecular weight of 70 to 90 kDa. Approximately, the average molecular weight is 45,000 kDa. Here, we propose a comparative study between PCL with different molecular weights to study the effect of polymer/solvent system and verify also effect of molecular weight towards the morphology of electrospun fibers. Next studies will be prepared only on higher molecular weights of PCL solution, currently available by Sigma-Aldrich.

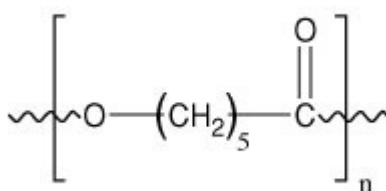


Figure 1: Poly-ε-caprolactone structures.

Solvents: Methylene Chloride and Methanol

Methylene Chloride (Dichloromethane) and also Methanol had been used for solvent and co-solvent. All these solvents were of analytical research grade from Sigma Aldrich and used without further purification. Some basic properties of the solvent are summarized in Table 1.

Methylene chloride is a clear, water white liquid at ordinary temperatures with a pleasant, ethereal odor. It is highly volatile and mobile. Methylene chloride is completely miscible with most organic liquids.). Whilst, Methanol is a polar solvent compared to Methylene Chloride and was used as a co-solvent in this work.

Table 1: Properties of solvent used in this work

Solvent	Chemical formula	Molecular weight	Boiling point (°C)	Density (g/cm ³)	Dipole moment (Debye)	Solubility parameter (MPa) ^{1/2}
Methylene Chloride	CH ₂ Cl ₂	84.93	39.8	1.325	1.55	19.8
Methanol	CH ₃ OH	32.04	64.7	0.790	1.7	29.7

3.3 Methods:

Solution preparation

In order to investigate the influence of solvent/co-solvent ratio on the formation of fibers and their morphology, polymer solution with a different solvent ratio were prepared. In this work, solvent ratio of 3:1, 2:1 and 1:1 has been used. The effect of main parameter such as voltage (V), flow rate (Q) and concentration of polymer solution towards the fiber diameter had been investigated in this work. Therefore, polymer solution with different concentration (8-12% wt) were prepared and used for these experiments. Hence, all solutions were prepared under magnetic stirring, for two days, at room temperature up to obtain homogenous and clear solutions.

Electrospinning Process.

Briefly, polycaprolactone (PCL) solutions were placed in a 5mL syringe. Electrospinning of the as-prepared solutions was carried out by using NANON electrospinning system (MECC, Japan). The working voltage was ranged from 10 to 20 kV while flow rate between 0.1 to 1.0 ml/hr. During the process, a fluid jet was ejected from the tip of the needle. The jet extends in a straight line for a certain distance and then bends and follows a looping and spiraling path. As the jet accelerated toward the target, the solvent evaporated and polymer nanofibers were collected on aluminum foil. All electrospinning were carried out at room temperature.

Fibre Morphology investigation: SEM and Image Analysis.

Electrospun PCL mats were coated with gold and preliminary observed by scanning electron microscopy (SEM; Phenom and Quanta 200 FEI). For quantification of fiber diameters, measurements were made on 20 random locations of the nanofibers using Image J software, (version 1.37) and the average of these twenty measurements was used as an average diameter of these nanofibers.

Bead area density was chosen to characterize uniformity in nanofibres. Beads are created by using not optimal processing parameters that result in a discontinuous in the electrospinning jet.

Bead area density was calculated by measuring bead diameters at the centre of each bead, also using the “Measure tool” in Image J towards SEM images. Assuming all beads were circular in shape, individual bead areas were calculated and added together to yield a total surface area covered by beads. The ‘Threshold’ tool in Image J was used to transfer the image to black and white in order to approximate the total surface area of PCL fibers, including both fibres and beads.

Differential scanning calorimetry (DSC)

Thermal analysis was performed using a TA Instruments Q20 Differential Scanning Calorimeter. Samples were heated from 20 °C to 250 °C at 10 °C/min. TA Instruments Universal Analysis 2000 software package was used to identify melting temperatures and measure the enthalpies of melting and fusion for each cycle.

3.4 Results and discussion

Effect of solvent/co-solvent

PCL, $M_n=42,500$ kDa

Studies on effect of solvent/co-solvent had been investigated. PCL with $M_n=42,500$ and 45,000 kDa were used in this experiment. Since, PCL is hydrophobic and linear semi crystalline polymer; it can be dissolved in organic solvent such as methylene chloride. However, solubility is not the sole criteria to explain the nanofiber formation from a polymer solution. For instance, Methylene chloride (MC) is a common solvent for PCL, which is not suitable for electrospinning process due to its moderate dielectric constant. PCL solution prepared in MC cannot be converted into nanofibers with good morphology; therefore a co-solvent such as Methanol had been used to enhance the spinning process. In order to investigate the effect of MC/Methanol system, a solvent/co-solvent ratio (3:1, 2:1, 1:1) had been tuned to get smooth and fine fibers. The electrospinning process was carried out under the following conditions: the applied voltage was 13 kV, solution concentration was (11-10% w/v), nozzle to collector distance was fixed at 10 cm and flow rate of polymer solution was adjusted in 0.5 mL/hr.

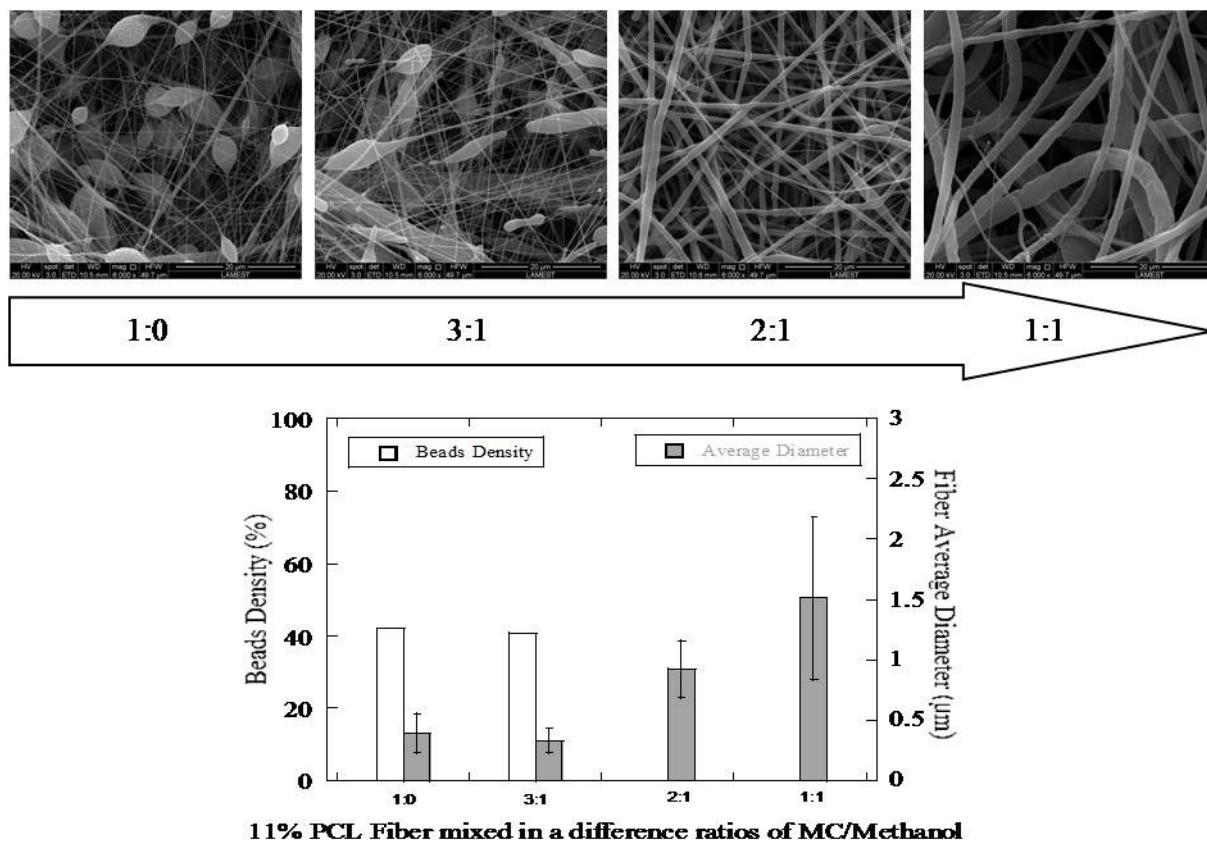


Figure 1: SEM of electrospun PCL ($M_n = 42,500$ kDa) fibers obtained from solution of PCL at a concentration 11% w/v in a mixed solvent ratio of DCM and Methanol at various compositional ratios: 1:0, 3:1, 2:1 and 1:1 (magnification 1800 x, scale bar = 50 µm). Graph bead density and fiber average diameter vs. ratio solvent/co solvent.

In the first experiments, 10% w/v PCL; $M_n = 42,500$ kDa was used. When MC was used as solvent, many microsphere-shaped beads and few fine fibers were detected in SEM micrographs (Figure 1). On the other hand, when the solvent mixed with co-solvent (Methanol) at 3:1 ratio, there were a lot of beads on string with smaller size). As the MC/Methanol ratio increase up to 2:1, smooth and fine fibers were observed (2.34 ± 0.7 µm average diameters). Moreover, when the MC/methanol ratio was 1:1; fiber diameter decreased (2.06 ± 0.42 µm average diameter) attributed to the higher boiling point of methanol.

In a second experiment, PCL; $M_n = 45,000$ kDa had been used. The electrospun of fibers was optimum at 10% w/v of PCL ($M_n = 45,000$ kDa). In order to investigate the solvent/co-solvent (MC/Methanol system that had been chosen, three various ratios had been used; 3:1, 2:1 and 1:1. PCL dissolved in MC still showed microspheres-beads (beads density: 33.8%) and no fiber

formation (Figure 2). However, in a mixed solvent (MC/Methanol) at 3:1 ratio showed the beads density was slightly decreased (33.3%) and accompanied with small fibers. The beads formation was getting decreased when methanol amount was increased up to 2:1 ratio. The beads density was also decreased; approximately 31.7%. A smooth and fine electrospun fibers ($0.25 \pm 0.07 \mu\text{m}$ average diameter) and with a less beads formation had been obtained by using mixed solvents (MC/Methanol) at ratio (1:1). The mixed solvent ratio (1:1) demonstrated the polymer solution had enough conductivity values to be electrospun. The boiling point of Methanol (boiling point: $64.7 \text{ }^\circ\text{C}$) solvents tends to increase the boiling point of the solution. Hence, the mixed solvents has had controlled the evaporation rate instead of using MC solvent alone. Then, the polymer solution had enough time to be yield and gave smooth and fine nanofibers.

PCL, $M_n = 45,000$

Methanol (co-solvent) is a polar solvent and contributes to modulate the solubility of the solvent solution. Nevertheless, in both experiments the beads formation on the morphology had been observed. This is referred to the poor interaction of PCL and solvent molecules. The polymer-solvent interactions must be strong enough to break the polymer-polymer bond (as discussed in chapter 2.2.2) to be electrospinnable. Otherwise, it leads to the formation of beads on the string. Moreover, dielectric constant value is low and therefore enhances the difference in the distribution of charges in the solvent-rich and polymer-rich regions. However, the amount of beads decreased and the beads appeared to be more elongated in shape up to reach a fibrous structure.

Obviously, the addition of Methanol resulted in a marked reduction in fiber diameter. Indeed, Methanol into MC solution enhanced the electrospinnability of PCL solutions by tuning dielectric properties and also higher boiling point of the solution. Solvents tend to give higher electrical susceptibility of the solutions when they are subjected to an electrostatic field, thus promoting the mass throughput of the solutions from a spinneret.

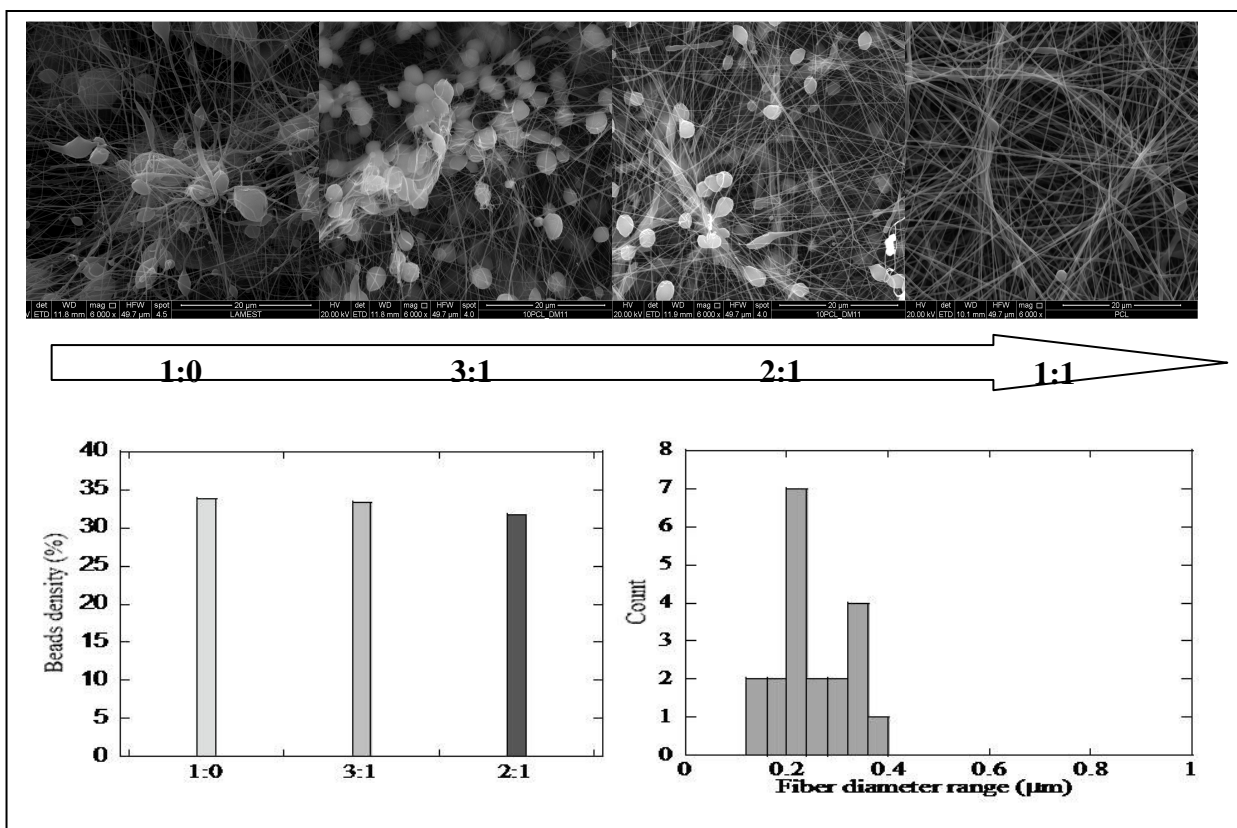


Figure 2: SEM of electrospun PCL (Mn= 45,000 kDa) fibers obtained from solution of PCL at a concentration 10% w/v in a mixed solvent ratio of DCM and Methanol in various compositional ratios of 1:0, 3:1, 2:1 and 1:1 (magnification 6000 x, scale bar = 20 μm). Graph Bead density vs ratio solvent/co-solvent; Histogram for PCL with solvent/co solvent (1:1).

The dielectric constant of the solvent plays a main role on predicting the final properties of electrospun membranes, more than other parameters such as dipole moment and other properties [24]. The dielectric constant is related to the dipole moment and generally, reflects the polarity of the molecules [17]. According to Guarino et al. [24], polar solvents and higher permittivity values ensured stronger polar interactions among the polymer chains mediated by solvent molecules, producing enhanced stretching of fibers and therefore the formation of thinner fibers [4]. The effect of solvent on the bead formation also was studied by Fong & Reneker [18]. When ethanol was added into the PEO/water system, less bead formation was found. They attributed that the phenomenon was about the higher viscosity, lower surface tension, and faster evaporation rate (leaving less time for the uniform fibers to form beads).

Effect of molecular weight on morphology of electrospun fibers.

In order to elucidate the effect of molecular weight on morphology of the electrospun fibers, two differences PCL molecular weight had been used in this experiment. As we can see in Figure 3, a comparison between PCL fibers with differences molecular weights ($M_n=42,500$ and $45,000$ kDa) had been observed using 10% w/v PCL concentration. The parameters of the electrospinning ($V=13$ kV and $Q=0.5$ ml/hr) had been fixed. There were two differences ratio solvent/co-solvent ratio been used, i.e. 2:1 and 1:1. Beneath on the ratio 2:1, electrospun PCL ($M_n=42,500$) fibers showed an irregular fibers formation and obtained 1.0 ± 0.4 μm average diameters. However, the electrospun of PCL ($M_n=45,000$) demonstrated fine fibers with beads on the strings. The average diameter was 0.29 ± 0.1 μm . On the other hand, under the ratio (1:1), electrospun PCL ($M_n=42,500$) fibers appeared rough fibers formation without any beads defect on the string (2.0 ± 0.9 μm average diameters).

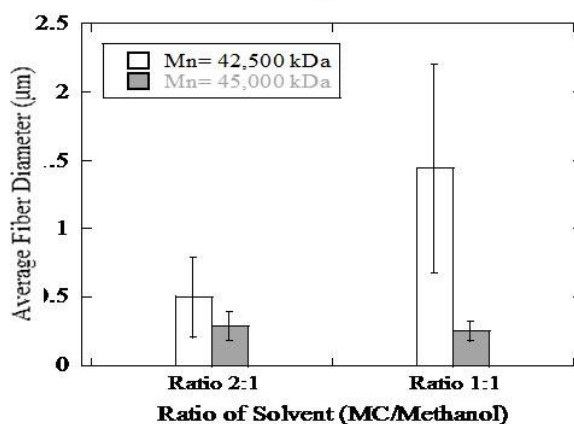
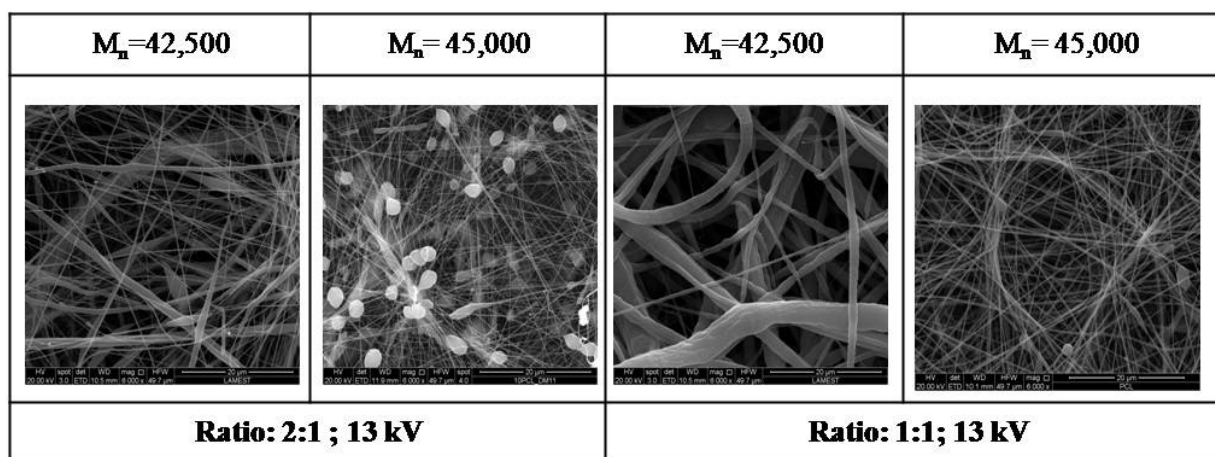


Figure 3: A comparison between PCL fibers with differences molecular weights ($M_n=42,500$ and $45,000$ kDa). (Magnification 6000 x, scale bar = 20 μm). Graph of PCL average fiber diameter vs ratio solvent/co-solvent.

Meanwhile, PCL ($M_n=45,000$) showed smooth and fine fibers morphology with $0.25 \pm 0.07 \mu\text{m}$ average diameters. Overall, PCL fibers diameters were decreased in these two cases as using PCL higher molecular weights.

As been discussed in Chapter 2.5.2, the molecular weight of the polymer is related to the length of the polymer chain and it can affect the solution viscosity. It means that the use of low molecular weight PCL ($M_n=42,500$) allows for the spinning of less viscous solutions. Indeed, in the case of low molecular weights, an higher chain mobility occurs due to less frequent molecular interactions with a consequent reduction of viscosity as confirmed by DSC thermograms (see Figure 4 and Table 2).

Some differences have been also detected in the case of dissolution of PCL in solvent mixture (2:1 v/v). PCL ($M_n=42,500$) solution exhibited different intermolecular interactions differently mediated by solvent molecules which ultimately can prevent jet break up, thus yielding nanofibers. On the contrast, PCL fibers ($M_n=45,000$) show the presence of several beads probably due to the less efficacious interaction of solvent with polymer chains groups.

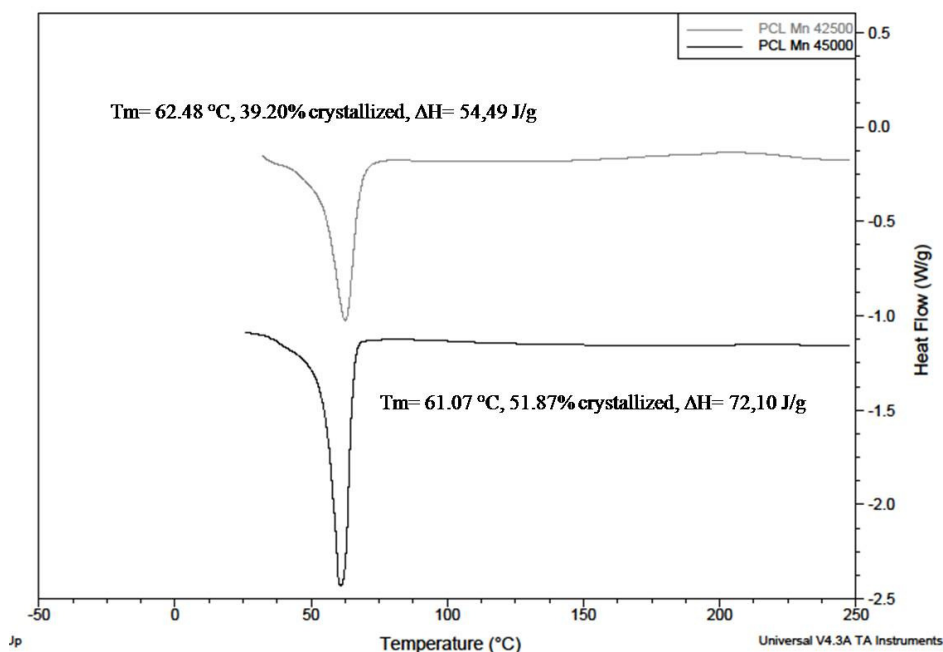


Figure 4: DSC thermogram curve of PCL with difference molecular weight; 42,500 and 45,000 kDa.

Table 2: DSC data of PCL Mn 42500 and Mn 45000 pure pellets.

Sample	Enthalpy of fusion (ΔH_m) (J/g)	Crystallinity (χ_c) (%)	Melting Temperature (T_m) (°C)
PCL (Mn 42500)	54.49	39.20	62.48
PCL (Mn 45000)	72.10	51.87	61.07

In a mixed solvent (1:1 v/v), PCL ($M_n=42,500$) fibers morphology demonstrated rough fibers diameters due to the higher amount of co solvent, methanol. A low viscosity of solutions indicates higher solvent molecules and thus the polymer-solvent interactions are weak and effect fibers morphology. Nevertheless, PCL ($M_n=45,000$) solution increased the viscosity and the polarity of methanol support a fiber formations. Therefore, an appropriate of higher polymer viscosity with a lower surface tension and higher boiling point (prevent dryness on the tip of the jet) had leads to the smooth and fine fibers.

Influence of main process parameters on the final fiber morphology.

Nanofibers morphology: Voltage

The effect of the applied voltage on electrospun PCL fibers morphology can be seen in Fig 5. These fibers were spun from the solution of 10 % (w/v) of PCL in MC/Methanol (ratio 1:1), using an applied potential ranging from 10 to 16 kV over a collection distance of 10 cm and a flow rate of 0.5 ml/hr. Generally, applied voltage was induced to the polymer solution and charge transport across the gap between the charged needle and the collector. In this study, the minimum voltage (initiation of the jet) was 10 kV. If voltage lower than 10 kV, it is not possible to electrospun the fibers. It is because; a charge is not enough to overcome the ionic conduction

of charge in the polymer solution. Hence, a broad fiber diameter was recorded ca. 1.21 ± 0.39 μm . The voltage had been increased to 13 kV and displayed a jet mode of whipping (bending stability) and go through the elongation process, which allows the jet become very long and thin (as been discussed in Chapter 2.3.3). The fiber diameter was found decreased; ca. 0.25 ± 0.06 μm . However, with further increased of the voltage (15 kV and 16 kV), showed a formation of beads on string with beads density; ca. 50%. The effect of applied voltage on electrospun PCL fibers diameter can be explained by considering the effects of all forces acting on a small segment of a charged jet. Six types of force may be considered; they are: (1) body or gravitational force, (2) electrostatic force which carries the charged jet from the spinneret to the target, (3) Coulombic force which tries to push apart adjacent charged carriers being present within the jet segment and is responsible for the stretching of the charged jet during its flight to the target, (4) viscoelastic force which tries to prevent the charged jet from stretching, (5) surface tension which also acts against the stretching of the surface of the charged jet, and (6) drag force from the friction between the charged jet and the surrounding air[17].

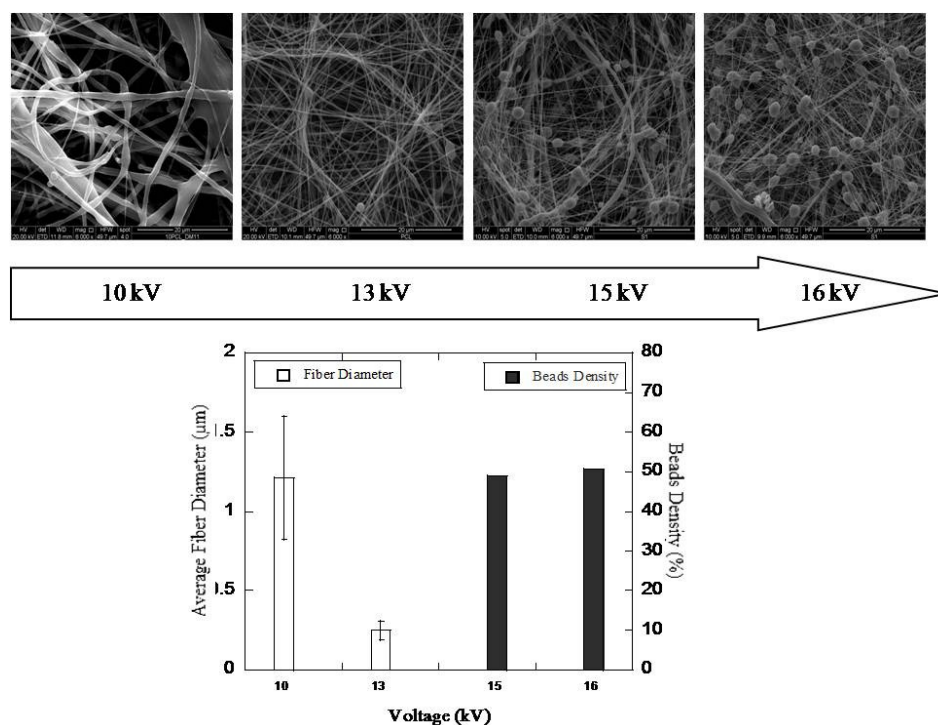


Figure 5: Effect of voltage from 10% (w/v) PCL/solvent [methylene chloride/methanol] =1:1 ratio. Flow rate=0.5 ml/hr and voltage: 10kV, 13kV, 15kV and 16kV. (Magnification 6000 x, scale bar = 20 μm). Graph Average Fiber Diameter and Beads Density vs. various voltages

Therefore, the effect of applied potential on the obtained fiber diameters can be explained in terms of the relationships among the three major forces (ie the Coulombic, the viscoelastic and the surface tension forces) influencing the fiber diameters.

At low applied potentials (eg 10 kV), the Coulombic force was not high when compared with that of the surface tension. This resulted in electrospun fibers with large diameters (ca. $1.21 \pm 0.39 \mu\text{m}$). At moderate applied potentials (eg 13 kV), all three forces were well-balanced, resulting in a narrow distribution of the fiber diameters. With further increase in the applied voltage (ie; 15 kV and 16 kV), the Coulombic force was much greater than that of the viscoelastic force. This might result in an increased possibility of the breakage of an over-stretched charged jet during its flight to the target (the jet undergoes a greater degree of strain than a lower voltages). Moreover, with increasing applied potential, a charged jet travels to the grounded target much faster. The solvent, therefore, has less time to evaporate. Retraction of the charged jet can then occur as soon as some of the charges carried in the jet are neutralized (causing the reduction in the Coulombic force), which, finally leads to the formation of beads defect (see Figure 4). [17].

Nanofiber morphology: concentration

Polymer concentration is important parameter in the electrospinning process. This fact is due to its strong relation with viscosity of the polymer. The effect of concentration for electrospun PCL fibers were showed in Figure 6. A difference concentration had been investigated (8, 10, 12% w/v of PCL solution) and exhibit various fiber diameter. As we can see, changing the polymer solution could change the solution viscosity. One of the factors that influenced the viscosity is polymer molecular weight as been mentioned in Chapter 2.5.2. In electrospinning process, a polymer solution required a sufficient polymer molecular weight (shows degrees chain entanglements) to obtain nanofibers without any defects (beads or fused fibers). In this study, at low concentration; 8% w/v of PCL solution, a large number of beads on string were presented and the beads density was 75%. Essentially, at low viscosity, the viscoelastic force (a result of the low degree of chain entanglements) in a given jet segment was not large enough to counter the higher Coulombic force, resulting in the break-up of charged jet, into smaller jets, which as a result of the surface tension, were later rounded up to form droplets [19,20].

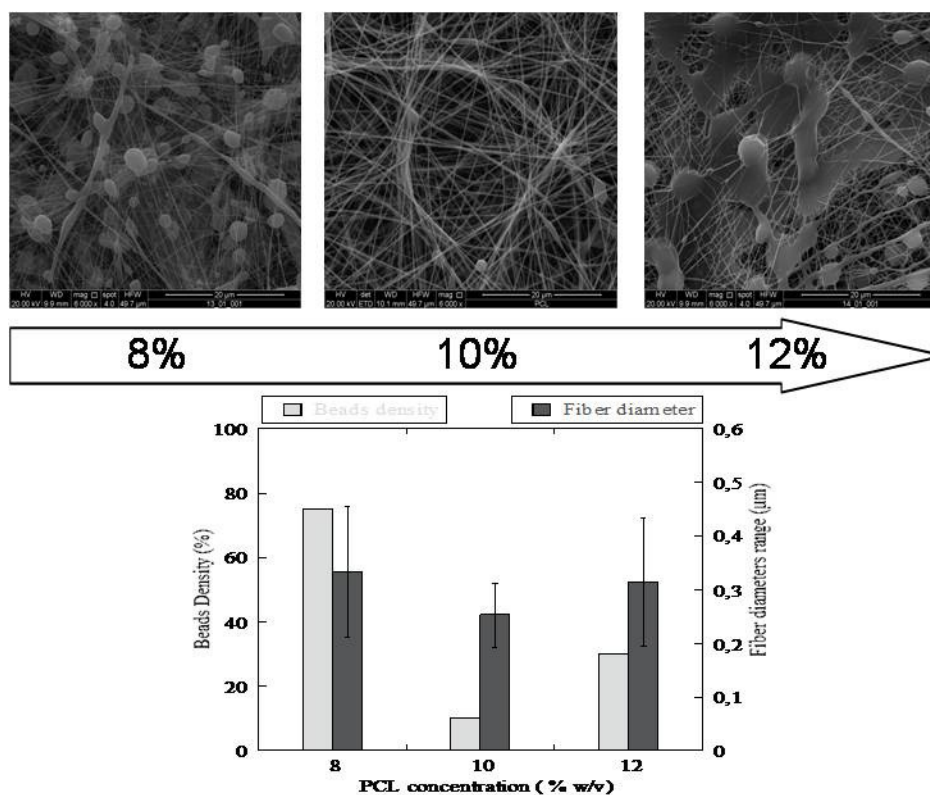


Figure 6: SEM micrographs of electrospun fibers from PCL solution at a difference concentration: 8%, 10%, 12% w/v of PCL/solvent [methylene chloride/methanol] = ratio 1:1. Flow rate=0.5 ml/hr and voltage =13kV. (Magnification 6000 x, scale bar = 20 µm). Graph of beads density and fiber distribution diameter vs. various concentration (8 – 12 % w/v) of PCL solution.

In this case, there is a high concentration of free solvent molecules and it means the solvents molecules are have a tendency to congregate and adopt a spherical shape due to the surface tension (as mentioned in Chapter 2.2.3). Even reported by Liu and co-workers [17] showed that when the polymer concentration was low, many beads or droplets appeared in the poly(butylene succinate) (PBS) nanofibrous webs, and the process converted to electro spraying when the concentration became low enough.

As soon as the concentration is increased (higher viscosity) at 10% w/v PCL solution, the charged jet did not break up into small droplets, a direct result of the increased chain entanglements (and hence an increase in the viscoelastic force) which were sufficient to prevent the break-up of the charged jet and allow the Coulombic stress to further elongate the charged jet during its flight time, which is ultimately thinned down the diameter of the fibers [21] ca. $0.25 \pm$

0.06 μm (as seen in Figure 5). Nevertheless, when the concentration is slight increased to 12% w/v, a mixed big droplets with fibers there on the surface. The fiber diameter was $0.31 \pm 0.12 \mu\text{m}$ and the beads density was 3.15 %.

When the concentration was slightly higher (12% w/v), the solutions became too viscous to be drawn into fibers before the dielectric breakdown of air took place and thus the formation of beads and fused fibers had occurred. It showed that a high chain entanglement in polymer solution and it is effect the intermolecular interaction between polymer and solvent (as mentioned in Chapter 2.2.2) and hence gives an effect to the surface tension. The formation of beads along the electrospun fibers could be a result of a number of different phenomena. For example, it could be a result of the viscoelastic relaxation and the work of the surface tension upon the reduction of the Coulombic force once the fibers are in contact with the grounded target that drives the formation of the beads [18]. Therefore, a suitable polymer concentration is essential to fabricate nanofibers without any beads or beads on-a string appearance. For instance, increase in viscosity or polymer concentration results in fiber diameter increase. By changing polymer concentration alone it is possible to fabricate the fiber diameters in the range of few nanometer to several micrometers while keeping other electrospinning parameters at a constant [22].

Nanofibers morphology: flow rate

Flow rate is a rate at which the polymer solution is pumped into the tip to replenish the Taylor's cone. Ideally, the feed rate must match the rate of removal of solution from the tip [23]. In this experiment evaluating the effect of flow rate on morphology, the applied voltage was kept constant. Moreover, 10% w/v PCL solution had been undergo for a difference flow rate to see an effect on the morphological of PCL fibers (Figure 7). Flow rate has to been maintained and enough to obtain a stable Taylor cone with a given voltage (as mentioned in 2.5.3). At a low flow rate (0.1 ml/hr), branched fiber were observed and the fiber diameter was ca. $0.77 \pm 0.47 \mu\text{m}$. In this condition, low flow rates electrospinning may only be intermittent with the Taylor's cone being depleted (with the cone even receding into the needle in some cases). Upon increasing the flow rate to 0.3 ml/hr and 0.5 ml/hr, the fiber diameter became thinner to ca. $0.41 \pm 0.14 \mu\text{m}$ and $0.25 \pm 0.06 \mu\text{m}$. However, if the flow rate increased up to 1.0 ml/hr, the fibers diameter was

decreased (ca. $0.47 \pm 0.24 \mu\text{m}$) and together with a lot of beads on the string (beads diameter was ca. $2.9 \pm 1.0 \mu\text{m}$).

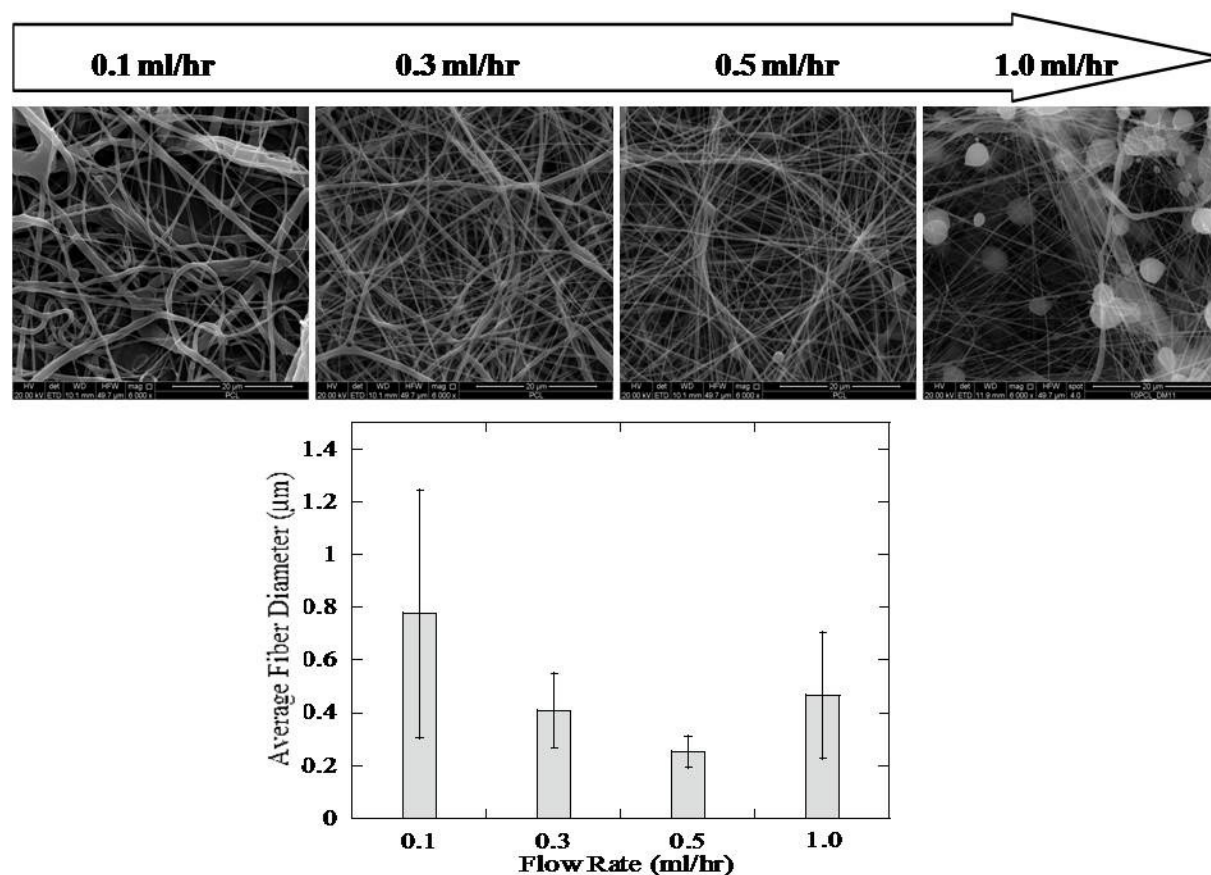


Figure 7: SEM micrographs of electrospun fibers from 10% w/v of PCL solution at a various flow rate: 0.1 ml/hr, 0.3 ml/hr, 0.5 ml/hr and 1.0 ml/hr. PCL/solvent [methylene chloride/methanol] =1:1 v/v ratio at 13kV. (Magnification 6000 x, scale bar = 20 μm). Graph of average fibers diameter vs. various flow rate (0.1-0.5 ml/hr) of PCL solutions.

When the flow rate exceeded a critical value, the delivery rate of the solution jet to the capillary tip exceeded the rate at which the solution was removed from the tip by the electric forces. This shift in mass balance resulted in a sustained, but unstable, jet, and fibers possessing big beads were formed. Instead of that, due to the high volume of solution, the fibers don't have enough time to evaporate and therefore, the residual solvents may cause the fibers wet and showed of bead defects on the fibers strings. When the size of the droplet is too big to suspend at the tip of the spinneret, it either drops from the tip or is carried along with a charged.

3.5 Conclusion

In this study, PCL nanofibers had been prepared with two differences of molecular weight (42,500 and 45,000 kDa) and showed influence to the ratio of solvent/co solvent. A suitability of Methanol as a co solvent is definitely evidence thru the morphologies that had been obtained. The most interesting of this study is the apparent change in the diameter and phenomenon of electrospinning observed in the electrospun PCL nonwoven mats. In deeply, the solution properties such as dielectric properties, viscosity and conductivity have demonstrated correlate strongly on the morphology of electrospun PCL nonwovens mats. Therefore, it is really important to understand on how to control the electrospun nanofibers. This will allow scientists to have the ability to produce fibers optimal for their specific use.

References:

- [1] Cipitria, A., Skelton, A., Dargaville, TR., Dalton, PD. & Hutmacher, DW. **2011**. *J. Mater. Chem.*
- [2] Hohman MM, Shin M, Rutledge G, Brenner MP. **2001**. *Phys. Fluids* 13:2201–2220
- [3] Hohman MM, Shin M, Rutledge G, Brenner MP. **2001**. *Phys. Fluids* 13:2221–2236.
- [4] Reneker, DH., Yarin, AL. & Fong, H & Koombhongse, S. **2000**. *Journal of Applied Physics* 87 (9) 4531-4547.
- [5] Yarin, AL., Koombhongse, S & Reneker, DH. **2001**. *J. Appl. Phys.*, 89 (5) 3018-3026
- [6] Yarin AL, Koombhongse S, Reneker DH. **2001**. *J. Appl. Phys.* 90:4836–4846.
- [7] Burger, C., Hsiao, BS. & Chu, AB. **2006**. *Annu. Rev. Mater. Res.*, 36, 333–368.
- [8] McKee MG, Layman JM, Cashion MP, Long TE. **2006**. *Science* 311:353–55
- [9] Nair, LS. & Laurencin, CT. **2007**. *Prog. Polym. Sci.*, 32: 762–798.
- [10] Kanani, AG. & Bahrami, SH. **2011**. *Journal of Nanomaterials*. 1-10.
- [11] Place, ES et al., **2009**. *Chem. Soc. Rev.*, 2009, 38, 1139–1151.

- [12] Lee, K.H., Kim, H.Y., Khil, MS, Ra, YM. Lee, DR. **2003**. *Polymer*, Vol 44 (4):1287-1294.
- [13] Jeun, JP., Lim, YM. & Nho, YC. **2005**. *J.Ind. Eng.Chem.* Vol 11 (4): 573-578.
- [14] Qin, X. & Wu, D. **2011**. *J Therm Anal Calorim.*
- [15] Beachley, V & Wen,X. **2009**. *Materials Science & Engineering C*, vol. 29, no. 3, pp. 663–668, 2009.
- [16] Baji, A. Mai, YW., Wong, SC., Abtahi, M & Chen, P. **2010**. *Composites Science and Technology*, vol. 70, no. 5, pp. 703–718.
- [17] Wannatong, L., Sirivat, A. & Supaphol, P.**2004**. *Polym Int* 53:1851–1859.
- [18] Fong, H., Chun, I. & Reneker, DH. **1999**. *Polymer* (40) 4585–4592.
- [19] Mit-uppatham, C., Nithitanakul, M. & Supaphol, P. **2004**. *Macromol. Chem. Phys.* (205) 2327.
- [20] Kumbar SG, Bhattacharyya S, Sethuraman S, Laurencin CTA.**2007**. *J Biomed Mater Res Part B: Appl Biomater*; 81B:91–103.
- [21] Buchko C.J., Chen, LC., Shen, Y., Martin, DC.**1999**. *Polymer* (40) 7397–7407.
- [22] Kumbar, SG., James, R., Nukavarapu, SP. & Laurencin, CT.**2008**. *Biomed. Mater.* 3: 1-15.
- [23] Andradý, A. L.**2008**. *Science and technology of polymer nanofibers*. John Wiley & Sons,
- [24] Guarino V., Cirillo, V., Taddei, P., Alvarez, MA. & Ambrosio L. 2011. *Macromolecular Science Journal*. [DOI: 10.1002/mabi.201100204].

CHAPTER 4

Chitosan Nanoparticles for Drug Delivery System

4.1 Introduction

For the past few decades, there has been a considerable research interest in the area of drug delivery using particulate delivery systems as carriers for small and large molecules. Particulate systems like nanoparticles have been used as a physical approach to alter and improve the pharmacokinetic and pharmacodynamic properties of various types of drug molecules as well as macromolecules such as proteins, peptides or genes [1]. They have been used in vivo to protect the drug entity in the systemic circulation, restrict access of the drug to the chosen sites and to deliver the drug at a controlled and sustained rate to the site of action. Various polymers have been used in the formulation of nanoparticles for drug delivery research to increase therapeutic benefit, while minimizing side effects [2].

The major goals in designing nanoparticles as a delivery system are to control particle size, surface properties and release of pharmacologically active agents in order to achieve the site-specific action of the drug at the therapeutically optimal rate and dose regimen [2]. Though, liposomes have been used as potential carrier with unique advantages including protecting drugs from degradation, targeting to site of action and reduction toxicity or side effects, their applications are limited due to inherent problems such as low encapsulation efficiency, rapid leakage of water-soluble drug in the presence of blood components and poor storage stability. On the other hand, polymeric nanoparticles offer some specific advantages over liposomes. The advantages of using nanoparticles as a drug delivery system included; (a) particle size and surface characteristics of nanoparticles can be easily manipulated to achieve both passive and active drug targeting after parenteral administration, (b) nanoparticles control and sustain release of the drug during the transportation and at the site of localization, altering organ distribution of the drug and subsequent clearance of the drug, as to achieve increase in drug therapeutic efficacy and reduction in side effects, (c) controlled release and particle degradation characteristics can be readily modulated by the choice of matrix constituents. Drug loading is relatively high and drugs can be incorporated into the systems without any chemical reaction; this is an important factor

for preserving the drug activity, (d) Site-specific targeting can be achieved by attaching targeting ligands to surface of particles or use of magnetic guidance and (e) the system can be used for various routes of administration including oral, nasal, parenteral, intra-ocular etc [2]. In spite of these advantages, nanoparticles do have limitations. For example, their small size and large surface area can lead to particle -particle aggregation, making physical handling of nanoparticles difficult in liquid and dry forms. In addition, small particles size and large surface area readily result in limited drug loading and burst release. These practical problems have to be overcome before nanoparticles can be used clinically or made commercially available [2].

Nanoparticles are defined as particulate dispersions or solid particles with a size in the range of 10-1000 nm. The drug is dissolved, entrapped, encapsulated or attached to a nanoparticle matrix. Depending upon the method of preparation, nanoparticles, nanospheres or nanocapsules can be obtained. Nanocapsules are systems in which the drug is confined to a cavity surrounded by a unique polymer membrane, while nanospheres are matrix systems in which the drug is physically and uniformly dispersed (as can be seen in Figure 1) [2,3].

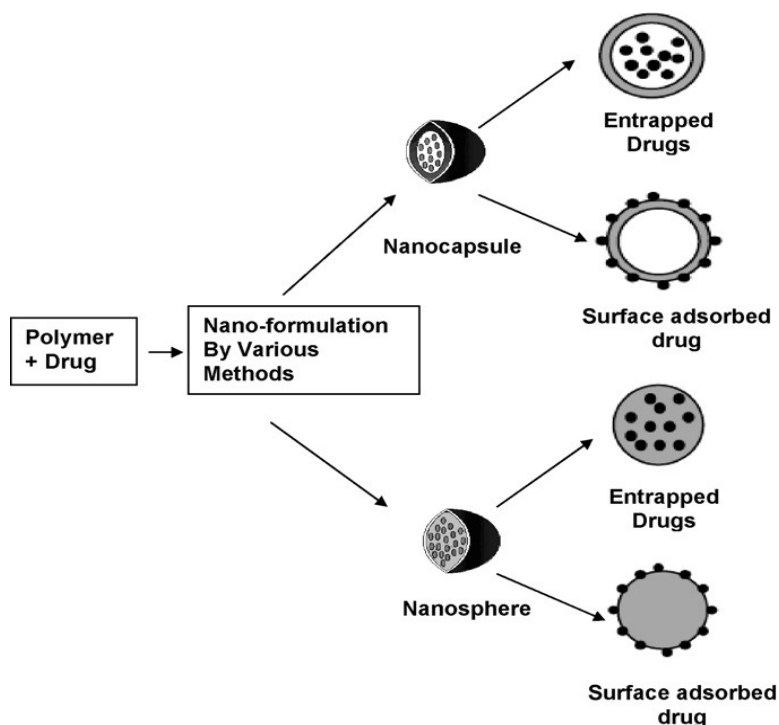


Figure 1: Type of nanoparticles; (a) nanocapsules, (b) nanospheres [4,5].

However, there were effects of characteristic of nanoparticles on drug delivery system such as particle size and surface properties. The particle size and size distribution are the most important characteristics of nanoparticle systems. They determine the in vivo distribution, biological fate, toxicity and the targeting ability of nanoparticle systems. In addition, they can also influence the drug loading, drug release and stability of nanoparticles [2]. Smaller particles have larger surface area, therefore, most of the drug associated would be at or near the particle surface, leading to fast drug release. Whereas, larger particles have large cores which allow more drug to be encapsulated and slowly diffuse out [6]. In addition, smaller particles also have greater risk of aggregation of particles during storage and transportation of nanoparticle dispersion. It is always a challenge to formulate nanoparticles with the smallest size possible but maximum stability [2].

Hence, to upgrade a surface properties of drug targeting by nanoparticles, it is necessary to minimize the opsonization (binding of these opsonins onto the surface of nanoparticles called opsonization acts as a bridge between nanoparticles and phagocytes) and to prolong the circulation of nanoparticles in vivo. This can be achieved by (a) surface coating of nanoparticles with hydrophilic polymers/surfactants; (b) formulation of nanoparticles with biodegradable copolymers with hydrophilic segments such as polyethylene glycol (PEG), polyethylene oxide, polyoxamer, poloxamine and polysorbate 80 (Tween 80) [2].

To develop a successful nano-particulate system, both drug release and polymer biodegradation are important consideration factors. In general, drug release rate depends on: (1) solubility of drug; (2) desorption of the surface bound/adsorbed drug; (3) drug diffusion through the nanoparticle matrix; (4) nanoparticle matrix erosion/degradation; and (5) combination of erosion/diffusion process. Thus solubility, diffusion and biodegradation of the matrix materials govern the release process [2]. In the case of nanospheres, where the drug is uniformly distributed, the release occurs by diffusion or erosion of the matrix under sink conditions. If the diffusion of the drug is faster than matrix erosion, the mechanism of release is largely controlled by a diffusion process. The rapid initial release or 'burst' is mainly attributed to weakly bound or adsorbed drug to the large surface of nanoparticles [7]. It is evident that the method of incorporation has an effect on release profile. If the drug is loaded by incorporation method, the system has a relatively small burst effect and better sustained release characteristics [8]. If the nanoparticle is coated by polymer, the release is then controlled by diffusion of the drug from the core across the polymeric membrane. The membrane coating acts as a barrier to release,

therefore, the solubility and diffusivity of drug in polymer membrane becomes determining factor in drug release.

Biodegradable Chitosan in drug delivery system

Chitosan is a copolymer of glucosamine and N-acetylglucosamine derived from the natural polymer chitin. Compared to many other natural polymers, chitosan has a positive charge and is mucoadhesive [9]. For these reasons, chitosan has been used in many applications in the formulations employed in drug delivery [10,11]. Since chitosan can be hydrolyzed by lysozyme, it is also one of the biodegradable polymers in nature. The degradation rate of chitosan can be controlled by changing its polymer composition (i.e., the co-polymerization ratio of glucosamine to N-acetylglucosamine or the length of acetyl side-chain on N-acetylglucosamine) and/or its molecular weight. Furthermore, the degradation products of chitosan are nontoxic, nonimmunogenic and noncarcinogenic [11,12].

Different methods have been used to prepare CS particulate systems. Selection of any of the methods depends upon factors such as particle size requirement, thermal and chemical stability of the active agent, reproducibility of the release kinetic profiles, stability of the final product and residual toxicity associated with the final product. Previous authors [3, 9, 13-15] had reviewed a preparation of chitosan micro/nanoparticles with a different methods such as emulsion cross linking, coacervation/precipitation, spray drying, emulsion-droplet coalescence method, ionic gelation, reverse micellar method, sieving method and up to date method is electrospraying. Overall, chitosan has been successfully used as a scaffolding material for cartilage, nerve, and liver cells. Therefore, chitosan is a natural candidate polymer for tissue scaffold applications.

Design of chitosan particles via Electrospraying

Electrospraying is a novel technique for the generation of micro/nanospheres for biomedical applications. Droplets produced by electrospraying are highly charged, that prevents their coagulation, and promotes self dispersion. When a droplet of liquid is subjected to strong electric field, due to mutual repulsion of electrical charges inside the droplet, it changes its shape to

conical. [16]. When these drops continue to accelerate away from the cone tip, their diameter decreases as a result of evaporation. As voltage is applied and increased, the frequency of the drops increases while the diameter of the individual drops decreases. This is because the electrostatic force on the drop decreases the “apparent” surface tension of the liquid in the drop. It has also been observed that for a given flow rate in this mode, reduction of the capillary diameter results in an increase in drop frequency and a decrease in drop size.

Much research has been focused on the preparation of chitosan nanoparticles using electro spraying techniques. Arya and co workers [14], had manipulated process and system parameters of electro spraying to produced chitosan micro/nanoparticles. The ampicilin loaded micro/nanoparticles had been developed for sustained nasal and gastrointestinal tract delivery with the potential for better patient compliance and enhanced control of bacterial pathogenesis. In Songsurang [17], they prepared doxorubicin (drugs) loaded chitosan nanoparticles by using electro spray ionization method with the presence of tripolyphosphate (TPP) as the stabilizer. They obtain nanoparticles in spherical shape with a narrower size distribution and high encapsulation efficiency (over 60%). The doxorubin loaded chitosan nanoparticles prolonged the release of doxorubin for up to 7 - 8 h. Zhang and co workers [18] reported that electro sprayed chitosan/acetic acid solution were prepared by using high negative voltage. In their study, the addition of ethanol had effectively stabilized the electro spraying by decreasing the solution conductivity and increasing the solution viscosity.

These researches showed that chitosan polymeric micro/nanoparticles can be easily synthesized by using electro spraying method. Therefore, the electro spraying is promising in producing solid micro/nanoparticles for drug delivery system. The electro spray process may similarly influence the morphology of polymer fibers formed using the electro spinning process [19].

Use of nanoparticles for LDD (Local Drug Delivery) in periodontal surgery

Recently, a new approach using local delivery systems containing antimicrobial has been introduced. This produces more constant and prolonged concentration profiles. Both topical delivery systems and controlled release systems have been termed as local delivery. The potential therapeutic advantage of local delivery approach has been claimed to be several fold. Local delivery devices are systems designed to deliver agents locally into periodontal pocket but

without any mechanism to retain therapeutic levels for a prolonged period of time. The periodic use of local delivery systems in reducing probing depths, stabilizing attachment levels and minimizing bleeding would allow better control of the disease [20].

Periodontal pocket provides a natural reservoir bathed by gingival crevicular fluid that is easily accessible for the insertion of a delivery device. Controlled release delivery of antimicrobials directly into periodontal pocket has received great interest and appears to hold some promise in periodontal therapy. Some techniques for applying antimicrobial subgingivally, such as subgingival irrigation, involve local delivery but not controlled release. Controlled release local delivery systems, in which the antimicrobial is available at therapeutic levels for several days, have been evaluated in several forms and using different antimicrobials. Controlled delivery systems are designed to release drug slowly for more prolonged drug availability and sustained drug action [20].

Different drugs had been used for local delivery such as tetracyclines, doxycycline, minocycline, metronidazole and chlorhexidine [20]. Tetracyclines are bacteriostatic for many pathogens at concentrations found in the gingival crevicular fluid after systemic administration (3-6 microgram/ml). However, local delivery of these agents provides high concentrations that are bacteriocidal. Local application of tetracyclines has been associated with minimal side effects. Metronidazole's spectrum of activity is relatively specific for obligate anaerobes. Chlorhexidine is an antiseptic, which adheres to organic matter and demonstrates low toxicity when applied topically and not adsorbed well into the tissues [20].

The present study investigated the preparation of chitosans micro/nanoparticles and the preparation of tetracycline loded chitosan micro/nanoparticles using electrospraying techniques. This study was to understand the influence of fabrication parameters of the process on the morphology and size of the particles formed and to optimize the same for the synthesis of micro/nanoparticles that are appropriate for drug loaded chitosan micro/nanoparticles. The application is strive for the periodontal tissue engineering applications.

4.2 Materials and Methods

Materials

A commercial Chitosan with low molecular weights was supplied by Sigma Aldrich (Italy). Acetic Acid (pure analytical grade) from JT Baker (Italy) was used to dissolve Chitosan. Meanwhile, distilled water used throughout the studies. All other chemicals used were of analytical grade. Tetracycline hydrochloride was also obtained from Sigma.

Nanoparticles Preparation

The electrostatic spraying (electrospraying) process was carried out by using NANON01 electrospinning system (MECC, Japan). Differences concentration of Chitosan particles were produced by using various parameters (as seen in Table 1). 90% v/v of acetic acid had been used as a solvent and distilled water as a co solvent. Chitosan is insoluble in most solvents but is soluble in dilute organic acids such as acetic acid, formic acid, succinic acid, lactic acid, and malic acid. The use of chitosan is limited because of its insolubility in water, high viscosity, and tendency to coagulate with proteins at high pH [21]. According to Arya et al [14], by using 90% v/v acetic acid solution, viscosity of the solution provides the most appropriate environment for the electrical forces to act adequately thereby facilitating distinct spherical particle formation and thus had been used in preparation of chitosan particles. Due to the low degree of dissociation of the acetic acid, the conductivity values will be decreased upon increase in acetic acid concentration [18]. While the surface tension decreased slightly upon an increase in acetic acid concentration [22]. Therefore, the acetic acid solution properties must have a low conductivity values and moderate viscosity to stabilize the electrospaying process.

The chitosan solutions were magnetically stirred for 2 days at room temperature and/or until the chitosan powder is completely dissolved before the electrospaying. At the tip of the nozzle, a liquid cone was formed and a thin jet was ejected from the apex of the cone. Single spray cone was achieved by adjusting the electric potential of the nozzle. The thin jet than broke up into monodisperse droplets. As the solvent evaporated from the surface of the liquid droplets, smaller solid particles were obtained on the collector. All the samples were dried overnight under a fume

hood and used for specific characterization. Overall, the experimental design is to study particle formation and to optimize the fabrication parameters (with using typical range operating parameters as seen in Table 2) involved in electrospaying for reproducible synthesis of chitosan based micro/nanoparticles (as seen in Figure 3).

Table 2: A typical range of operating parameters used for electrospaying experiments

Parameter	Range
Flow rate	0.1-0.3 ml/hr
Electrode spacing	7 cm
Capillary diameter	0.8 mm
Voltage	13kV-28kV
Chitosan Concentration	1%-3%wt

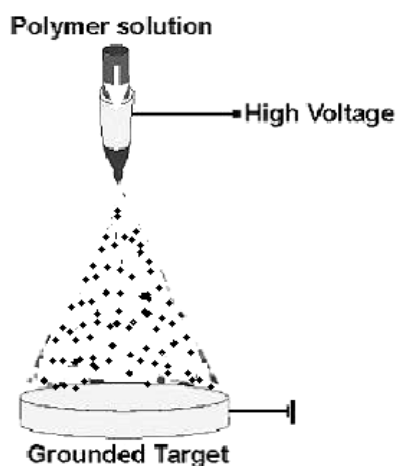


Figure 3: Schematic illustration of the used electrospaying configurations - a simple set-up consisting of a nozzle through which a polymer solution is fed with applied high voltage and a grounded collector.

Preparation of drug loaded chitosan nanoparticles

Tetracycline hydrochloride (TCH) loaded chitosan particles were prepared by using the results from the optimization of chitosan particles studies. The drug concentration was in the range of 1–5% w/w with respect to the polymer used and loaded in 2% w/v chitosan in 90%v/v acetic acid solution. The solutions were stirred until the complete dissolution of the drug. Moreover, TCH loaded chitosan solution appears dark yellow also due to the TCH addition. The electro spraying process have been conducted at a voltage of 17 kV, flow rate 0.1 ml/hr and with a tip to collector distance of 7 cm. In this experiment, we study the effect of percentages of TCH loaded chitosan particles by using the electro spraying process. The TCH loaded chitosan particles will be used for next experiments such as encapsulation and also drug release studies.

Scanning electron microscopy

For high-resolution images, the electro sprayed particles were deposited onto scanning electron microscopy (SEM) stubs. The electro sprayed samples on the stubs were gold-coated and ready to be investigating with SEM (Quanta 200 FEI). For quantification of particle size diameters, measurements were made on 20 random locations of the particles using Image J software, (version 1.37) and the average of these 20 measurements was used as an average diameter of these micro/nanoparticles.

In vitro drug release experiments

Encapsulation efficiency and loading capacity of tetracycline loaded micro/nanoparticles were determined by centrifugation of samples at 5,000 g for 30 min. A Chitosan sample was suspended in 35 mL PBS (pH7.4) for 24 hours and after centrifuging, the amount of free drug in clear supernatant was determined by UV spectrophotometry (Cary 100 Varian) at 380 nm. A linear calibration curve with different concentrations of tetracycline in PBS (pH 7.4) was established to find the relation between the absorbance and the drug concentration (as shown in Figure 4).

The encapsulation efficiency and drug loading were calculated using the following relations:

$$\text{Encapsulation Efficiency} = \frac{\text{Total amount of tetracycline} - \text{Free amount Tetracycline}}{\text{Total amount of tetracycline input}} \times 100\%$$

$$\text{Loading Capacity} = \frac{\text{Total amount of tetracycline} - \text{Free amount Tetracycline}}{\text{Total amount of chitosan}} \times 100\%$$

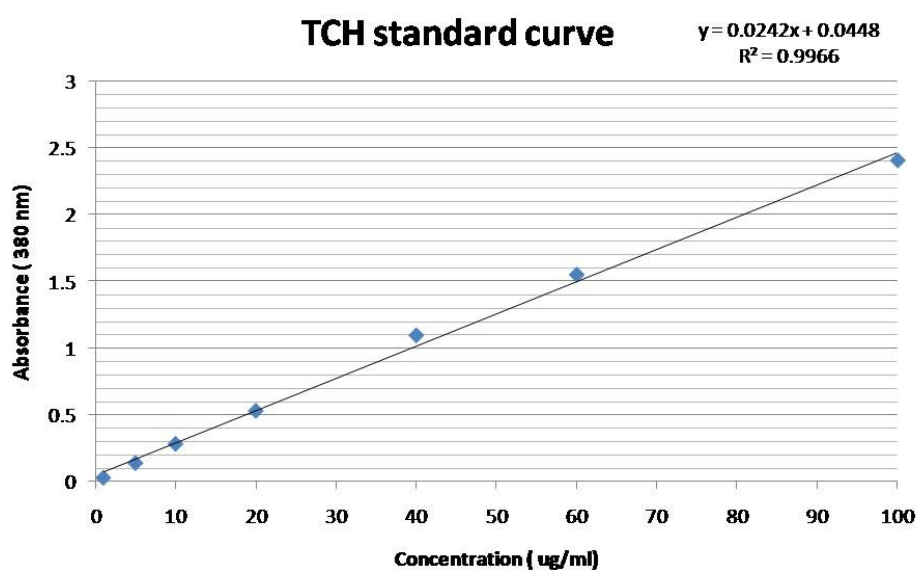


Figure 4: Tetracycline standard calibration curve ($R^2 = 0.9966$).

For the purpose of tetracycline hydrochloride release study, TCH loaded chitosan samples were diluted into the medium of phosphate buffer saline (PBS) (pH 7.4) for 35 mL (37 ± 0.5 °C). All the samples had been mixed using vortex in 2-3 minutes. The amount of TCH in the samples was determined using a UV-spectrometer at a λ max of 380 nm. The time intervals were read to determine the release of TCH start on 5 mins up to 48 hours. The detected UV absorbance of TCH was converted to its concentration according to the calibration curve of TCH in the same buffer. Then the relative percentages of the released TCH were calculated as a function of incubation time. Moreover, a graph was plotted determining cumulative release of TCH (%) vs time (hours).

Cell Culture

Biological assays were performed using bone marrow derived human mesenchymal stem cells line (hMSC, PT-2501) obtained from LONZA. hMSC were cultured in 75 cm² cell culture flask in Eagle's alpha minimum essential medium (α -MEM) supplemented with 10% fetal bovine serum, antibiotic solution (streptomycin 100 μ g/mL and penicillin 100U/ml, Sigma Chem. Co) and 2 mM L-glutamin. The cells were incubated at 37°C in a humidified atmosphere with 5% CO₂ and 95% air. For hMSC cells 4-6 passages were used for all the experimental procedures.

Cell viability and proliferation

The cell adhesion of hMSC onto electrosprayed particles of CHI and TCH loaded CHI was evaluated by using the vibrant cell adhesion assay kit (MolecularProbes). hMSC cultured in 75 cm² cell culture flask were washed with PBS and incubated with calcein AM stock solution to a final concentration of 5 μ M in serum free medium for 30 min. After incubation, the cells were washed with PBS, trypsinized and the cell pellet was collected and diluted with cultured medium to get the required cell concentration. hMSC were seeded onto electrospun fibres and incubated for 4 and 24 h. The fluorescence was quantified by using fluorescein filter set with a Wallac Victor3 1420 spectrophotometer (PerkinElmer, Boston, MA). Percentages of cell adhesion were obtained by dividing the corrected (background subtracted) fluorescence of adherent cells by the total corrected fluorescence of control cells and multiplying by 100%. Conventional polystyrene 24-well culture plates were used as a control.

Cell viability of hMSC (1×10^4 cells) plated in triplicate onto electrosprayed particles of CHI was checked by the MTT assay for 1, 3 and 5 days of culture. This assay is based on the ability of mitochondrial dehydrogenases of living cells to oxidize a tetrazolium salt (3-4,5-dimethylthiazolyl-2-y-2, 5-diphenyltetrazolium bromide), to an insoluble blue formazan product. The concentration of the blue formazan product is directly proportional to the number of metabolically active cells. The hMSC seeded onto integrated scaffolds at prescribed time were washed with PBS and incubated with fresh cultured medium containing 0.5 mg/mL of MTT for 4 h at 37°C in the dark. Then, the supernatant was removed and dimethyl sulfoxide (DMSO) was added to each well. After 60 minutes of slow shaking the absorbance was quantified by spectrophotometry at 570 nm with a plate reader. The culture medium was renewed every day.

Statistical analysis

All numerical data are presented as mean \pm standard deviation. All results were subjected to statistical evaluation using an unpaired Student's t-test to determine significant differences between groups. The significance level was set at $p < 0.05$.

4.3 Results and Discussion

Synthesis of chitosan particles by electrospraying and optimization of fabrication parameters

Electrospraying was successfully tested as a tool for fine particle production [14,23]. The solvent from the electrosprayed droplets evaporates and the remaining solid material forms a fine particles powder on the collector. The size of such particles can be controlled by tuning a right voltage, concentration and also flow rate. An optimization of chitosan particles with processing parameter had been studied.

- *Effect of Voltage*

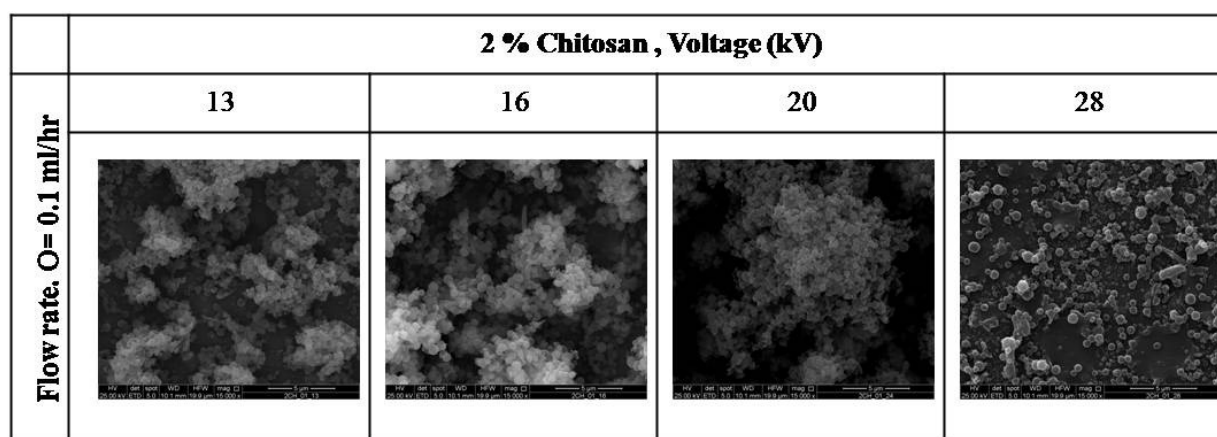


Figure 5: SEM of 2% w/v of Chitosan micro/nanoparticle at differences voltages (a) 13 kV; (b) 16 kV; (c) 20 kV; (d) 28 kV (magnification 15000 x, scale bar = 5 μ m).

The electrospraying process can be sustained in a variety of modes characterized by the shape of the surface from which the liquid jet originates. These modes (cone-jet mode, pulsating mode)

occur at different voltages and have significant effects on droplet size distribution and current transport. It is expected that the degree of instability of the liquid surface from which the jet originates should produce changes in the electrospayed morphology [19]. The change in fiber morphologies with voltages also correlates to changes in the originating droplet shape. Thus, the effect of voltage on micro/nanoparticle formation was studied by conducting the experiments with differences voltage values; 13, 16, 20 and 28 kV (Figure 5). At low voltages (13 kV), a droplet of solution remains suspended at the end of the syringe needle, and the liquid jet originates from a cone at the bottom of the droplet. The particles obtained under this voltage showed polydispersion and clumps of nanoparticles with 513 ± 900 nm average diameters. According to Deitzel and co-workers, the electrospinning current increased slowly with increasing voltage. Therefore, an increase in the electrospinning current generally reflects an increase in the mass flow rate from the capillary tip to the grounded target when all other variables (conductivity, dielectric constant, and flow rate of solution to the capillary tip) are held constant and can be observed with changes in jet initiation modes. As voltage is increased (16 and 20 kV), the cone has receded and the jet originates from the liquid surface within the syringe tip. As a consequence, the volume and size of the droplet increased. The particle size distribution showed a decrease around 564 ± 100 nm average diameters (16 kV) and 581 ± 113 nm average diameters (20 kV). Nevertheless, in terms of microparticles size and size range (monodispersity) had been obtained with electrospaying voltage at 16 kV. Moreover, when the voltage was increased up to 28 kV, it's led to the formation of distinct particles with 641 ± 132 nm average diameters. At high voltage, the high electrical potential lead to the uniform particle without cluster and therefore increased the particle size of chitosan. However, in this study, the polymer concentration that had been used was too low to allow for fiber formation and hence led to breaking of the jet in mid-air resulting in irregular shaped particles. It was only at the voltage of 28 kV was the particles with spherical shape and non clustered morphology observed. This effect was probably as a result of balanced combination of thinning due to bending instability and breaking up into spheres due to Raleigh forces at 28 kV.

- *Effect of Concentration*

In electrospayed process, a solution concentration is vigorous and gives a significant effect on the final size and distribution of particles [24]. Hence, an experiment was conducted to study the effect of chitosan concentration on the morphological properties of formed particles (Figure 6).

A low molecular weight of Chitosan had been diluted in 90% v/v of acetic acid had been used. The chitosan concentration was varied from 1% to 3% (w/v), with increments of 1% in concentration. At the initial chitosan concentration of 1% (w/v), the microspheres obtained were less volume and spherical particles with the average particle size ca. 468 ± 95 nm.

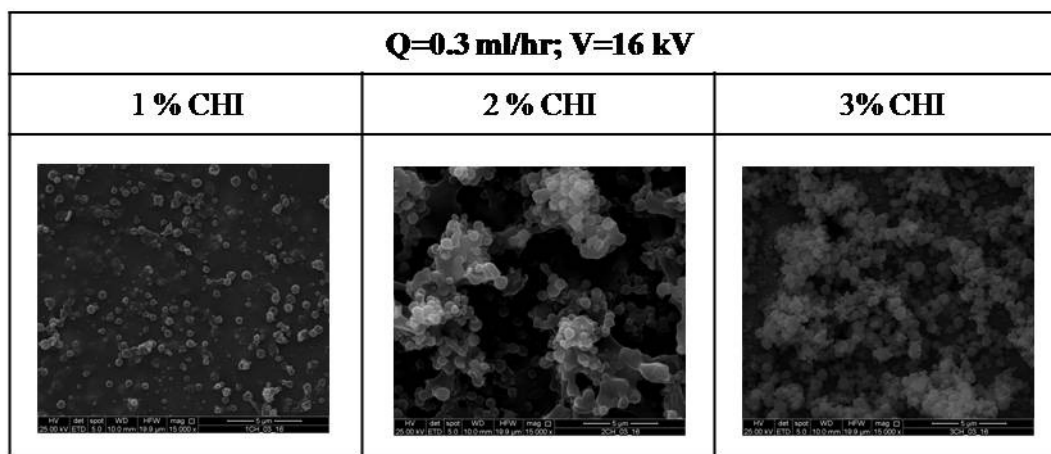


Figure 6: SEM of Chitosan micro/nanoparticle at differences concentrations (a) 1% w/v; (b) 2% w/v; (c) 3% w/v (magnification 15000 x, scale bar = 5 μ m). The parameter had been used: voltage= 16 kV and flow rate= 0.3 ml/hr.

When the concentration is lower, the micro/nanoparticles could not completely dry before to reach the collector due to the high solvent concentration. Thus, turn resulted in particles of irregular shapes. At 2% chitosan concentration, cluster and spherical particles with minimal polydispersity were observed (ca. 650 ± 128 nm average particle size distribution). The probable reason for the above may be that the Raleigh forces [25], which assist in particle formation, were able to overcome the viscous forces to enable the formation of spherical particles. As the polymer concentration was increased to 3% w/v, clumps monodisperse particles were formed with ca. 600 ± 741 nm average particle size.

For higher viscosity solutions (more than 3% w/v chitosan) proved extremely difficult to force through the jet within in these parameters (Q= 0.3 ml/hr and V= 16 kV). On the other hand, the polymer concentration was not high enough to give sufficient chain entanglements. Thus, the jet produced could not result in fiber formation, instead led to the microparticles formation. In other words, the viscosity was not high enough to resist Raleigh forces, and by using low flow rate and also high voltage can brings to the particle formation. Moreover, increasing viscosity is thought

to increase resistance of the solution to be separated into droplets [26]. In this study, a low concentration of (1-3% w/v) chitosan had been proved in generate particles instead of fibers.

- *Effect of Flow rate*

When the voltage is properly tuned, the jet disintegrates into a stream of droplets of uniform size. The size of the droplets can be controlled by the voltage magnitudes and also flow rate of the liquid. The only mechanism of charge transport is the flow of polymer from the tip to the target. Hence, the production rate of particles can be controlled by the flow rate. Therefore, an experiment had been conducted with using 2% w/v chitosan at 16 kV. As we can see in Figure 7, two differences flow rate affected the size particles and also the morphology of chitosan. Low flow rate, 0.1 ml/hr, showed a strict monodispersion of spherical particles. However, at higher flow rate, 0.3 ml/hr, showed a clustered of irregular shape of spherical particles. An increase in the flow rate allows droplet generation with higher frequency [23]. Particle size was increased when the spray flow rate was increased. For the specific case of the cone-jet mode, the average droplet size decreases while the droplet frequency increases if the flow rate is decreased or the solution conductivity increases [19].

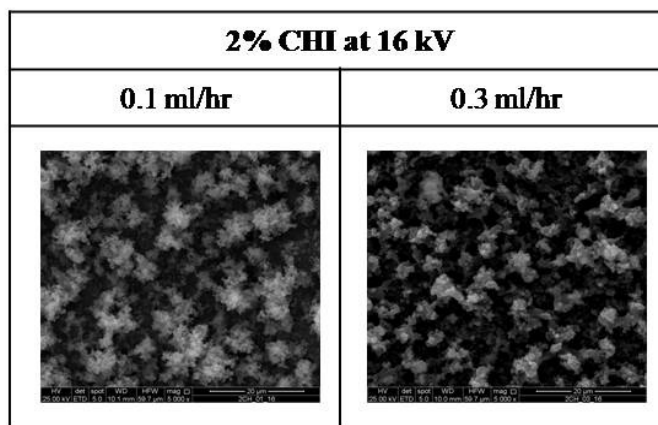


Figure 7: SEM of 2% w/v of Chitosan micro/nanoparticle at differences flow rate (a) 0.1 ml/hr; (b) 0.3 ml/hr; (magnification 5000 x, scale bar = 20 μ m). The parameter had been used: Voltage = 16 kV, distance = 7cm.

Electrospraying is a versatile tool for liquid atomization that has the advantage of uniform droplet generation from inexpensive equipment. Electrospray devices can operate under atmospheric conditions, and the rate of particle production is easy to control via voltage and flow

rate. Electro spraying is a single-step, low-energy, and low-cost material processing technology, which can deliver products having unique properties.

In this work, micro/nano particles of chitosan and drug loaded chitosan particles had been successfully fabricated by using a higher acetic acid (>95%v/v). In addition, it has been founded that the morphology of the particles produced is influenced strongly by parameters such as voltage, concentration and flow rate. Moreover, increasing voltage produced a cluster of particles and polydisperse. The particle size distribution seems increased within the voltages. Meanwhile low concentration of chitosan needed to obtain particles rather than fibers. Even tough, a low flow rate of the solution required in order to produce a monodisperse particles and homogenous.

A potential application: CHI particles as coating for PCL fibers

A coating composed of a dispersion of micro/nanoparticles from 2% CHI solution was collected onto PCL fibers membranes. CHI particles were electrosprayed at a voltage of 16 kV and different flow rates: 0.1 and 0.3 ml/hr respectively (Figure 8) to evaluate the role of flow rate on final particle morphology. Therefore, at 0.1 ml/hr, a higher amount of CHI particles appears on the surface of PCL fibers showing an average particle size of $2.187 \pm 0.534 \mu\text{m}$.

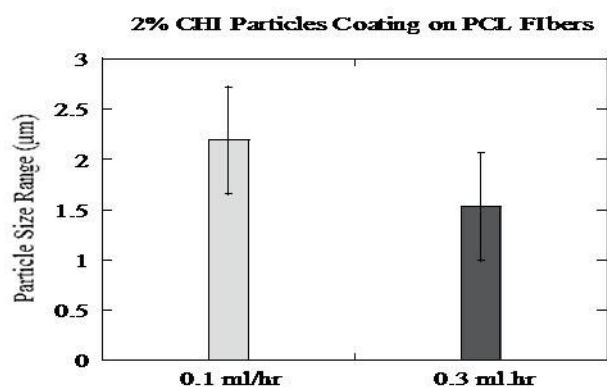
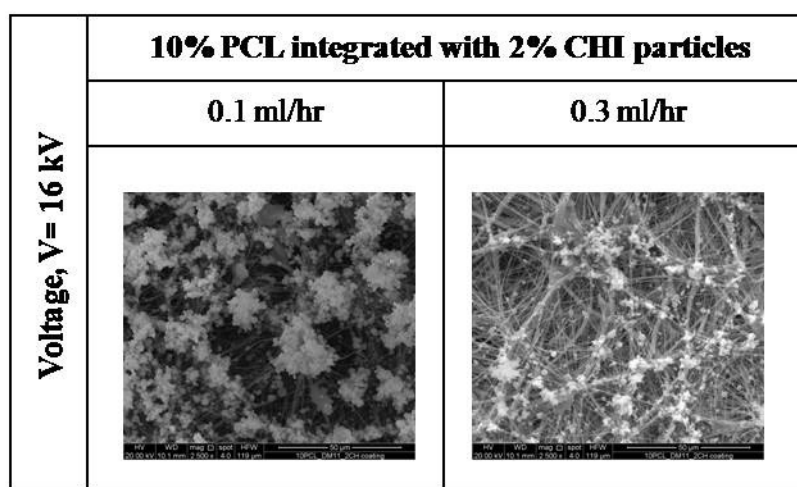


Figure 8: SEM of 2% w/v of Chitosan micro/nanoparticles coating on PCL fibers at differences flow rate (a) 0.1 ml/hr; (b) 0.3 ml/hr; (magnification 2500 x, scale bar = 50 µm). The parameter had been used: Voltage= 16 kV; distance to collector = 7cm.

Contrariwise, at 0.3 ml/hr, a more sparse distribution of CHI particles on the surface of PCL fibers was detected with smaller average sizes ($1.523 \pm 0.281 \mu\text{m}$). Hence, CHI particles successfully coated the PCL fibers at 0.1 ml/hr rather than 0.3 ml/hr due to an improved droplet stability. Noteworthy, larger particles have been obtained in the case of both

flows, probably due to the less effectiveness of collector conductivity in the presence of fiber coating.

Synthesis of Tetracycline Loaded Chitosan Particles by Electro spraying Techniques

In this study, TCH loaded chitosan particles have been examined in terms of particle size distribution, as a function of the concentration of the TCH. As shown in Figure 9, 1% w/w of TCH loaded chitosan particles showed a narrow dispersion of spherical particles with a average diameter of 803 ± 128 nm.

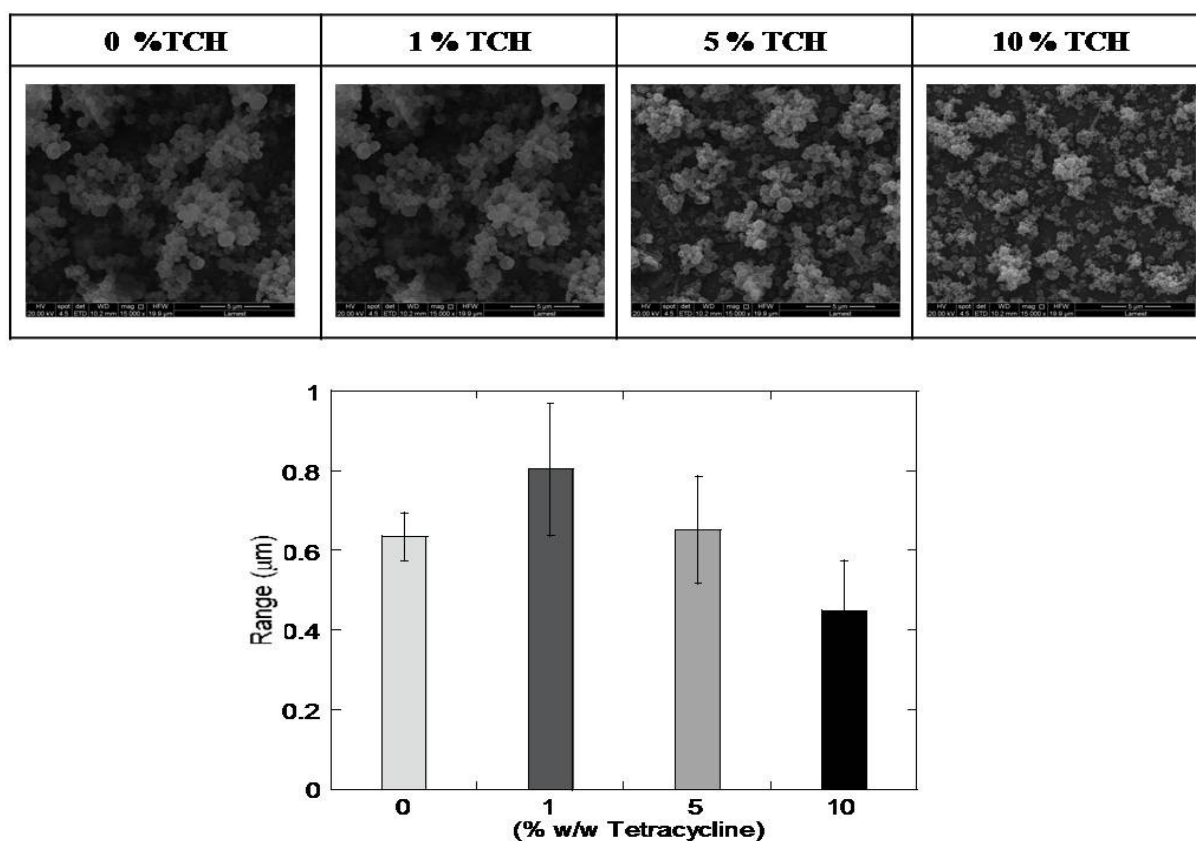


Figure 9: SEM of 2% w/v of Chitosan micro/nanoparticle with controlled sample and various TCH concentration (1, 5 and 10% w/w TCH) (magnification 5000 x, scale bar = 20 µm). The parameters have been used: Voltage= 17kV, Flow rate= 0.1 ml/hr, distance = 7cm.

As the concentration increases up to 10% w/w of TCH, more heterogenous particle size was detected. In particular, the average particle size diameter varies from 652 ± 132 nm for 5% w/w

TCH to 447 ± 127 nm for 10% w/w TCH. In overall, the nanosized particles provides higher surface area to volume ratio thus augmenting an uniform release of encapsulated TCH. This makes efficacious them for any type of mucosal or nasal delivery. Indeed, delivery carrier needs to carry a positive surface charge while the mucosa which lining the intestinal wall and nasal passages carry a negative charge. Chitosan as a drug carrier has been established through several studies as showing excellent mucoadhesive properties [27].

In Vitro Drug Release Study

Biodegradable micro/nano particles allow the drug release to be accurately tuned for the treatment of the specific disease through the appropriate choice and formulation of specific drugs and polymers. Based on various microencapsulation techniques, micro/nano particles can be designed for optimum delivery of a selected bioactive agent [27].

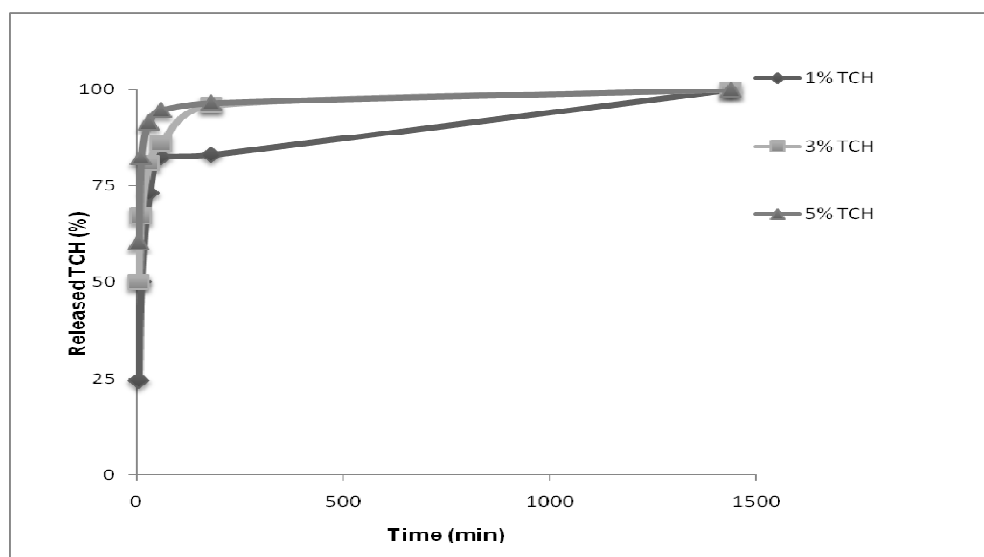


Figure 10: In vitro drug release from the chitosan microspheres against the tetracycline released as function of time at 37 °C

Therefore, a TCH loaded chitosan micro/nano particles formulation had been proposed to tailor for long term drug release with specific release rates. The release profile of tetracycline loaded chitosan micro/nanoparticles is shown in Figure 10. Tetracycline release in vitro showed a rapid initial burst in the first 3 hours, due to elution of the drugs from the outer surface and cut edges of the matrix and sustained drug release occurred after 4 hours released. The release rate

was found increase as the concentration of TCH increased. For the delivery of antibiotic drugs, an initial burst release is required to achieve enough initial dosage, because it is important to eliminate the intruding bacteria before they begin to proliferate [28]. Hence, the burst release of drug was associated with the molecules close to the micro/nanoparticles surface, which easily diffused in the initial incubation time. The further dissolution processes indicated the release medium penetrates into the particles due to the hydrophilic nature of chitosan, and dissolves the entrapped tetracycline by time. Additionally, Chitosan polymeric had a slow degradation behavior and thus affect the drug release rate and confirmed by the encapsulation efficiency and drug loading experiments. 1, 3 and 5% w/w of TCH loaded into CHI particles and showed high encapsulation efficiency with the value 97.8%, 98.1% and 98.0 % respectively. It has been observed that encapsulation efficiency was increased as increased of the TCH concentration. It is due to the low concentration of CHI and thus facile the solubility between drug and polymer. In fact, TCH is a typical water soluble drug and easy to be encapsulate. Moreover, 1%-5% w/w TCH loaded chitosan particles showed loading value approximately 0.97%, 2.9 % and 4.9% accordingly. The drug loading efficiency is increased as the increased of TCH concentration. It may be attributed to the water soluble nature of TCH. Therefore, it may lead to its rapid migration into the aqueous phase and, hence, decreased drug entrapment into the microspheres. However, low drug incorporation efficiencies of TCH into CHI particles (physically bound to the polymer by weak forces) is due to the high encapsulated TCH into the particles and thus gives a slow drug release of the system. Low drug incorporation efficiencies of water soluble drugs into nanoparticles and microspheres have also been reported for other preparation methods using an aqueous external phase during particle preparation [29,30].

In Vitro Biocompatibility tests

A confocal microscope image for TCH loaded chitosan micro/nanoparticles was shown in Figure 11. Green staining by confocal images qualitatively indicates a good vitality of hMSC either onto chitosan with 1% and 5% w/w (TCH). In particular, it showed, the cells growth on chitosan with 1% TCH extended and aligned to a spindle like shape and therefore supported improved cell growth.

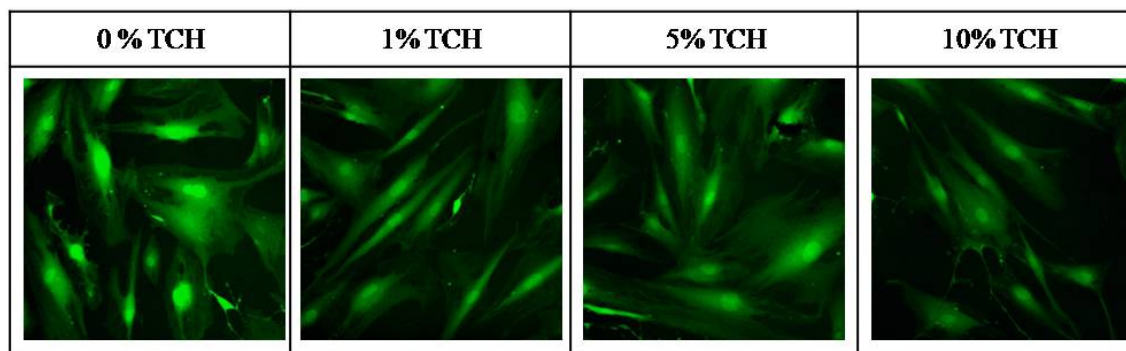


Figure 11: Confocal microscope image of TCH loaded chitosan micro/nanoparticles with difference TCH loading (1%, 5% and 10 % w/w).

Contrariwise, cells spread without any preferential orientation on chitosan with 5% TCH. This evidence is confirmed by the indirect MTT and AB reduction experiment (Figure 12) test performed on samples with different TCH loading. After 1, 3 and 5 days of hMSC exposure to eluant, in-direct test indicates that cell activity is progressively reduced as TCH amount increases, so confirming the cytotoxicity of TCH overdosing.

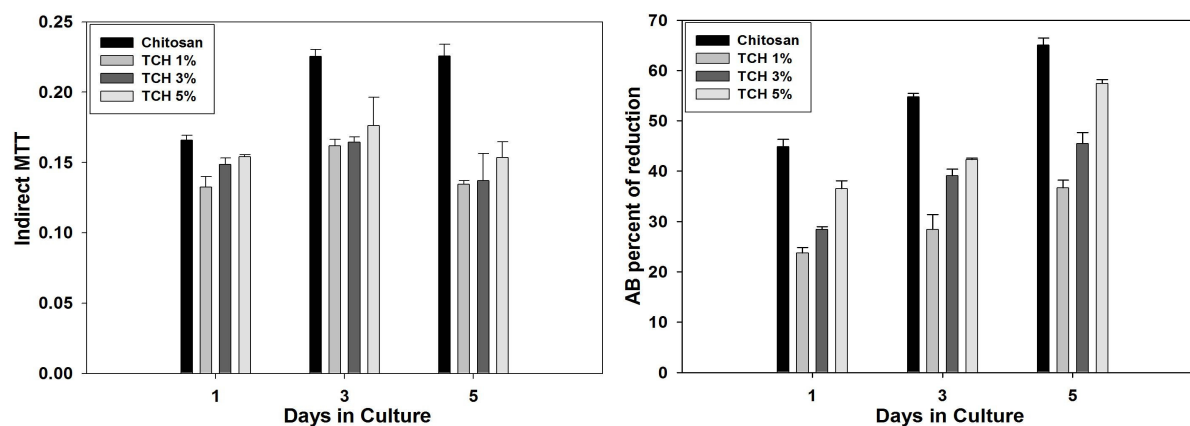


Figure 12: Indirect MTT and AB reduction vs time of culture for the various TCH concentrations (0, 1, 5 and 10% w/w) loaded chitosan micro/nanoparticles.

4.4 Conclusion

Different delivery systems have been investigated for use in periodontal disease, but still an ideal targeted delivery system is yet to be developed. The greatest advantage associated with the use of intra-pocket delivery systems over systemic delivery is that the administration is less time consuming than mechanical debridement and only lower amount of drug are needed to achieve the effective concentration at the site. In this work, we demonstrate that chitosan nanoparticles and tetracycline loaded chitosan nanoparticles generated from electrospraying techniques are potentially useful as drug delivery vehicles system capable in delivering the therapeutic agents by targeted and/or sustained delivery. However, other progress will require enhanced the mechanism of drug release in time. Hence, the proposed particles will be promising to control bacterial pathogenesis for sustained periodontal drug delivery. In perspective, the electrospraying technique could be a interesting technique to synthesize micro/nanoparticle-based drug delivery systems for periodontal tissue engineering.

References

- [1] Moghimi, S.M., Hunter, A.C., Murray. **2001**. J.C.Pharmacol. Rev. 53: 283–318.
- [2] Monhanraj, VJ. & Chen Y. **2006**. Tropical Journal of Pharmaceutical Research, 5 (1): 561-573
- [3] Soppimatha, KS., Aminabhavia, TM, Kulkarnia, AR. & Rudzinski. 2001. Journal of Controlled Release 70 (2001) 1–20.
- [4] Kumari, A., Sudesh Kumar Yadav, Subhash C. Yadav. **2010**. Colloids and Surfaces B: Biointerfaces 75 (2010) 1–18.
- [5] Tiyaboonchai, W., Woiszwillo, J., Sims, R. C. and Middaugh, C. R.: **2003**, Int. J. Pharm. 255, 139–151.
- [6] Redhead H.M. , Davis S.S., Illum. L. **2001**. J Control Release. 70: 353-363.
- [7] Magenheim B., Levy M.Y, Benita S. **1993**. Int. J. Pharm. 1993; 94: 115-123.
- [8] Fresta M, Puglisi G, Giammona G, Cavallaro G, Micali N, Furneri PM. **1995**. J. Pharm. Sci. 84: 895-902.
- [9] Andradý, A. L. **2008**. *Science and technology of polymer nanofibers*. John Wiley & Sons, Inc.
- [10] Sinha, V.R. , A.K. Singla, S. Wadhawan, R. Kaushik, R. Kumria, K. Bansal, S. Dhawan. **2004**. International Journal of Pharmaceutics 274:1–33.
- [11] Nair, R., Haritha, B., Reddy Ashok C.K. Kumari, K. Jayraj Kumar. **2009**. J. Pharm. Sci. & Res. 1(2) 1-12.
- [12] Mia, F.L., Tanb, Yu-Chiun Hsiang-Fa Liangb, Hsing-Wen Sung. **2002**. Biomaterials 23: 181–191.
- [13] Sunil A. Agnihotri, Nadagouda N. Mallikarjuna, Tejraj M. Aminabhavi. **2004**. Journal of Controlled Release 100 (2004) 5 –28.
- [14] Arya, N., Chakraborty, S., Dube, N., Katti, Mater Res Part B: Appl DS. **2008**. J Biomed Biomater 88B: 17–31.
- [15] Singla, AK., Chawla, M. **2001**. Journal of Pharmacy and Pharmacology. 53: 1047–1067.

- [16] Prajapati, BG., Patel, M. **2010**. International Journal of Pharmaceutical Sciences Review and Research. Volume 1, Issue 1,
- [17] Songsurang, K., Praphairaksit, N., Siraleartmukul, K & Muangsin, N. **2011**. Arch Pharm Res 34, No 4, 583-592.
- [18] Zhang, S., Kawakami K. **2010**. International Journal of Pharmaceutics 397: 211–217.
- [19] Deitzel, J.M., Kleinmeyer, J., Harris, D. Tan, N.C.B. **2001**. Polymer 42: 26-272.
- [20] Divya, P.V, K. Nandakumar. **2006**. Trends Biomater. Artif. Organs, 19(2)74-80.
- [21] Rabea EI, Badawy ME-T, Stevens CV, Smagghe G and Steurbaut W, **2003**. Biomacromolecules 4:1457–1465.
- [22] Geng, X., Kwon, O., Jang, **2005**. J. Biomaterials 26 (2005) 5427–5432.
- [23] Jaworek, A., Sobczyk, A.T. **2008**. J. Electrostat. 66(3–4) (2008) 197–219.
- [24] Chen, D.R., Pui, D.Y.H., Kaufman S.L. **1995**. J. Aerosol Sci., Vol. 26, No. 6. 963-977.
- [25] Shin Y., N., Hohman M.M., Brenner MP, Rutledge GC. **2001**. Appl Phys Lett 2001;78:1149–1151.
- [26] Hartman, R.P.A., Brunner, D.J., Camelot, D.M.A., Marijnissen, J.C.M., Scarlett, B., **2000**. J. Aerosol Sci. 31: 65–95.
- [27] Park, JH., Ye, M. Park, K **2005**. Molecules, 10, 146-161
- [28] Xu, X., Zhong, W., Zhou S., Trajtman, A., Alfa, M. **2010**. Journal of Applied Polymer Science 118: 588–595.
- [29] Govender T., Riley T., Ehtezazi T., Stolnik S., Garnett M.C., Illum L., Davis S.S. **2000**. International Journal of Pharmaceutics 199: 95–110.
- [30] Singla, A.K., Sharma, M.L., Dhawan, S., **2001**. Biotech. Histochem. 76, 165–171.

CHAPTER 5

Integrated System of PCL Nanofiber/ Chitosan Particles for Periodontal Tissue Engineering

5.1 Introduction

Periodontal disease is major concern in dentistry. Periodontal tissue is often lost with the progression of periodontal disease. Loss of periodontal tissue compromise the prognosis for retention of teeth in the dental arch, often creates an unhealthy environment in the mouth and may be unsightly [1]. One of the most important clinical features of periodontitis is periodontal pocket [2]. The epithelium of the gingiva migrates along the tooth surface forming 'periodontal pocket' that provides an ideal environment for the growth and proliferation of microorganisms [3]. Moreover, surgical implantation of periodontal pockets can be associated with infection and inflammation. Infection and excessive inflammation can adversely affect tissue regeneration with the use of periodontal barriers for guiding healing. The immediate goal is to control or eliminate periodontitis and to restore the lost, form, function, esthetics and comfort [2]. Therefore, it would be beneficial to be able to treat the tissue regeneration site with antibiotic, anti-inflammatories or chemotherapeutic agents as required to facilitate periodontal tissue regeneration [1].

Recently a new approach using local delivery systems containing antimicrobial has been introduced. This produces more constant and prolonged concentration profiles. The potential therapeutic advantage of local delivery approach has been claimed to be several fold. Local delivery devices are systems designed to deliver agents locally into periodontal pocket but without any mechanism to retain therapeutic levels for a prolonged period of time. The periodic use of local delivery systems in reducing probing depths, stabilizing attachment levels and minimizing bleeding would allow better control of the disease. The effectiveness of this form of therapy is that, it reaches the base of periodontal pocket and is maintained for an adequate time for the antimicrobial effect to occur. Periodontal pocket provides a natural reservoir bathed by gingival crevicular fluid that is easily accessible for the insertion of a delivery device. Controlled release delivery of antimicrobials directly into periodontal pocket has received great interest and appears to hold some promise in periodontal therapy [2]. For instance, Esposito and co workers [4] had developed a microparticles containing tetracycline, designed for periodontal disease

therapy and showed controlled released of tetracycline in the microparticles. Moreover, Tetracycline (TCH) is the most abundant test and used antibiotics in the treatment of periodontal disease. Clinical studies using tetracycline have shown it to have an effective spectrum of activity against many of the anaerobic microbes associated with the various periodontitis patients [5].

The present work describes a reliable and efficient method designed to fabricate biocomposite nanofibrous patches via simultaneous electrospinning (PCL fibers) and electrospaying (TCH loaded Chitosan nanoparticles) as an interface/implant between alveolar bone and epithelial tissue. A suitable biodegradable polymer such as PCL had been chosen to be electrospinning due to the degradability and biocompatibility properties [6]. Moreover, chitosan nanoparticle generated from electrospaying are suitable drug carrier for tetracycline [7]. This periodontal patch with a spatially controlled design structure is using dual injection system. The configuration of the design was easy and simple hence required two difference nozzles and ready to be electrospinning/electrospaying at the same time. The idea of the design is to integrate PCL nanofibers by using electrospinning and drug loaded nanoparticles via electrospaying. Electrospaying of chitosan nanoparticles on electrospun nanofibers helped to attain rough surface morphology ideal for cell attachment and proliferation than PCL nanofibers. Instead of that, drug loaded chitosan particles can controlled the rate of the drug delivery on the periodontal pocket. Significantly, fabrication of periodontal patches with integrated structure is to retain its structural, dimensional and mechanical integrity long enough to permit periodontal tissue regeneration.

A design of integrated membranes by using electrospinning/electrospaying techniques for tissue engineering had been attempted by a numerous researchers. The fabrication of a periodontal membrane with osteoconductive/inductive behavior provided by nano-sized hydroxyapatite particles and metronidazole to combat periodontal pathogens has been reported by Bottino et al. [8]. He had developed multilayered of poly (DL-lactide-co-e-caprolactone) (PLCL) layer surrounded by two composite layers composed of a protein/polymer ternary blend by using co-electrospinning. It consists of a core layer and two functional surface layers interfacing with bone (nano-hydroxyapatite, n-HAp) and epithelial (metronidazole, MET) tissues.

Wang et al. [9] had demonstrated Chitosan nanoparticles/ PCL composites by using co-axial electrospinning. He encapsulated Rhodamine B (drug) into Chitosan particles and mixed with PCL to obtain composite electrospun nanofibers with core-sheath structures for tissue engineering applications. Additionally, in Gupta study [10], a biocomposite nanofibrous scaffolds were fabricated using poly(L-lactic acid)-co-poly(3-caprolactone) (PLACL), gelatin and HA by blending and spraying methods to create an in vitro environment resembling the lowest level of hierarchical organization of bone, for the mineralization of osteoblasts. The results of the studies demonstrated nanofibrous scaffolds showed high pore size and porosity up to 90% with fiber diameter in the range of 200–700 nm. Electrospayed HA had showed better cell proliferation and thus enhanced mineralization and alkaline phosphatase activity. In their study, they showed that electro spraying in combination with electrospinning had produced superior and more suitable biocomposite nanofibrous scaffolds for bone tissue regeneration.

Interestingly, electro spraying and electrospinning processes were also employed for the production of nanocomposite material of polymer nanofibers made of PVC, PSU or nylon blended with metal oxide nanoparticles of TiO_2 , MgO , and Al_2O_3 [11]. Three configurations of electro spray/electrospun nozzles had been used for the nanocomposite production were tested: i.e. simultaneous electro spraying during the electrospinning process, electro spraying onto the same rotating drum after the electrospinning is completed, and. electro spraying onto the electrospun mat removed from the drum and placed onto a heated table. This type of nanocomposite could be used for the production of masks, filter or scaffolds in biotechnology [11].

Francis [12] had developed nanofibrous scaffolds of Gelatin/Hydroxyapatite by using the simultaneous electrospinning and electro spraying techniques. They used a rotating cylinder set up instead of using a flat collector plat to produce nanocomposite for bone tissue regeneration. Moreover, results of cell proliferation, ALP activity and FESEM studies revealed that the combination of electrospinning of gelatin and electro spraying of HA yielded biocomposite nanofibrous scaffolds with enhanced performances in terms of better cell proliferation, increased ALP activity and enhanced mineralization, making them potential substrates for bone tissue regeneration.

The versatility of existing electrospinning/electrospraying technology for fabricating biomimic nanocomposite scaffold had significant potential for regeneration of different tissue. The design by using electrospinning techniques allowed to be altered and controlling the spatial arrangement of the scaffold by using nozzle and collector configurations. In addition, the nanoparticles added in the fibers environment, are useful in retain the structure of multifunctional of the scaffold. The formation of a thin layer of fiber/particles open an interesting route for the development of membranes with more predictable physico-chemical, mechanical and biological characteristics that could ultimately lead to enhanced periodontal regeneration.

5.2 Material and Methods

Materials

Polycaprolactone (PCL; Mn 45,000 kDa) and Chitosan (CHI; low molecular weight) were purchased from Sigma-Aldrich (Italy). Methylene Chloride (Dichloromethane) and Methanol both purchased from Sigma Aldrich (Italy) had been used as solvent and co-solvent in the preparation of PCL nanofibers. Acetic Acid (pure analytical grade) from JT Baker (Italy) was used to dissolve Chitosan. All other chemicals used were of analytical grade. Tetracycline hydrochloride was obtained from Sigma Aldrich and used without any purification.

Here we proposed the development of integrated PCL fibres and Chitosan particles. The optimization of PCL nanofibers was done in Chapter 3 by selecting 10% w/v PCL nanofibers in MC/Methanol (1:1) for further studies. Meanwhile, 2% w/v Chitosan in 90% v/v acetic acid was selected to obtain particles for this study as reported in Chapter 4. Both electrospinning and electrospraying of the as-prepared solutions were carried out by using NANON electrospinning system (MECC, Japan).

Preparation of TCH embedded PCL electrospun fibers

Tetracycline (TCH) in various amounts (i.e., 0.5 % and 2% w/v of TCH) was embedded in 10% w/v PCL solution. The influence of process parameters such as voltage and flow rate had been investigated. In addition, the effect of TCH amounts was examined too. TCH was mixed with PCL solutions and then electrospun into fiber mats under a range of 15-20 kV and the flow rate was 0.2-0.5 ml/hr. A distance between tips of the needle and collector was fixed at 10 cm.

Electrospinning and Electrospraying integrated system (PCL fibres-Chitosan nanoparticles).

PCL solution (10% w/v) was prepared by dissolution in MC/Methanol (1:1) up to form a clear solution. Chitosan (CHI) (2% w/v) was diluted in 90% v/v acetic acid until the chitosan is dissolved. Drug concentration was fixed in the range of 1– 5% w/w with respect to the used polymer fraction.

The idea of the integrated systems consists in the mixing of the PCL nanofibers and chitosan particles. Therefore, electrospinning and electrospraying by using two nozzles in one spinneret was used using NANON electrospinning machine in this experiment. 10% w/v PCL solution was used to obtain nanofibers meanwhile 2% w/v CHI solution to obtain nanoparticles. The integrated system technology is schematically illustrated in Fig. 1. The operating parameters used in this experiments are showed in Table 2. The integrated system (via simultaneous of electrospinning and electrospraying) was developed by using two separate nozzles with a different flow rate but same voltages. Nevertheless, the spinneret was adjusted with a minimum speed (5 mm/sec) and 100 mm width to improve samples homogeneity. Finally all the samples were dried overnight under a fume hood and used for specific characterization.

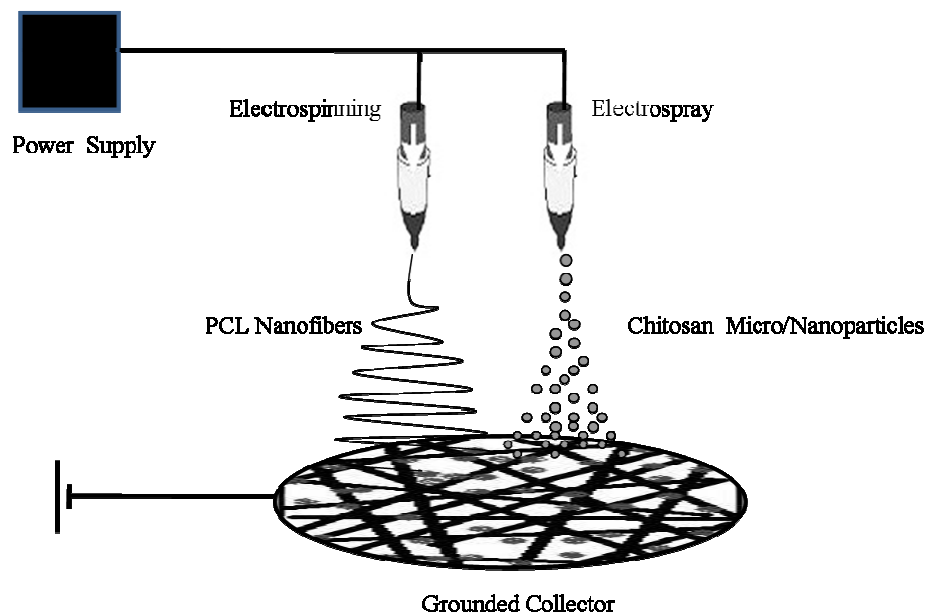


Figure 1: Schematic method of Integrated System mixing of PCL Nanofibers and Chitosan Particles.

Table 2: A typical range of operating parameters used for integrated system experiments.

Parameter	Range
PCL in MC/Methanol	10% w/v
Chitosan in AA	2% w/v
Voltage (kV)	13-17
Flow rate (ml/hr)	0.1-0.5
Electrode spacing (cm)	10
Spinneret speed (mm/sec)	5
Spinneret width (mm)	100

SEM analysis

Morphology of TCH embedded in PCL fibers and integrated membranes (PCL nanofibers with CHI particles) was observed by scanning electron microscopy (SEM, Quanta 200 FEI). The estimation of fibers and particles diameters was assessed on 20 random locations of the samples using Image J software, (version 1.37) while the average of these twenty measurements was used as an average diameter of these samples.

In vitro drug release

Encapsulation efficiency and loading capacity of integrated membranes (PCL nanofibers and TCH loaded chitosan particles) were determined by centrifugation of samples at 5,000g for 30 min. An integrated sample was suspended in 35 mL PBS (pH7.4) for 24 hours and after centrifugation, the amount of free drug in clear supernatant was determined by UV spectrophotometry (Cary 100 Varian) at 380 nm. A linear calibration curve with different concentrations of tetracycline in PBS (pH 7.4) was established to find the relation between the absorbance and the drug concentration (as shown in Figure 2).

The encapsulation efficiency and drug loading were calculated using the following relations.

$$\text{Encapsulation Efficiency} = \frac{\text{Total amount of tetracycline} - \text{Free amount tetracycline}}{\text{Total amount of tetracycline input}} \times 100\%$$

$$\text{Loading Capacity} = \frac{\text{Total amount of tetracycline} - \text{Free amount tetracycline}}{\text{Total amount of chitosan}} \times 100\%$$

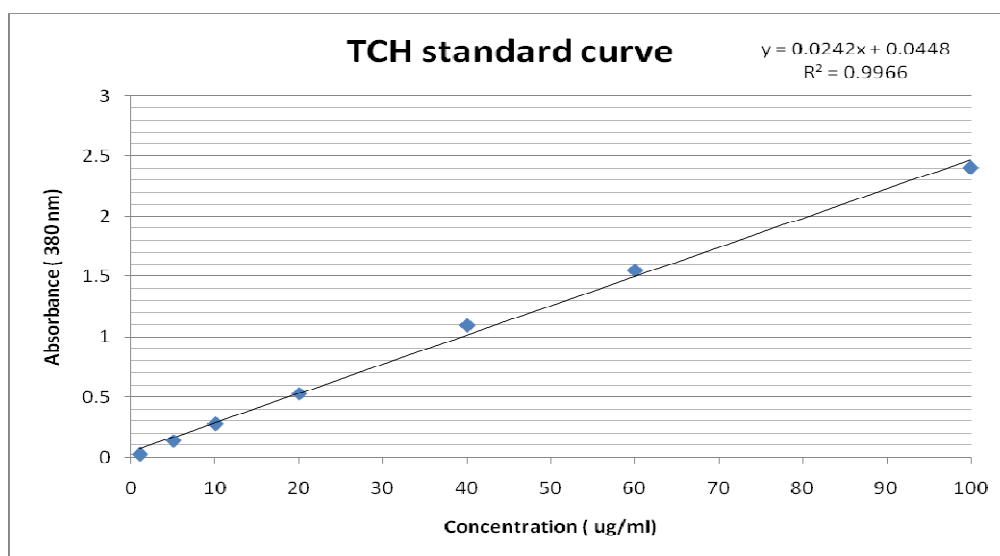


Figure 2: Tetracycline standard calibration curve ($R^2 = 0.9966$).

For the purpose of tetracycline hydrochloride release study, integrated membranes (PCL nanofibers and TCH loaded chitosan particles) samples were diluted into the medium of phosphate buffer saline (PBS) (pH 7.4) for 35 mL (37 ± 0.5 °C). All the samples were mixed using vortex in 2-3 minutes. The amount of TCH in the samples was determined using a UV-spectrometer at a λ max of 380 nm. The time intervals were read to determine the release of TCH start on 30 mins up to 24 hours. The detected UV absorbance of TCH was converted to its concentration according to the calibration curve of TCH in the same buffer. Then the relative percentages of the released TCH were calculated as a function of incubation time. Moreover, a graph was plotted determining cumulative release of TCH (%) vs. time (hours).

Cell Culture

Biological assays were performed using bone marrow derived human mesenchymal stem cells line (hMSC, PT-2501) obtained from LONZA. hMSC were cultured in 75 cm² cell culture flask in Eagle's alpha minimum essential medium (α -MEM) supplemented with 10% fetal bovine serum, antibiotic solution (streptomycin 100 μ g/mL and penicillin 100U/ml, Sigma Chem. Co) and 2 mM L-glutamin. The cells were incubated at 37°C in a humidified atmosphere with 5% CO₂ and 95% air. hMSC passages 4-6 passages were used for all the experimental procedures.

Cell viability and proliferation

The cell adhesion of hMSC onto electrospun fibres mats of CHI/PCL integrated systems was evaluated by using the vibrant cell adhesion assay kit (MolecularProbes). hMSC cultured in 75 cm² cell culture flask were washed with PBS and incubated with calcein AM stock solution to a final concentration of 5 μ M in serum free medium for 30 min. After incubation, the cells were washed with PBS, trypsinized and the cell pellet was collected and diluted with cultured medium to get the required cell concentration. hMSC were seeded onto electrospun fibres and incubated for 4 and 24 h. The fluorescence was quantified by using fluorescein filter set with a Wallac Victor3 1420 spectrophotometer (PerkinElmer, Boston, MA). Percentages of cell adhesion were obtained by dividing the corrected (background subtracted) fluorescence of adherent cells by the total corrected fluorescence of control cells and multiplying by 100%. Conventional polystyrene 24-well culture plates were used as a control.

Cell viability of hMSC (1x10⁴ cells) plated in triplicate onto electrospun fibres mats of PCL scaffolds was checked by the MTT assay for 1, 3 and 5 days of culture. This assay is based on the ability of mitochondrial dehydrogenases of living cells to oxidize a tetrazolium salt (3-4,5-dimethylthiazolyl-2-y-2, 5-diphenyltetrazolium bromide), to an insoluble blue formazan product. The concentration of the blue formazan product is directly proportional to the number of metabolically active cells. The hMSC seeded onto integrated scaffolds at prescribed time were washed with PBS and incubated with fresh cultured medium containing 0.5 mg/mL of MTT for 4 h at 37°C in the dark. Then, the supernatant was removed and dimethyl sulfoxide (DMSO) was added to each well. After 60 minutes of slow shaking the absorbance was quantified by spectrophotometry at 570 nm with a plate reader. The culture medium was renewed every day.

Statistical analysis

All numerical data are presented as mean \pm standard deviation. All results were subjected to statistical evaluation using an unpaired Student's t-test to determine significant differences between groups. The significance level was set at $p < 0.05$.

5.3 Results and Discussion

Tetracycline embedded in PCL nanofibers: Effect of process parameters

In this work, 0.5% w/w TCH was embedded in 10% w/v PCL solution. The addition of TCH in the PCL solution imposes to change the process parameters, i.e.; voltage, flow rate and concentration. In Figure 3, the increase of voltage determines an increase of the nanofibers diameters while kept the flow rate constant at 0.5 ml/hr.

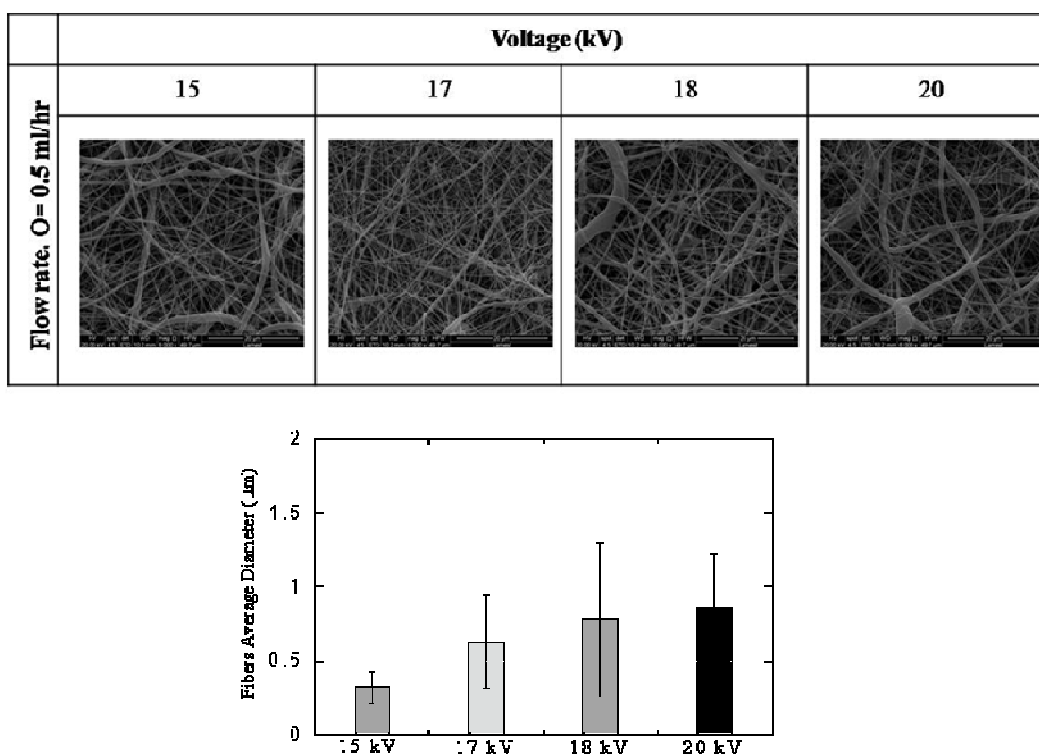


Figure 3: SEM micrographs of 0.5% w/w TCH embedded fibers from 10% w/v of PCL solution at various voltage: 15, 17, 18 and 20 kV and fixed flow rate 0.5 ml/hr. (Magnification 6000 x, scale bar = 20 μ m).

The electrospinning process starts at 15 kV just producing fibers diameter with average of $0.318 \pm 0.111 \mu\text{m}$. As the voltage increases to 17 and 18 kV, the fibers diameters also increases with an average fibers diameter of $0.627 \pm 0.317 \mu\text{m}$ and $0.779 \pm 0.524 \mu\text{m}$ respectively. Further increase of voltage up to 20 kV also appeared increased in the fibers diameters with average $0.861 \pm 0.360 \mu\text{m}$.

Although, TCH molecules do not interact with the solution, the addition of TCH significantly affects the fibre morphology which do not shows beads over a voltage of 20 kV.

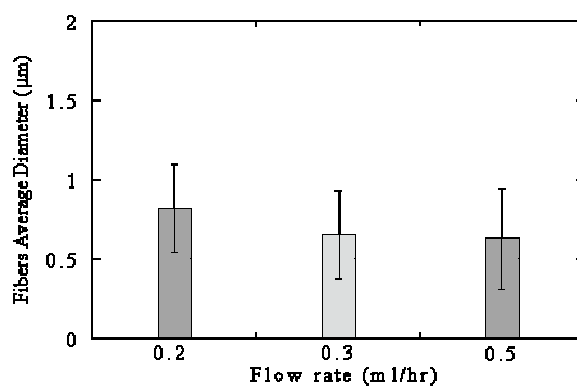
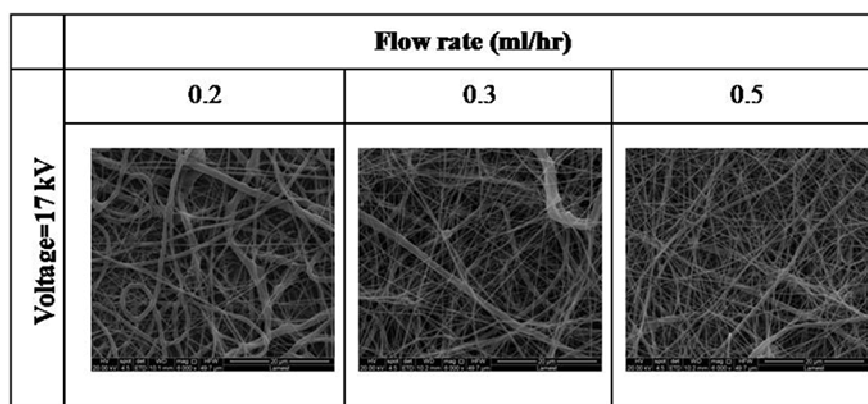


Figure 4: SEM micrographs of 0.5% w/w TCH embedded in PCL nanofibers at various flow rates: 0.2, 0.3 and 0.5 ml/hr and voltage of 17 kV (Magnification 6000 x, scale bar = 20 μm). Average Fiber Diameter as a function of the flow rates (0.2-0.5 ml/hr).

The illustrated effect of the flow rate towards the morphologies can be seen in Figure 4. Thus, the voltage is kept constant at 17 kV. Upon the flow rate 0.2 ml/hr, average diameter was $0.821 \pm 0.278 \mu\text{m}$. By increasing the flow rate up to 0.3 and 0.5 ml/hr, the average diameters showed

$0.653 \pm 0.482 \mu\text{m}$ and $0.627 \pm 0.317 \mu\text{m}$. As the flow rate increased, the fibers diameters progressively decreased.

Ideally, the feed rate must match the rate of removal of solution from the tip [6]. Furthermore, the interaction among polymer chain with macromolecules had increased the conductivity in the solution. Indeed, when macromolecular drug is embedded in a PCL solution, it provides to improve the stability of jet during the fiber formation.

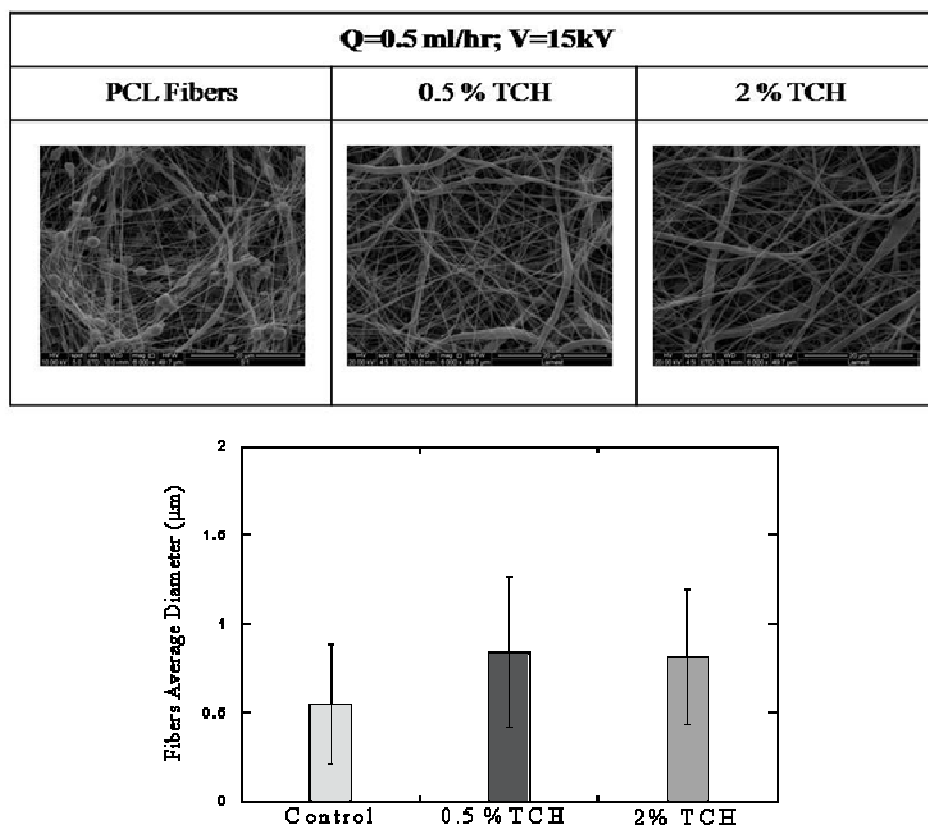


Figure 5: SEM images of PCL fibers with different TCH loading (0.5 % and 2 % w/w TCH) at voltage: 15 kV and flow rate: 0.5 ml/hr. (Magnification 6000 x, scale bar = 20 µm). Average fibers diameter vs. various concentration of TCH (0, 0.5 and 5% w/w).

Morphologies of 10% w/v PCL with various concentrations i.e.; 0, 0.5 and 5% w/w TCH were reported in Figure 5. 10% w/v PCL was used as control and shows an average fibre diameter of electrospun nanofibers of $0.544 \pm 0.337 \mu\text{m}$. By adding TCH in the PCL solution (from 0.5 to 5% w/w), an increase of the average diameter of electrospun nanofibers was detected with $0.840 \pm 0.427 \mu\text{m}$ and $0.814 \pm 0.384 \mu\text{m}$. However, the morphology of PCL fibers frequently presents

beads on strings due to the effect of conductivity and viscoelastic force (i.e., a result of the low degree of chain entanglements). When these forces do not counter the higher Coulombic repulsion force and surface tension, the formation of beads results along the fibres [13]. On the contrary, the addition of drug (TCH) in PCL solution promotes the formation of free-beaded fibers. The TCH embedded PCL fibers were larger, less uniform and with higher average fiber diameter.

PCL fibers integrated with CHI Particles by using electrospinning and electrospraying technique (One spinneret case).

- Effect of process parameters (voltage and flow rate)

Electrospinning and electrospraying were used simultaneously to produce a non woven PCL fibers integrated with CHI particles to create biomimetic nanofibers/nanoparticles suitable for periodontal tissue engineering. Therefore, the construction of a scaffold from biodegradable PCL nanofibers integrated with CHI particles can be considered effortless by this technique.

In this study, an effect of process parameter such as voltage, flow rate was observed by the SEM morphologies. As reported in Figure 6, two differences voltages, 13 kV and 15 kV, were applied and the flow rate was kept constant at 0.2 ml/hr. At the 13 kV, the morphology showed uniform fibers (average fibers diameter; $0.647 \pm 0.229 \mu\text{m}$) with small CHI particles (average particles diameter; $0.691 \pm 0.158 \mu\text{m}$) attached on the fibers surface.

When the voltage increases up to 15 kV, fibers with beads appeared (average fibers diameter; $0.537 \pm 0.429 \mu\text{m}$) and CHI particles with higher average particles diameter ($0.795 \pm 0.188 \mu\text{m}$). Apparently, voltage is one of the important parameters to obtain fine fibers and homogenous particles. PCL fibers morphology showed beads on strings due to the low surface tension and the instability of the Taylor cone. Contrariwise, the CHI particles size increases with the applied voltage due to the higher ability of the liquid jet to form a droplet.

The effect of the applied voltage on diameter size distribution needs to be considered together with other parameters, particularly the feed rate. Therefore, a study on the effect of flow rate towards the morphology was examined as shown in Figure 7. The SEM micrographs showed

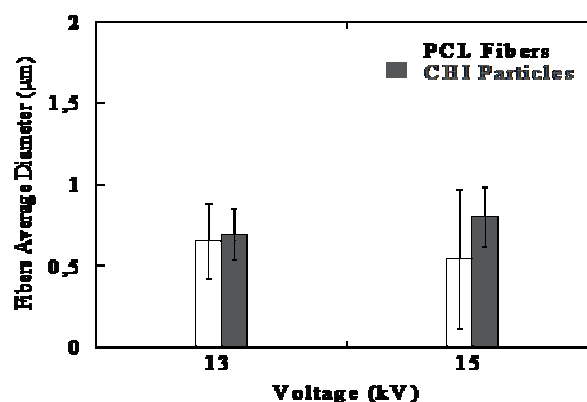
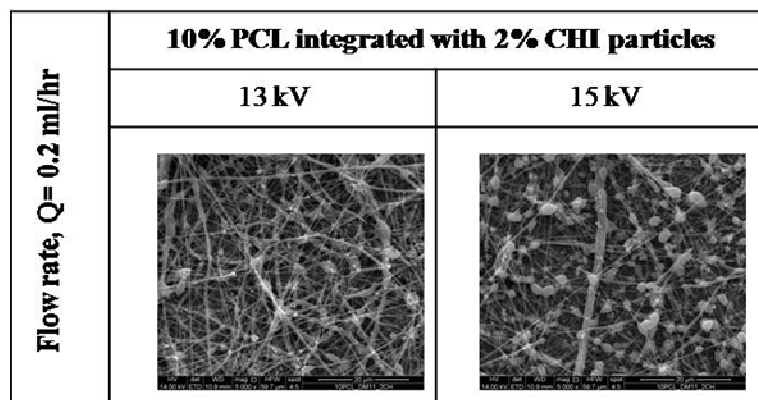


Figure 6: SEM micrograph of PCL nanofibers/Chitosan particles at differences voltage; 13 and 15 kV with fixed flow rate: 0.2 ml/hr. (Magnification 5000 x, scale bar = 20 µm). Graph Fiber Average Diameter vs. difference voltages.

PCL fibers integrated with CHI particles at a different flow rate (0.1, 0.3 and 0.5 ml/hr) at 13 kV was kept constant. At low flow rate, 0.1 ml/hr, PCL fibers illustrated fine fibers without any defects with average fiber diameter $0.377 \pm 0.107 \mu\text{m}$ and CHI particles with average particle size diameter $0.421 \pm 0.087 \mu\text{m}$. At 0.3 ml/hr, PCL fibers with beads on string (average fiber diameter $0.414 \pm 0.115 \mu\text{m}$) appeared and CHI particles (average particle size diameter $0.670 \pm 0.128 \mu\text{m}$) were collected on PCL fibers surface. Upon increasing the flow rate to 0.5 ml/hr, average PCL fibers diameter ($0.774 \pm 0.617 \mu\text{m}$) increases and as well as CHI particles size ($0.700 \pm 0.245 \mu\text{m}$). The PCL fibers showed a bi-modal distribution and reduced amount of CHI particles was observed. This is due to the high mass flow rate over the critical rate (the rate at which the solution was removed from the tip by the electric forces) with applied voltage, 13 kV. On the other side, high mass flow rate also affects the electrospayed CHI which is unable to

spray and produce homogenous particles. This is probably due to the low voltage (13 kV) applied in this case, which hinder to generate droplets on PCL fibers.

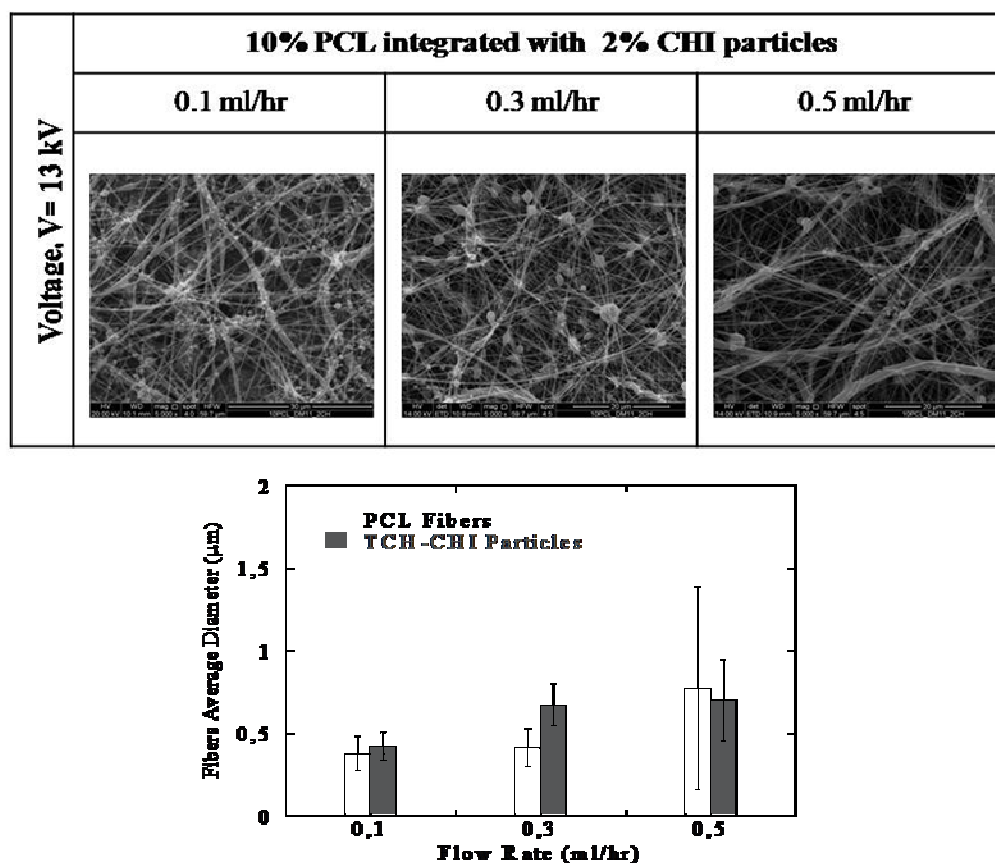


Figure 7: SEM micrographs of PCL/CHI integrated system by imposing different flow rates: 0.1, 0.3 and 0.5 ml/hr and fixed voltage, 13 kV. (Magnification 5000 x, scale bar = 20 µm). Fiber Average Diameter vs. difference flow rate.

Overall, high flow rates (0.3-0.5 ml/hr) and low voltages (13 kV) proved to be a suitable parameter for PCL fibers. However, CHI particles need high voltage (more than 15 kV) and low flow rate to produce monodisperse particles. Therefore, it is proposed to use two spinnerets to allow two different flow rates to be used at the same voltage for the next experiments.

PCL fibers integrated with CHI Particles by using electrospinning and electrospraying technique (two spinnerets case).

-Effect of process parameters (voltage and flow rate)

A dual integrated system used with two spinnerets to able to vary two flow rates and equal voltage at the same time. Hence, 10%w/v PCL solution will use flow rate at 0.5 ml/hr and kept constant for further studies.

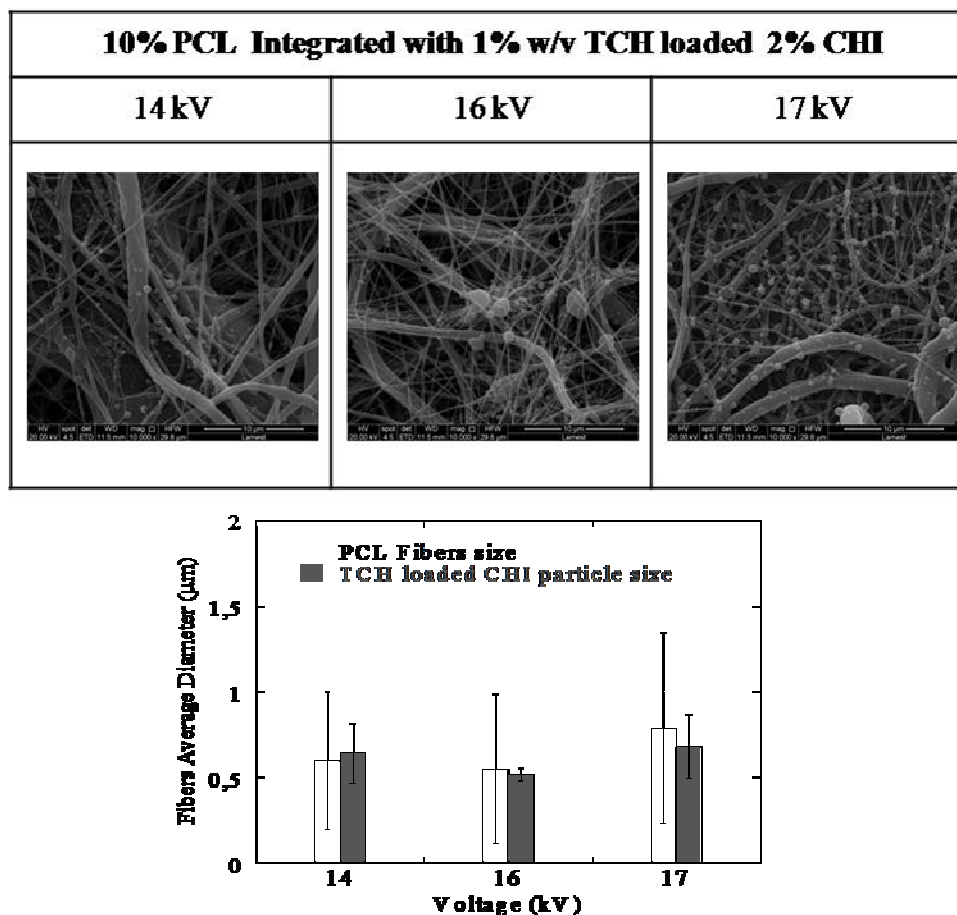


Figure 8: SEM micrograph of PCL /Chi integrated systems at differences voltage; 14, 16, 17 kV. (Magnification 10000 x, scale bar = 10 µm). Fiber Average Diameter vs. voltage.

In these experiments we used a dual integrated system to produce non woven membranes consisting of PCL nanofibers integrated with 1% w/w TCH loaded 2% w/v CHI particles. The effect of process parameters needs to be optimized to control the morphologies of the membranes. Three different voltages were tested, i.e.; 14, 16 and 17 kV with the TCH loaded CHI solution where flow rate was kept constant at 0.3 ml/hr (as seen in Figure 8). At 14 kV, PCL average fiber diameter was $0.6015 \pm 0.405 \mu\text{m}$ and CHI particles size diameter was $0.642 \pm 0.175 \mu\text{m}$. Upon increasing the voltages to 16 and 17 kV, the fiber diameters increased with average fiber diameter $0.549 \pm 0.437 \mu\text{m}$ and $0.788 \pm 0.558 \mu\text{m}$ respectively and CHI particles

showed fluctuating values with average particle size diameter $0.519 \pm 0.345 \mu\text{m}$ and $0.680 \pm 0.188 \mu\text{m}$, respectively. Voltage induces instability of the Taylor's cone which results in changes in diameter distribution. At a constant gap and feed rate, very high values of V (kV) may result in the Taylor's cone receding into the needle and the spinning occurs on the tip of the needle [14]. Therefore, the voltage affects PCL nanofibers diameters distribution, which appears uneven and bi modal. Moreover, a larger amount of CHI particles is produced increasing voltage, as seen at 17 kV. Higher voltages are necessary to overcome the viscoelastic forces leading to the TCH loaded CHI particle formation.

In figure 9, SEM micrograph showed the effect of the flow rates on the morphologies of integrated membranes. At low flow rate 0.1 ml/hr, the PCL fibers obtained average fiber diameter $0.567 \pm 0.260 \mu\text{m}$ and the TCH loaded particle size gives average particle size diameter $0.712 \pm 0.166 \mu\text{m}$. Hence, flow rate of 0.2 and 0.3 ml/hr showed slightly reduced fibers diameter with $0.505 \pm 0.183 \mu\text{m}$ and $0.491 \pm 0.415 \mu\text{m}$ respectively. Moreover, for TCH loaded CHI particles decreased with, the average particle size diameter $0.664 \pm 0.232 \mu\text{m}$ and $0.519 \pm 0.034 \mu\text{m}$ respectively. However, the increase of the flow rate determined a reduction of the volume of TCH loaded particles inside while the increase in voltage determined an increase of the volume of TCH loaded particles. The generation of particle seems affected greatly by both the voltage and flow rate.

The instability jet from PCL solution tends to affect the formation of CHI particles and thus showing fewer particle amounts on the surface of PCL fibers. Moreover, by controlling the motion of the spinneret (moving left to the right), it is also possible to control the solvent evaporation. However, the evaporation mechanism is often too fast so that the PCL fibers are usually unsmooth and rough fibers.

The PCL fibers integrated with numerous concentrations (1, 3 and 5% w/w) TCH loaded in 2% CHI particles were shown in Figure 10. By using 1% TCH loaded in CHI particles, SEM morphology showed a monodispersity of particles and thus gives average particle size diameter $0.712 \pm 0.166 \mu\text{m}$.

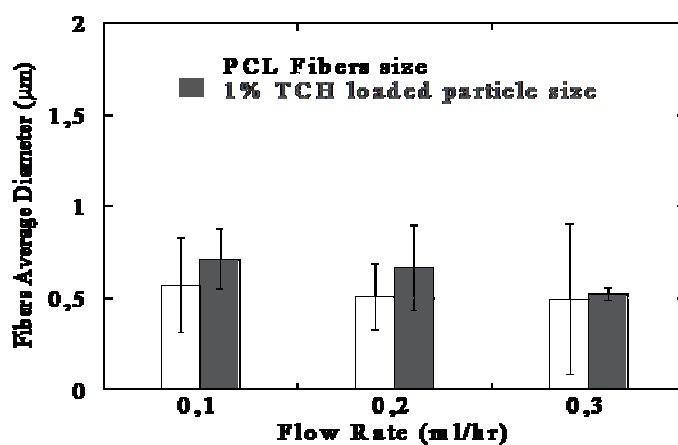
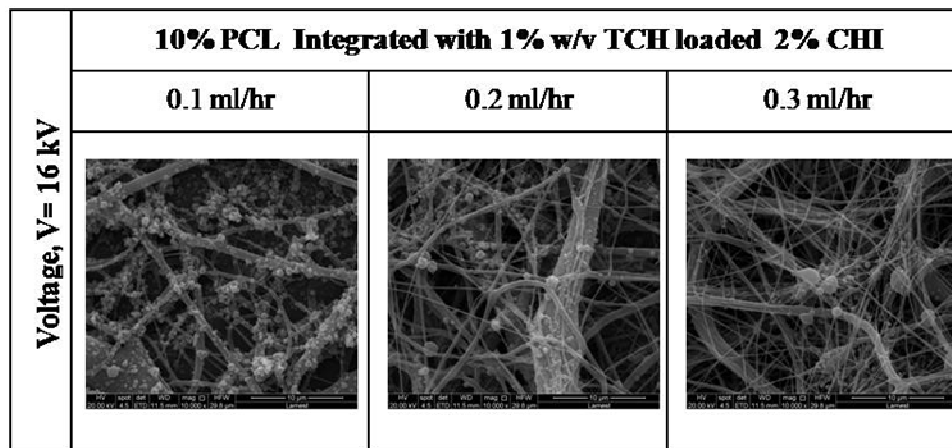


Figure 9: SEM micrograph of PCL nanofibers/Chitosan particles at different flow rate; 0.1, 0.2 and 0.3 ml/hr with fixed voltage: 16 kV. (Magnification 10000 x, scale bar = 10 µm). Graph Fiber Average Diameter vs. difference flow rate.

As TCH concentrations increases up to 5% w/w, TCH loaded CHI particle size decreased from $0.639 \pm 0.154 \mu\text{m}$ to $0.485 \pm 0.147 \mu\text{m}$ respectively. Probably, it has to be considered also the interaction between hydrophilic chitosan particles and hydrophobic PCL fibers which affects the final particle size during the spinning.

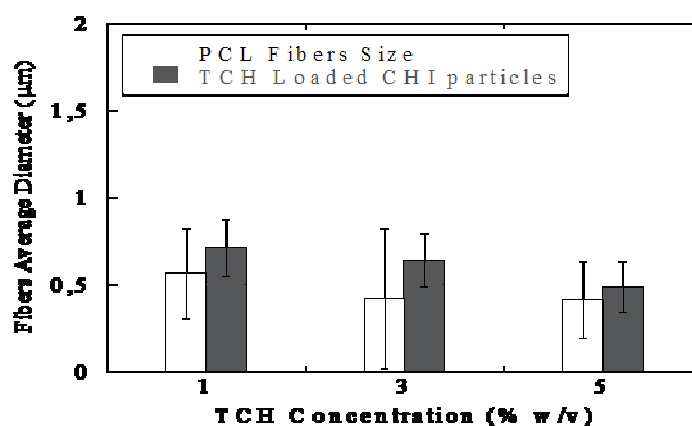
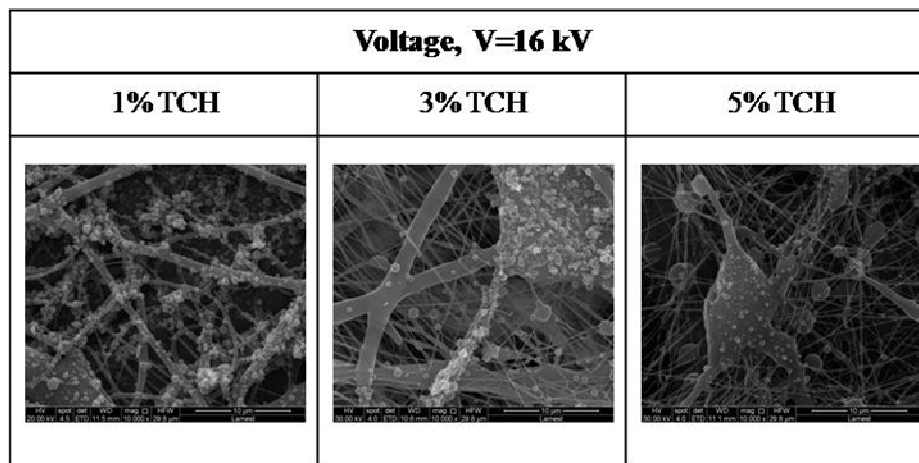


Figure 10: SEM micrographs of PCL nanofibers/TCH loaded Chitosan particles with various concentration of TCH; 1, 3 and 5% w/w with flow rate; 0.1 ml/hr and voltage; 16 kV. (Magnification 10000 x, scale bar = 10 µm). Graph Fiber Average Diameter vs. difference TCH loading.

In Vitro Tetracycline Release from integrated membranes

Figure 11 shows a release profile of (1, 3 and 5% w/w) TCH from PCL integrated with TCH loaded CHI particles. In this profile, an initial burst release occurred after 30 minutes, followed with sustained release. The release is driven by diffusion of the drug through the pores of wall and thus diffusion is the rate determining step and the initial phase of release was thought to occur mainly by dissolution and diffusion of drug entrapped close to or at the surface of the microparticles.

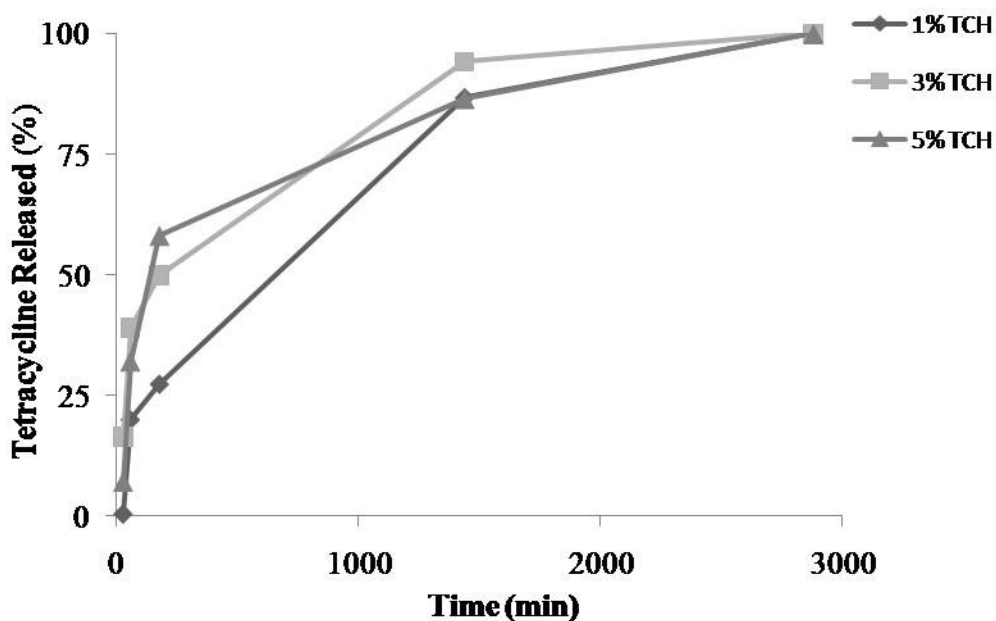


Figure 11: Tetracycline release profile of PCL nanofibers integrated with (1-3% w/w) TCH loaded chitosan particles membranes at various time intervals.

The initial burst release was commenced after 30 minutes and showed 1, 3 and 5% TCH release was 0.36, 16 and 7% correspondingly. Subsequently after 24 hours, 1, 3 and 5% w/w TCH releases were getting slowed. In this second step is called sustained release. Generally, a sustained release (slower phase release) was thought to involve the diffusion of drug entrapped within the inner part of the polymer matrix by means of aqueous channels of a network of pores. This sustained release pattern is also due to the depletion of the drug content and is due to the microparticle shape, both affecting the mode of diffusing medium into the particle, from the center from the surface [15].

TCH loaded CHI particles showed a slower release in the case of integrated systems, compared to TCH loaded CHI particles alone (as discussed in Chapter 4). This is due to the effect of hydrophobic behavior of PCL nanofibers, when hydrophilic CHI with hydrophilic drug have a contact with them, thus favouring inhomogeneous regions.

Moreover, this turns TCH are well entrapped in the microparticles as confirmed by the high encapsulation efficiency (Table 2). The result showed that high encapsulation efficiency ca. 100% was obtained with PCL/ 1% w/w TCH loaded CHI particles. In particular, the

encapsulation efficiency is independent on the TCH content (Table 2). This could be explained with TCH solubility was higher in the polymer solution (during mixing of polymer and drug) and therefore yielded more homogenous TCH/CHI solution. It thus formed a better drug dispersion that can hold more TCH during microsphere formation. The encapsulation of TCH with CHI particles brings out an advantage over CHI particles since higher encapsulation efficiency is desired goal for controlled drug release studies.

Moreover, the release profile shows a slower release with the respect to particles alone. Therefore, it can be stated that it is possible to construct biodegradable fiber integrated with drug loaded particles release systems which would deliver the drug directly into the periodontal pockets avoiding transport, metabolism and distribution problems as well as the need for removal.

Table 2: Drug encapsulation efficiency and drug loading for various concentration of TCH

% w/w TCH loaded in CHI particles	Drug encapsulation (%)	Drug loading (%)
1%	100	1
3%	99.91	2.99
5%	99.69	4.98

*Encapsulation efficiency (%): percentage of the initially used drug that could be encapsulated within microparticles.

In vitro Proliferation Test

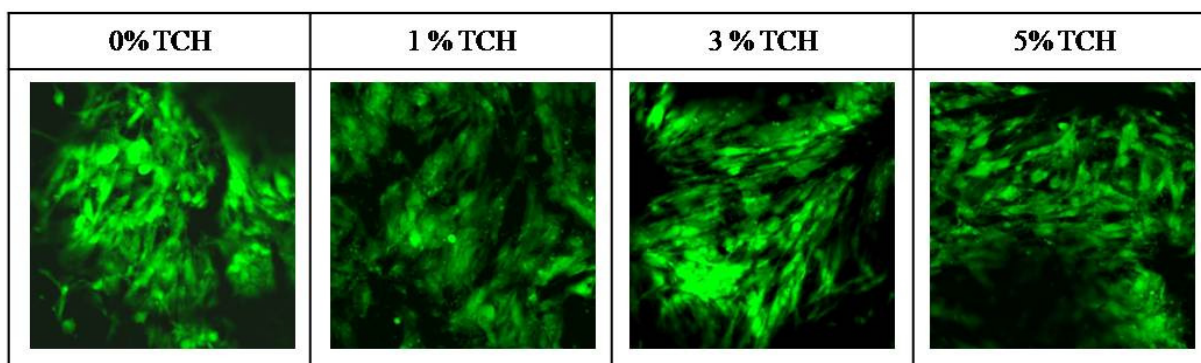


Figure 12: Confocal microscope image of PCL/CHI membranes and PCL/ TCH loaded CHI micro/nanoparticles with difference TCH loading (1%, 3% and 5 % w/w).

Figure 12 shows the confocal images of different scaffolds. Green staining was detected in all the TCH loaded CHI/PCL (with 1, 3 and 5% w/w TCH loading), indicating an higher number of grown cells on PCL/TCH-CHI integrated systems than controls. Both qualitative and quantitative analysis of green staining (Figure 12 and 13) confirm that hMSc cells growth with a good vitality.

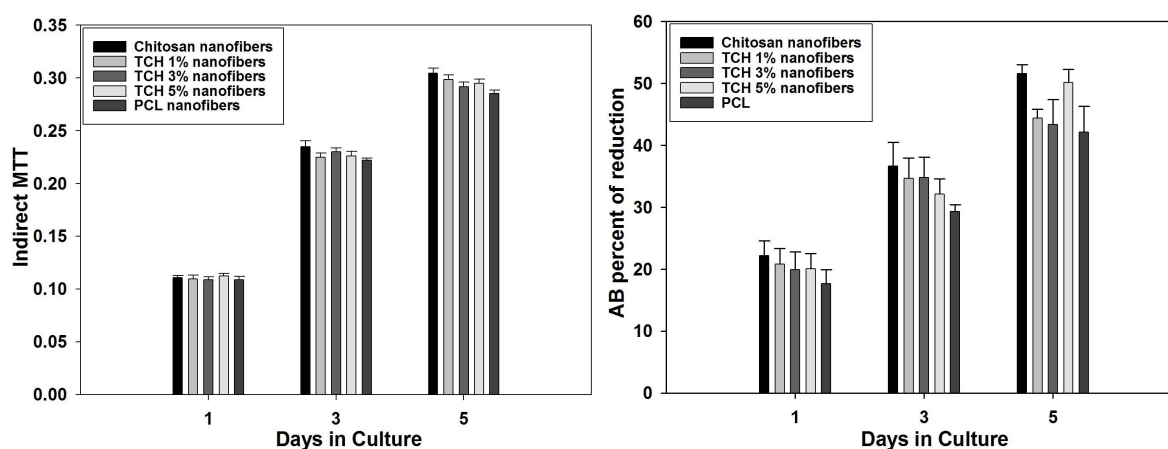


Figure 13: MTT assay and AB percent reduction for hMSC proliferation on PCL fibers, PCL/CHI scaffolds and PCL/TCH-CHI patches.

Scaffold properties play a pivotal role in controlling the cell growth and morphology and impose a direct influence on intra-cellular response. Cell behavior such as adhesion, spreading and proliferation represent the initial phase of cell-scaffold communication. In this study, the effect

of PCL integrated TCH loaded chitosan patches with the controlled samples were analyzed on cell morphology, growth and phenotypic expression of hMSc cells. The results for MTT assay (Figure 13) showed an increase for day 3 and 5 of cell culture, in the proliferation of hMSC cells on both PCL fibers, PCL/CHI and PCL/TCH-CHI. Moreover, the TCH/CHI showed a similar amount of cell culture as compared to controlled samples. On the other hand, AB reduction percentages for all the samples showed decreased of proliferation as increasing culture times (3 and 5 days). Therefore, the proliferation on the PCL/TCH-CHI particles was observed to be comparatively less than PCL/CHI scaffolds.

5.4 Conclusion

A new approach of integrated system of 3D patches had been successfully prepared by using simultaneous electrospinning and electrospraying technique. PCL fibers and Chitosan particles show been appropriate configuration by using dual nozzle system. Molecular signals (drug) loaded into chitosan particles allows for an homogeneous arrangement into the scaffolds for a time and space controlled release. Hence, PCL fibers integrated with TCH loaded chitosan particles showed a better attachment and proliferation of hMSc cells. This allows to propose PCL fibers integrated with TCH loaded chitosan particles as periodontal pockets patches.

References:

- [1] Jernberg, Gary R. Mankato. European Patent Specification EP 0 528 998 B1.
- [2] Divya, P.V., Nandakumar, K. **2006**. Trends Biomater. Artif. Organs 19: 74–80.
- [3] Vyas, S.P., Sihorkar, V., Mishra, V. J. **2000**. Clin. Pharm. Ther. 25:1–42.
- [4] Esposito, E., Cortesi, R. Cervellati, F., Menegatti, E. Nastruzzi, C. **1997**. J. Microencapsulation 14 (2) 175-187.
- [5] Palmer, R.M., Watts, T.L.P., Wilson, RF. **1996**. J. Clinical Periodont. 670-674.
- [6] Andradý, A. L. Science and technology of polymer nanofibers. John Wiley & Sons, Inc. 2008.
- [7] Govender, S., Lutchman, D. Pillay, V. Chetty, DJ., Govender, T. **2006**. Journal of Microencapsulation. 23(7) 750-761.
- [8] Bottino, MC., Thomas, V., Janowski, GM. **2011**. Acta Biomaterialia. 7 :216–224.
- [9] Wang, Y., Wang, B., Qiao, W., Yin, T. **2010**. Journal of Pharmaceutical Sciences. 99 (12) 4805-4811.
- [10] Gupta, D., Venugopal, J., Mitra, S., Giri Dev VR. & Ramakrishna, S. **2009**. Biomaterials 30, 2085–2094.
- [11] Jaworek, A., Krupa, A., Lackowski, M., Sobczyk, AT., Czech, T., Ramakrishna, S., Sundarrajan, S., Pliszka, **2009**. D. Journal of Electrostatics 67: 435–438.
- [12] Francis, L., Venugopal, J. Prabhakaran, MP., Thavasi, V., Marsano, E., Ramakrishna, S. **2010**. Acta Biomaterialia 6: 4100–4109.
- [13] Kannawung, K., Panitchanapan, K., Puangmalee, S., Utok, W. Ongarjnukool, Nk., Rangkupan, R. Meechaisue, C., Supaphol. P. **2007**. Polymer Journal, Vol. 39, No. 4, Pp. 369–378.
- [14] Deitzel, J.M., Kleinmeyer, J., Harris, D., Tan, NCB. **2001**. Polymer 42 26-272.
- [15] Sendil, D., Gü rsel, I., Wise, D.L., Hasirci, V. **1999**. J Control Release 59:207–17.

SUMMARY

This thesis deals with the design of integrated nanofibers and nanoparticles as multifunctional scaffolds for periodontal tissue regeneration. Sub-micron diameters of electrospun fibers with similar magnitude to the fibrils of the native extra cellular matrix demonstrate great promise for tissue engineering and skin grafts.

In designing scaffolds for tissue regeneration, the principal objective is to recapitulate extracellular matrix (ECM) function in a temporally coordinated and spatially organized structure. An alternative strategy in design scaffold is by the development of material structures arranged in the shape of polymeric fibers at nanometer scale. Both approaches should allow structural modulation at nano- and micro-scale. Therefore, one of up to date technique is electrospinning and electrospraying. It is an interesting tool to reproduce the fibrous component of the ECM at nanometric resolution.

Among the common techniques for the production of nanofibers, electrospinning is the most simple and cost effective one. It is a process which uses a strong electrostatic force by a high static voltage applied to a polymer solution placed into a small nozzle. The electrospinning technology are recently emerging as a novel technique for tissue regeneration because it is versatile and relatively economical to manufacture micro- and nanofibers similar to natural extracellular matrix. Electrospinning is increasingly being used to produce fibers from a wide range of polymers that are attractive as tissue culture scaffolds.

Once a preliminary description of state of art in scaffold and particle design (chapter 1 and 2), the optimization of PCL membranes by using electrospinning techniques has been developed in chapter 3. The effect of co-solvent and process parameters was investigated to identify the best solvent and co solvent combination. We demonstrated that the use of methanol as a co solvent enhance the stability of the jet, by affecting evaporation and polarity of solvent mix. Likewise, we verified that fibre diameters is also influenced by molecular weights and polymer concentration. Furthermore, process parameters such as voltage and flow rate also play an important role in define fiber size scale, also affecting the bead formation along the fibers. Here, the optimization of PCL fibers was obtained with 10% w/v PCL with solvent ratio (1:1) with an average fiber diameter of $0.25 \pm 0.07 \mu\text{m}$.

Significant efforts have been devoted to develop nanoparticles for drug delivery since they offer a suitable instrument to deliver small molecules as drugs in the local implant site. The preparation of chitosan nanoparticles by using electrospraying technique was investigated. In chapter 4, the optimization study of chitosan particles was assessed in terms of effect of process parameter on the final fiber morphology. Thus, a chitosan solution (2% w/v in 90% v/v acetic acid) have been electrosprayed to obtain an narrow distributed population of particles with average size of 564 ± 100 nm. The optimum parameter set was 16 kV as voltage and 0.1 ml/hr as flow rate.

To guide periodontal tissue regeneration, we propose to incorporate one carrier agent in nanocarriers of Chitosan to reach a controlled time release of antibiotics (i.e tetracycline) into a periodontal barrier. In the chapter 5, periodontal patches were design and fabricated via integrated electrospinning and electrospraying system. The utility of this integrated system is to develop periodontal patches made of PCL nanofibers and integrated with tetracycline loaded particles. Chitosan particles with optimized parameters were encapsulated with tetracycline at various concentrations (1, 5 and 10% w/w). A study on the effect of the process parameters such as voltage and flow rate on the morphologies was performed, evidencing an homogenous distribution of particles into the fiber network. The average diameter for PCL fibers was 0.56 ± 0.26 μm and for tetracycline loaded chitosan particles was 0.71 ± 0.16 μm . The in vitro drug release showed that tetracycline showed an initial release after 30 minutes and sustained release occurred after 24 hours. Finally, proliferation test confirm a good vitality of hMSC cells independently on the final TCH concentration. However, as a tetracycline amount increases, the cytotoxicity of tetracycline was overdosing. However, biocompatibility tests confirm that green staining on the PCL nanofibers/tetracycline loaded chitosan particles showed hMSC cells within the culture time.

It can be concluded that, a periodontal patches had been successfully design by using electrospinning and electrospraying technique. The integrated system appeared as one of the superior technique to control the architecture of the membranes by controlling the spatial arrangement and added a molecular signal. Therefore, it is suitable in aiding and guiding the periodontal tissue regeneration. Given the versatility of existing electrospinning/electrospraying technology for fabricating biomimic nanofibers and nanoparticles made of various polymers, it has significant potential for regeneration of different tissues at different sites. The advances in

this scaffold design move towards the use of dual spinneret systems that allow the formation of nanofibers integrated with nanoparticles. PCL fibers integrated with drug loaded chitosan can be used to develop thicker tissue and ideal as a drug carrier depends on sites of target. This will provide an opportunity to study drug release at the different pH to see the release system and hence to determine a sites to be targeted. Further, new challenges in signaling molecules could help in decoding various disease mechanisms and developing surrogate models for disease.

ACKNOWLEDGEMENTS

To start with, all the thanks and appreciations go to my advisors Prof. Luigi Ambrosio and Dr. Vincenzo Guarino for their unconditional support and help, without them this work would have never been accomplished. I have gained tremendous knowledge and experience, academically and professionally, from interacting with them and being part of their research groups. I also thank the entire faculty members of the *Department of Materials Engineering and Structure (DIMP)* for their unhesitant aid whenever they are approached.

Special thanks and gratitude go to all my friends, for the fun time spent together. Valentina Cirillo, Marco Alvarez Perez, Maria Grazia Raucci, Alfredo Ronca, Mauro Petretta, Teresa Russo, Luisa Russo, Maria Assunta Autiello, Ugo D'Amora, Mariagemiliana Dessi and Valeria Panzetta.

I wish to express my gratitude to my friends who have had a great influence in my life during the PhD program; Rene Birke, Nassim Chikhi and Dalel and Elisabetta Damiano.